Biofouling growth risk assessment on Atlantic Salmon (*Salmo salar*) farm nets: exploring links to environmental factors

by

Devan Johnson

B.Sc., Vancouver Island University, 2015

A Thesis Submitted in Partial Fulfillment of the Requirements for the Degree of

MASTER OF SCIENCE

in the Department of Geography

Biofouling growth risk assessment on Atlantic Salmon (*Salmo salar*) farm nets:

exploring links to environmental factors

by

Devan Johnson

B.Sc. Vancouver Island University, 2015

Supervisory Committee:
Dr. Mark Flaherty, Co-supervisor

Department of Geography

Dr. Chris Pearce – Co-supervisor

Department of Geography

Dr. Laura Cowen – Outside Member

Department of Mathematics and Statistics

Abstract

Recently, salmon aquaculture companies in British Columbia, Canada, have experienced significant fish losses resulting in tens to hundreds of millions of dollars in damages due to gill disorders and mouth lesions. Hydroids, the colonial stage of some cnidarians, are the most likely problematic species. Field studies were conducted to examine biofoulant composition, gill health, and the interactions between water parameters, biofoulants, and gill health. In 2020, biofouling was observed at two fish farm sites in the Broughton Archipelago from April 20 to October 30 by suspending 30x30 cm net patches at five depths (1, 5, 10, 15, and 20 m). Net patches remained in the water for 1-3 weeks between pen cleanings (via power washing). After collection, the biofoulants were identified and counted, with hydroids removed and weighed separately. In addition, tow samples were collected weekly to identify any free-swimming stinging-capable species. Biofoulant compositions were mainly composed of Mollusca (mostly *Mytilus* sp.) and Arthropods (mostly Harpacticoids), hydroids were mostly composed of *Obelia* sp., and tow samples were composed of mostly medusa-form *Obelia* sp. GLMMs were built to examine the relationships between the water parameters and the biofoulant species counts, hydroid biomass, and tow sample counts. Both sites saw nearly every parameter significantly associated with biofoulant counts, with the effects stronger at Wicklow Point. Similarly, nearly all parameters were associated with hydroid biomass, however the effects were stronger at Doctor Islets. Only two (ammonia and nitrate levels) and one (ammonia) parameters were associated with the counts of sting-capable species in the tow samples from Doctor Islets and Wicklow Point, respectively. CLMMs were built to examine the relationships between gill health, biofoulant counts and biomass, and water parameters. Iron, nitrate levels, and pH were significantly associated with gill health at Doctor Islets, and temperature, pH, and dissolved

oxygen were significant at Wicklow Point. No biofoulant species counts or hydroid biomass from the net patches were associated with gill health, however, when the gill health scores were sampled after a net patch collection gill scores were significantly higher at both sites. At Doctor Islets, no stinging-capable species counts were associated with gill health and at Wicklow Point, counts of *Sarsia* sp., *Bourgainvilla* sp., *Clytia gregaria*, and Diphydae spp. were significantly associated with gill scores. Like the net patch samples, when gill scores were recorded after a tow collection, gill scores were significantly higher.

Table of Contents

List of Tables

List of Figures

List of Abbreviations

AGD – Amoebic Gill Disease
AICc – Small-sample corrected Akaike Information Criterion
BC – British Columbia
BKD – Bacterial Kidney Disease
CGD – Complex Gill Disease
CLMM – Cumulative Link Mixed Models
CPG – Complex Proliferative Gill Disease
GLM – Generalized Linear Models
GLMM – Generalized Linear Mixed Models
HABs – Harmful Algae Blooms
iHNV – Infectious Hematopoietic Necrosis Virus
iPN – Infectious Pancreatic Necrosis
ISA – Infectious Salmon Anemia
NPLD – Net Pen Liver Disease
PGD – Proliferative Gill Disease
SGPV – Salmon Gill Poxvirus

Acknowledgements

Thank you to the Federal Student Work Exchange Program (FSWEP) through Fisheries and Oceans Canada and Mowi Canada West for the financial support and planning for this amazing opportunity.

I would also like to thank my committee members from UVic, Dr. Mark Flaherty, and Dr. Laura Cowen, for your guidance, support, and understanding of my year-long absence. I would especially like to thank my committee member Dr. Chris Pearce for the many years of guidance and support you've provided in this project and past projects.

Thank you to Bogdan Vornicu and Sandi Huynh from Mowi Canada West for your support was organizing the project, finding and setting up the warehouse lab, helping with the sample collections, processing, and going beyond expectations when answering my endless questions.

Also, a thanks to the folks at the Middlepoint warehouse in Campbell River for their generous allowance of the improvised lab space and site access right at the beginning of the COVID outbreak.

I am also extremely grateful for the support of my friends, family, and coworkers from UVic and the Pacific Biological Station. Especially to my partner, Angus Valleau for the countless and sleepless hours taking care of our newborn, now toddler, so I could work on this thesis, to Morgan Black for the many hours spent explaining ecological statistics to me, and to Raquel Greiter Loerzer for her companionship during the long lab hours.

Chapter 1 **Introduction to biofouling in commercial aquaculture**

1.1 Biofouling in aquaculture

Global fisheries production, consisting of both aquaculture production and commercial fishing, plays a significant role in feeding the world's ever-growing population. It is a fast-growing sector, with a global production in 2018 of 178.5 million tonnes, nearly 50 million tonnes more than predicted in 2009 (FAO, 2020, 2009). With this increased production comes an increased awareness of the environmental challenges the fisheries sector faces as technology and techniques progress towards the demand for sustainability. Biofouling is a costly and time-consuming issue that can interfere with these demands, especially in marine finfish aquaculture (Bosch-Belmar et al., 2019).

Biofouling can refer to anything biological that can foul the equipment or the surrounding environment. This includes macro-algae and other organic debris which can get caught and tangled on nets and immersed equipment, micro-algae blooms which can deprive fish of oxygen, and other factors such as increased ammonia and the accumulation of other waste products (Gormican, 1989).

Most commonly, biofouling can cause damages to net-rearing pens via occlusion, increasing drag which can damage equipment, waste fuel in the case of commercial fishing, and prevent proper circulation leading to low-oxygen events in net-rearing pens (Bosch-Belmar et al., 2020; Swift et al., 2006). In net-rearing pens, which are often submerged for weeks to months at a time, the issues of pathogen transfer and physical damage to fish via stinging or ingestion of hydroids are a major concern (Cornejo et al., 2020). In addition, net-rearing pens can act as an artificial reef by providing novel hard substrate and facilitate the invasion of nonindigenous species (Mineur et al., 2012; Simkanin et al., 2012). Costs incurred due to biofouling has been

estimated at one of Norway's largest salmon farms to be about 2.2% of the production costs of individual sites, although this doesn't include indirect costs such as net and equipment repairs or reduced growth due to impacts on fish. In addition, cleaning the nets is, at minimum, a labour-intensive process (Bloecher and Floerl, 2021).

Although most, if not almost the entirety of the literature regarding biofouling is regarding negative aspects, some positive aspects have been noted. A study examining the predation of fouled mussels in the Baltic Sea found that individuals with fouling, and especially those with hydroid fouling, were significantly less likely to be predated upon by sea stars (Laudien and Wahl, 1999). Additionally, another study examining the effect of biofouling on fish farm nets on the cleaning efficacy of lumpfish found that some presence of fouling on the nets had a significant and positive influence on the prevalence of sea lice in their diets (Eliasen et al., 2018).

1.1.1. Equipment damage

The two main methods in which biofouling causes problems in aquaculture are damaging the immersed infrastructure and harming the animals (Fitridge and Keough, 2013). Depending on factors such as size, shape, material, and current velocity, the panels of net-pens naturally change shape in the water. Fouling of the panels can amplify this natural change, which can cause problems due to wear and tear and thus an increased potential for escape incidents, and also cause problems with the fish due to decreased water exchange and volume (Swift et al., 2006). Cyclical fatigue damage to nets during cleaning and from the extra handling associated with frequent cleaning can drastically shorten the life span of the infrastructure (Cornejo et al., 2020; Fitridge et al., 2012). As an example, Tasmania's Atlantic salmon (*Salmo salar*) farms are

severely affected by biofouling as during the summers the nets need to be removed every 5-8 days to be cleaned (Hodson et al., 1997). Not only is this costly, labour-intensive, and damaging to the nets, but Hodson noted that the high frequency of cleaning also disrupted the feeding and behaviour of the Atlantic salmon which had a negative effect on the growth rates.

1.1.2. Injuries to animals

The deformation of nets caused by increased weight and drag on net-rearing pens can influence the fluid dynamics not only in the inside of the nets, but in the surrounding area as well. This can affect the transmission and dispersal of parasites and pathogens, potentially increasing loads by acting as a physical barrier (Cornejo et al., 2020; Øvrelid, 2017). Sea lice, which refers to several Northern hemisphere endemic members of the family Caligidae, is a common salmon-specific parasite that has been the focus of much research globally since a 1989 outbreak in Ireland (Tully et al., 1993) and Norway (Birkeland, 1996), and locally since an outbreak in British Columbia in 2001 (Morton and Williams, 2003). It has been shown that a decrease in water flow can increase the chance of infection of sea lice, and possibly other parasites, due to the increased contact time between parasite and fish (Samsing et al., 2015).

Biofouling organisms can function as hosts to various other parasites and pathogens, sea lice included. Some well-known pathogens include: *Piscirickettsia salmonis* which causes Salmon Rickettsial Septicemia (SRS), *Renibacterium salmonarum* which causes Bacterial Kidney Disease (BKD), *Vibrio* species which can cause bacterial septicemia, and net pen liver disease (NPLD) which is caused by the consumption of microcystins (Fitridge et al., 2012; Cornejo et al., 2020 and citations within). Other pathogens known to use biofouling shellfish as a

reservoir include Reovirus (or chum salmon virus), Japanese oyster virus, strains of infectious pancreatic necrosis (iPN), infectious hematopoietic necrosis virus (iHNV), and *Neoparamoeba perurans* which causes Amoebic Gill Disease (AGD) (Fitridge et al., 2012; Floerl et al., 2016). Some studied examples of parasites that use biofouling organisms as a host for part of their life cycles include *Gilquinia squali*, a metacestode that usually uses a crustacean host commonly found in fouling communities and can be harmful to farmed Chinook salmon (*Oncorhynchus tshawytscha*) in British Columbia (Fitridge et al., 2012). Another example is *Cardiocola forsteri*, a blood fluke that uses polychaetes as a host, which has negatively affected farmed Atlantic bluefin tuna (*Thunnus thynnus*) in Australia (Fitridge et al., 2012).

Cornejo et al. (2020) showed that the fouling impact on current velocity from net-rearing pens is marked but tends to be vastly reduced or disappears altogether 500-1000 m from the farm location. However, it is unknown how this would apply to a site with a very strong water exchange, such as those described in Gustafson et al. (2007) in the Bay of Fundy area between New Brunswick and Maine, where reoccurrences and spread of infectious salmon anemia (ISA) have been linked to the extreme tidal activity. Finally, another point to consider is the presence of harmful algae blooms. These blooms can cause damage to net-reared fish by the release of toxins, irritation caused by mechanical damage, and asphyxiation caused by low dissolved oxygen (Whyte et al., 2001). It has been suggested that the presence of fouling organisms can enhance phytoplankton blooms by the release of nutrients into the water column via waste products (LeBlanc et al., 2002).

1.1.3. Examples of hydroid damages in non-finfish aquaculture

The most common taxa of biofouling organisms are Porifera (sponges), hydroids (life

stage of/or closely related to jellyfish), bryozoans (small encrusting organism), barnacles, polychaetes (marine worms), ascidians (tunicates), and macroalgae (Bosch-Belmar et al., 2019). The most affected organisms are finfish, oysters, and scallops (Fitridge and Keough, 2013).

Hydroids are a sessile stage of life for most animals that belong to the class Hydrozoa, which are closely related to jellyfish. Most hydroids grow in colonies that can range from a few individuals to several thousand. Some hydroids are capable of reproducing both asexually through budding and sexually by the release of medusa, which is the free-swimming jellyfish stage (Piraino et al., 1996). The most common ways that hydroids can damage cultured shellfish is the tendency of colonies to grow on the lip regions of shellfish, which is especially a problem with scallops and oysters. This can smother or reduce the growth of the animals and due to the structure of hydroid colonies and provide a growing substrate for other harmful fouling organisms such as tunicates (Fitridge and Keough, 2013). The presence of hydroids can also damage the shells or be visually unappealing, further devaluing the product (Martell et al., 2018).

Ectopleura crocea is a species of hydroid that has caused problems with mussel (*Mytilus galloprovincialis*) aquaculture in Australia. This loss has mostly come through the excessive cleaning and damage to animals and nets, and it has also been shown that *E. crocea* can eat the planktonic larval stages of *M. galloprovincialis* preventing resettlement (Fitridge and Keough, 2013). *Obelia* species, a common genus of hydroids found world-wide in disturbed areas and fouling communities, have been the suggested cause of several mass mortalities in shellfish aquaculture, as well as causing water quality problems due to their capability of mass-production of medusae (Martell et al., 2018). *Pennaria disticha*, a small hydroid common in warmer waters around the world, is less of a problem in shellfish aquaculture, but contact with colonies growing on fouled lines in Turkey sent 9 people to the hospital with symptoms of painful and itchy

patches of skin (Tezcan and Sarp, 2013). Recently, fouling by hydroids has also been implicated in losses in kelp aquaculture via shading and thus reducing growth rates, physical damage via growth directly on the kelp blades, and nutrient competition (Visch et al., 2020).

1.2. Mortality and diseases related to Cnidarians

1.2.1. Hydroids and jellyfish in finfish aquaculture

Hydroids are key pioneering components of fouling communities, often being the quickest to colonize bare surfaces, crowding out other species due to their high growth rates, and by the colonies themselves acting as a substrate for secondary colonizers (Martell et al., 2018). Warming oceans due to climate change is considered to be a contributing factor for recent jellyfish blooms and the increased rates of recruitment and survival of both invasive and native species (Bosch-Belmar et al., 2020).

Many species of hydroids have the potential to do harm, but most scientific studies focus on members of the family Tubulariidae in the genus *Ectopleura* (Bosch-Belmar et al., 2019; Gansel et al., 2015; Martell et al., 2018). The reason *Ectopleura* has so much focus is because until recently, most studies on hydroid-related biofouling have taken place in the Mediterranean Sea and in Northern Europe, where *Ectopleura* is a common species. In a 'data-dive' literature review published by Bosch-Belmar et al. (2020), *Aurelia* species, *Pelagia noctiluca*, *Cyanea capillata, Muggiaea atlantica*, and *Solmaris corona* were among the top mentioned species in articles related to jellyfish interference with aquaculture activities globally, although many more species have been reported to cause problems.

1.2.2. Jellyfish

Hydroids are a popular focus of biofouling research because they contribute directly to the other fouling issues (e.g., equipment damage, pathogen/parasite transfer, harm via direct contact, etc.), but it is worthwhile to note the damages that free-swimming medusa-stage jellyfish can cause as they are a global issue in finfish aquaculture. In recent years, reports of sudden mass mortalities of fish stock from Asia, Australia, North and South America, and Europe as a result of observed blooms of jellyfish have been on the rise (Bosch-Belmar et al., 2017; Palma et al., 2007; Willcox et al., 2008).

Some of the more frequently reported species that are known to cause harm to finfish in aquaculture are: *Aurelia aurita* or moon jelly, which is globally distributed and was responsible for a mass mortality event in Ireland (Baxter et al., 2011) and *Pelagia noctiluca* or mauve stinger is known for its painful sting in humans as well as being responsible for mass mortality events in Ireland and in the Mediterranean Sea (Baxter et al., 2011; Bosch-Belmar et al., 2017; Marcos-López et al., 2016).

Other frequently reported species are: *Muggiaea atlantica*, a small globally distributed siphonophore known for many harmful stinging events in the Mediterranean Sea and Northern Europe (Bosch-Belmar, 2017; Baxter et al., 2011), *Solmaris corona*, a microscopic species found in the Northern Atlantic that has been determined to contribute to mouth and gill irritations leading to mortalities in Ireland and Scotland (Bosch-Belmar et al., 2017), and *Cyanea capillata*, or the lion's mane jellyfish. The Lion's mane jellyfish is one of the largest known species of jellyfish and can be found in colder oceans, such as the northern Pacific and Atlantic oceans as well as in areas around southern Australia and New Zealand. Due to its size, the lion's mane jelly is particularly vulnerable to breaking apart as currents and wave action push it through the mesh of net-rearing pens where small bits containing nematocytes can come into contact with fish,

causing skin and gill irritation (Powell et al., 2018). The lion's mane jelly can also act as a vector for several aquaculture pathogens including *Aeromonas salmoicida*, and *Vibrio* species (Clinton et al., 2020).

The most significant pathologies associated with exposure to jellyfish occur on the skin and gills. This is due to the discharge of cnidocytes, or stinging cells that contain venom, which is triggered by physical contact. (Mitchell et al., 2011). Some general symptoms of fish that have been exposed to jellyfish are lethargy, swimming close to the surface, excessive jumping, respiratory distress, abstaining from feeding, and mortalities. Closer examination of the gills can show mottling, discolouration, and damage or erosion of the gill rakers and operculum. In addition, skin and eye lesions are also commonly observed after contact (Rodger et al., 2011). Contact envenomation can also lead to a range of secondary infections including several gill related pathologies that jellyfish are frequently vectors of such as the bacterium *Tenacibaculum maritimum* (Ferguson et al., 2010), or *Neoparamoeba perurans*, a known causative of amoebic gill disease (AGD) (Downes et al., 2018).

These damages can be particularly severe, as exampled with *Cyanea capillata* previous, because jellyfish can be pushed into net-rearing pens via currents and wave action, and as cnidocytes are activated by contact, even macerated pieces of jellyfish pushed through the mesh can pose a threat (Purcell et al., 2013; Rodger et al., 2011).

1.2.3. Hydroids

Hydroids can cause injuries to finfish in similar ways to jellyfish in the forms of skin lesions from contact envenomation, gill pathologies, and secondary infections (Baxter et al., 2012; Bosch-Belmar et al., 2019). In addition, during in situ cleaning events hydroids can be

washed into the water column where they can be swallowed causing mouth injury and digestion issues (Baxter et al., 2012). In one example on an Atlantic salmon farm in Ireland, the salmon saw massive gill hemorrhaging due to contact with *Ectopleura larynx*, one of the most problematic hydroid species in Europe and the Mediterranean Sea. As further evidence that *E. larynx* was the culprit species, one severely affected salmon was found to have a piece of the colony lodged in its gills (Baxter et al., 2012).

Hydroids are key pioneering components of fouling communities, often colonizing bare surfaces the quickest, and by acting as substrates for secondary colonizers such as tunicates (Martell et al., 2018). Hydroids are also suspected reservoirs for pathogens; the AGD causing amoeba, *Neoparamoeba perurans*, has been detected in *Obelia* and *Ectopleura* species present in biofouling on farms in Norway (Hellebø et al., 2017) and in Ireland (Floerl et al., 2016). *Vibrio* and *Pseudomonas*, two bacterial infections that have resulted in mass mortalities of farmed finfish, have also been detected in a species of *Obelia* present in biofouling on several farms in Scotland (Clinton et al., 2020).

Several species of hydroids are of particular interest to biofouling research. Species from the genus *Ectopleura* contains several of these species of interest. One of the most common hydroid species studied in aquaculture, *E. larynx*, is found in the Northern Atlantic Ocean, the Mediterranean Sea, and Northern Europe. Other *Ectopleura* species are also commonly distributed in temperate waters in the Atlantic Ocean and both the North and South Pacific Ocean (Fofonoff et al., 2020).

E. larynx has caused mortalities relating mostly to gill pathologies leading to secondary infections in Spain (Bosch-Belmar et al., 2017), Ireland (Baxter et al., 2011), and Norway (Fitridge and Keough, 2013; Gansel et al., 2015). The gill pathologies commonly observed after

exposure to *E. larynx* are gill hemorrhaging, necrosis, and epithelial sloughing. In addition, corneal clouding had also been observed after exposure (Baxter et al., 2012). Bosch-Belmar's (et al., 2017) study correlated the appearance of the microscopic actinulae larvae (a free-swimming larval stage that can morph into either a medusa or hydroid colony, depending on the species) of *E. larynx* with fish mortality events at a farm site near Almeria, Spain. *E. crocea* is mostly a nuisance foulant species more of concern to shellfish aquaculture in Australia and New Zealand (Floerl et al., 2016; Sievers et al., 2019), but it has the potential to become harmful to finfish due its widespread distribution.

The genus *Obelia* is distributed world-wide, only excluding the Arctic and Antarctic regions. *Obelia* species are mostly observed in the colonial hydroid stage, but also have the ability to release massive amounts of small medusa-stage jellyfish, each capable of releasing cnidocytes or stinging cells upon contact (Piraino et al., 1996). *Obelia*-caused damages to finfish aquaculture has been reported in the Mediterranean Sea (Bosch-Belmar et al., 2019, 2017; Martell et al., 2018), the Northeastern Pacific (Edwards et al., 2015; Gartner et al., 2016), the North Atlantic (Martell et al., 2018), and New Zealand (Floerl et al., 2016).

Bosch-Belmar (et al., 2017) described a study in the Almerian Gulf off the coast of Spain in which European Sea Bass (*Dicentrarchus labrax*) suffered a mass mortality event with no evident causing agent (such as bacterial, viral, or parasitic pathogens) present. Clinical symptoms displayed were like those caused by jellyfish blooms on several finfish farms, as described by Rodger et al. (2011). A taxonomic analysis found *Obelia longissima* to be a consistent member of the fouling community and was found to occur at high concentrations during several of the mortality events. This study was unable to determine a significant relationship between *O. longissima* and mortality but suggests that *O. longissima* played a role in the increasing their

susceptibility to mortality inducing triggers. Recently, several Atlantic salmon farms in British Columbia have been experiencing similar issues – mortalities and gill, mouth, and digestive injuries commonly seen during hydroid and jellyfish blooms with no apparent causative agents. Analysis of the mesh of the net-rearing pens and the water column revealed high concentrations of *Obelia* species (J. Pudota, Mowi Canada West, pers. Comm).

In addition to hydroids, sea anemones, a closely related class of animals that also contain cnidocytes or stinging cells within their tentacles, has demonstrated their capacity to harm finfish in aquaculture. The white-striped anemone (*Anthothoe ablocincta*), the brown-striped anemone (*Haliplanella* sp.), and members of the genus *Bunodeopsis* have caused sublethal ulcers on the skin of salmon species that have come into contact with them on farms in New Zealand (Floerl et al., 2016). In a recent study examining the biofouling communities on net-rearing pens in British Columbia, the plumose anemone (*Metridium senile*) was found in low densities. The plumose anemone is not known to have caused any harm, but its presence demonstrates the potential for larger sting-capable animals to contribute to biofouling communities (R. Greiter Loerzer, pers. comm.).

Several other species of hydroids have been examined, but in general, information and data regarding injuries to finfish in aquaculture caused by hydroids is scarce. As Bosch-Belmar (et al., 2017) noted, there is a complete lack of information on the severity of injuries caused by different species of hydroids and jellyfish, as well as densities of blooms or colonies during injurious events. By far, most of the data collected about hydroids and finfish aquaculture biofouling is studying their ability to quickly colonize and grow on the mesh of net-rearing pens and other structures, which can cause a host of costly problems including compromised cage structure, occlusion of the net mesh which can decrease water exchange, decrease dissolved

oxygen, and facilitate parasite attachment rates (Cornejo et al., 2020; Fitridge et al., 2012; Samsing et al., 2015).

1.3. Aquaculture in BC

Aquaculture production is an important part of Canada's economy and British Columbia is Canada's largest farmed salmon producing province. BC consistently ranks as the 4th largest farmed Atlantic salmon producer in the world, producing over 84,000 tonnes worth nearly $700 million in 2021 (Statistics Canada, 2021).

In 2019, salmon aquaculture company Mowi Canada West in BC experienced significant fish losses resulting in tens to hundreds of millions of dollars in damages due to gill disorders and mouth lesions. Some of the potential causatives such as viruses, bacteria, parasites, and harmful algae blooms have been examined extensively and subsequently ruled out. With their stinging cells, hydrozoans are theorized to be the most likely problematic species. In previous European laboratory-based challenges, exposure to cleaning debris containing hydrozoans has been shown to cause gill disorders and mouth diseases similar to what was observed in BC (Mitchell and Rodger, 2011) and hydrozoans are a known constituent of the salmon farming biofouling community at Mowi Canada West farms (Jay Pudota, Mowi Canada West, pers. comm.).

1.4. Objectives and research questions

My objective is to examine the hypothesis that *in situ* cleaning of nets may release matter and organic debris that can impact the gill and mouth health of farmed Atlantic salmon, specifically by identifying if correlations between environmental parameters, biofouling growth

on fish farm nets, free swimming stinging-capable species in the water column, and gill health scores exist. To explore these relationships several methods will be applied and discussed in two parts. The first part (Chapter 2) will focus on the interactions between the environmental parameters and the biofoulant and hydroid growth on the fish farm net pens, and the free-swimming stinging-capable species collected from on-site tow samples. The question driving the methods of this chapter is:

1) Are there correlations between the environmental variables and the biofouling community, including hydroid species, as well as the local free-swimming sting-capable species?

The second part (Chapter 3) will focus on the interactions between the gill health of the farmed Atlantic salmon, the environmental parameters, the biofoulant and hydroid growth on the net pens, and the stinging species collected from the tow samples. The questions driving these methods are as follows:

1) Are there correlations between environmental variables and gill health?
2) Are there correlations between the biofouling community, including hydroid species, and local free-swimming sting-capable species and gill health?

The results from these questions will be used to discuss the hypothesis and provide insight into possible mitigation or management strategies when specific variables or combination of variables are present. The implementation of a model that predicts what variables are harmful at certain levels could reduce direct (e.g., gill disorders) or indirect (e.g., reduced growth from stress of injury) losses of revenue.

Chapter 2 **Exploring the biofouling communities at two Atlantic salmon farms**

2.1. Introduction

In finfish aquaculture, biofouling refers to the growth, accumulation, and clogging of nets by algae, animals, and other organic debris. Most damages to infrastructure caused by biofouling are net-mesh occlusion, which can increase the drag, damage equipment, and decrease water flow in the pens leading to low dissolved oxygen and the accumulation of waste products (Bosch-Belmar et al., 2020). In addition to physical damages, the issues of injuries caused by pathogen transfers or contact envenomation are of major concern (Cornejo et al., 2020).

The extra handling and cleaning associated with biofouling can lead to cyclical fatigue damage which can drastically reduce the lifespan of the equipment and is, at minimum, a costly and labour-intensive process (Cornejo, 2020; Fitridge et al, 2012). In addition, the fraying damage caused by cleaning increases the available surface area for new recruitment of biofoulants. This is of special concern in the case of hydroids, where some studies have shown that in situ power washing of *Ectopleura larynx*, a common hydroid responsible for fish and shellfish mortalities in Europe, induced the bursting of gonophores releasing the larval actinulae that then settled immediately on the clean nets in greater numbers (Carl et al., 2011; Guenther et al., 2010)

Many biofouling species of concern are cosmopolitan; however, the community composition of individual sites is dependant on abiotic and biotic factors that are unique to each area (Fitridge et al., 2012; Pica et al., 2019). Typical abiotic factors that drive community composition are seasonality and the associated light and temperature changes, nutrient availability, substrate, currents, and depth (Holloway and Keough, 2002; Howes et al., 2007). While some factors such as light, temperature, salinity, and currents are largely dependant on

geography; nutrient availability and substrate type can be heavily influenced by fish culturing activities. Excess feed, fecal material, and cleaning debris can all contribute to nutrient availability to the communities growing on the nets, which themselves can be made of a variety of substrate-providing materials (Cook et al., 2006).

2.1.1 Abiotic factors affecting community compositions

Ocean temperatures have risen 0.88˚C (0.68˚C-1.01˚C) since 1850-1900 levels, and despite national pledges to reduce human emissions, global projections are reaching as high as a 2-4˚C increase by the end of the century. This increase has already caused substantial losses and changes in coastal and open ocean ecosystems (IPCC, 2023; UNEP, 2022). Increasing ocean temperatures are facilitating the spread and survival of non-indigenous species, including those found in biofouling assemblages. As most of these non-indigenous species are from warmer waters, they are better able to survive, leading to out-competition of native biofoulant species (Bosch-Belmar et al., 2022; Kim and Micheli, 2013).

Changes in salinity can also be attributed to rising ocean temperatures via reduced or enhanced precipitation relative to evaporation. Decreases of salinity and increases of temperature can cause density stratifications and reduced winter mixing depths. This in turn can cause a reduction in available nutrients and dissolved oxygen (Dobretsov et al., 2019).

Dissolved oxygen is inversely and exponentially inversely related to temperature and salinity, respectively. As water temperatures increase the threshold for reaching 100% oxygen saturation decreases, resulting in lower dissolved oxygen levels. As salinity increases, dissolved oxygen decreases exponentially, additionally, typical saltwater environments can only hold 80% as much oxygen as freshwater of the same temperature. Atmospheric and hydrostatic pressure

also affect dissolved oxygen levels, increasing saturation with increasing pressure. In addition, dissolved oxygen levels can change throughout the day due to photosynthesis (Wetzel, 2001).

Anthropogenic atmospheric CO_2 is the overwhelming cause of ocean acidification. The air-sea gas exchange has resulted in a decrease of 0.1 pH units in the past 200 years, with an expected decrease of 0.2-0.3 pH units by the end of the century (Feely et al., 2009). When CO2 is absorbed by sea water it alters the calcium carbonate state, resulting in an increase in hydrogen ion concentration, lowering pH and reducing the amount of calcium carbonate available. This has significant effects on organisms that calcify, internal pH regulations of fish, growth rates, and photosynthesis (Dobretsov et al., 2019; Feely et al., 2009; Guinotte and Fabry, 2008).

Several studies have demonstrated that the community structures of biofoulants are significantly affected by various environmental parameters (Mangano et al., 2019; Mhaddolkar et al., 2019; Montalto et al., 2020; Nellis and Bourget, 1996), with some species, including hydroids, that can serve as indicators of environmental quality due to their sensitivity to changes in environmental parameters (Roveta et al., 2022). However, in the compositions and successions of hydroids specifically, temperature remains a key factor in their growth and phenology (Boero et al., 2016).

2.1.2. Biotic factors affecting community compositions

The most common biotic factors that impact the ecological success of biofoulant communities are recruitment, predation, and competition pressures (Greene and Grizzle, 2007). Initial recruitment can be important in the structuring of later assemblages by enhancing both settlement by entrapment (e.g., larvae caught on stems or edges of sessile invertebrates) and by protection from predation due to the structure or chemical cues of established residents

(Holloway and Keough, 2002; Russ, 1980). However, initial recruitment can also impede later assemblages via restriction of flow, predation, being an unsuitable substrate, and overgrowth (Holloway and Keough, 2002). Recruitment and succession are unique to local ecologies, and it was noted by Greene and Grizzle (2007) that the successional pattern on suspended net-pens compared to benthic areas was substantially different in the same areas. This is especially important when examining predation as net-pens are suspended approximately 50-70 m from the seabed (B. Vornicu, Mowi Canada West, pers. comm.) and it would require non-swimming predators (e.g., sea stars) to have settled during larval stages as part of the biofouling community.

Predation on biofoulant species often has a significant effect on biofoulant communities and this effect can both increase and decrease diversity. Intense and non-selective predation can decrease diversity by allowing only a few species capable of withstanding this pressure thrive, while selective removal of a few dominant species can prevent monopolization of space which results in a higher level of diversity (Russ, 1980). However very little information exists in relation to finfish farms, which can vary significantly from benthic communities. Some attempts have been made to utilize predation as a measure of biological biofoulant control on fish farms; lumpfish (*Cyclopterus lumpus*) (Eliasen et al., 2018) and California sea cucumber (*Parastichopus californicus*) (Fitridge et al., 2012) are examples that have shown some promise, although significant challenges remain.

Competition between biofoulant species is often intermingled with species succession and is closely associated with a multitude of other factors previously discussed as well as available food quality and available space (Brown et al., 2020). However, several studies have highlighted a common pattern of succession that is likely due in part to competition. Several studies from Norway and the Mediterranean Sea indicate that hydroids are among the earliest of

colonizers but are weak long-term competitors, and bivalves tend to be dominators of final stages of assemblages but usually take long immersion periods to reach that point (Bloecher et al., 2013; Guenther et al., 2010; Martell et al., 2018). However, it is unlikely that biofouling communities on finfish farms will ever reach final stages of assemblages due to repetitive cleaning. Repetitive cleaning of nets essentially "resets" the community and keeps it at an early succession stage, which selects for early colonizers to dominate for longer than an untouched substrate (Guenther et al., 2010).

Published data on the specifics of competition between biofoulant species is scarce and each locality will have its own unique assemblage, succession, and competition pressures dependant on the local abiotic and biotic factors. This chapter will examine the interactions between environmental parameters, biofoulant assemblages, hydroid growth, and stinging-capable free-swimming species on two Atlantic salmon farms in the Broughton archipelago.

2.2. Materials and Methods

2.2.1. Description of study sites

Mowi Canada West owns two Atlantic salmon farms (Doctor Islets and Wicklow Point) in the Broughton Archipelago, on the north-eastern coast of Vancouver Island, British Columbia, Canada. I chose these sites for study due to past fish mortalities, and in 2019 there was a progression of complex gill disease (CGD) at both sites through the first summer of rearing in saltwater that was likely caused by intense biofouling, including hydroid colonies of net-pens at Wicklow Point and, to a lesser extent, at Doctor Islets. For this study the sites were populated with S1 (first year) Atlantic salmon smolts in the weeks of April 20 and 27, 2020 at the Doctor Islets site and May 4, 11, and 18, 2020 at the Wicklow Point site.

Both sites are mainly influenced by the Knight Inlet and Queen Charlotte Strait, which is a remote and sparsely populated glacier valley created during the last ice age. It has been strongly suggested that there are three layers of flow in the Knight Inlet; an up-inlet flow around 25-90 m, and a down-inlet flow above and below that. The up-inlet flow layer brings highly oxygenated water from the Queen Charlotte Strait through Fife Sound into Tribune Channel and Knight inlet, which is not only important for aquaculture sites, but plays an important role in the migration corridor of juvenile salmon from upper Knight Inlet (Foreman et al., 2006). In addition, these routes also have important implications for the transportation of various buoyant organism, including viruses, bacteria, and sea lice (Krkošek et al., 2005).

Wicklow Point (Figure 2.1) is located on the western side of the Broughton Archipelago, in Fife Sound on the south shore of Broughton Island. Wicklow Point has had historical exposures to jellyfish blooms and significant hydroid colonies (*Obelia* spp.) were regularly detected on the nets in 2019. The water current follows a specific pattern of flow during tidal exchange, with less influence coming from nearby channels, resulting in less water exchange and greater exposure time to the conditions circulating in the bay. Fish are exposed to harmful plankton and jellyfish in the water column for a longer period than the Doctor Islets site (B. Vornicu, Mowi Canada West pers. comm.).

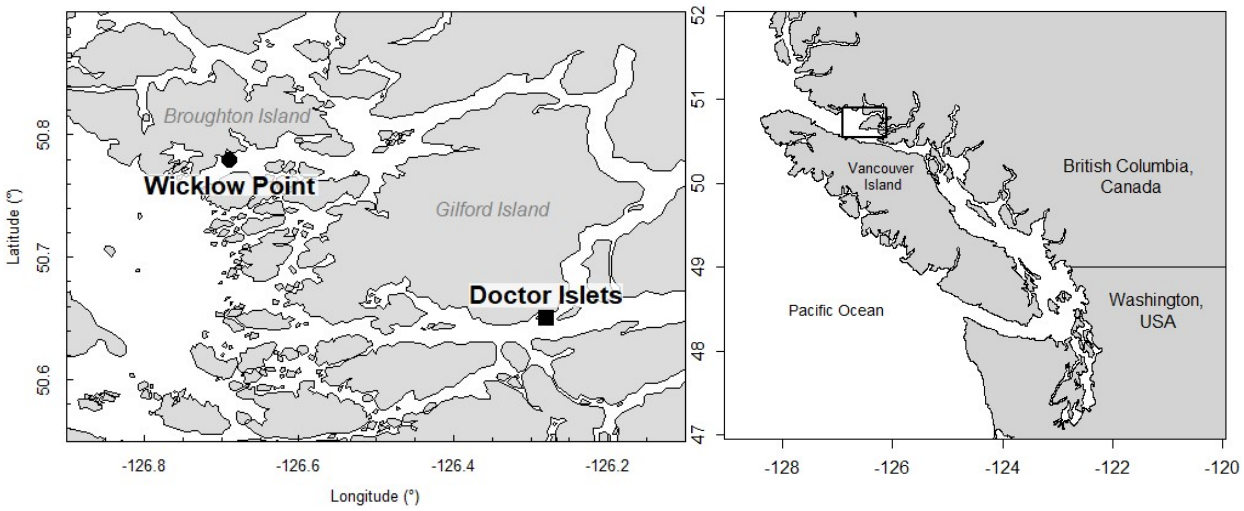

Figure 0.1: Right: inset map of the Wicklow Point (●) and Doctor Islets (■) farm sites in the Broughton Archipelago. Left: map of coastal British Columbia and Vancouver Island, the rectangle on the northern coast of Vancouver Island represents the inset.

Doctor Islets (Figure 2.1) is in Knight Channel on the south shore of Gilford Island. There is a significant influx of glacial water resulting in low salinity and a considerable amount of runoff from the northern end of Knight Inlet. There were no significant amounts of hydroid colonies (*Obelia* spp.) identified on the fish nets during the summer of 2019 and harmful plankton and jellyfish presence in the water column were noticed for shorter periods of times and with less intensity than the Wicklow Point site (B. Vornicu, Mowi Canada West. pers. comm.).

2.2.2. Sampling of water parameters and nutrients

Water quality was recorded in each pen at a depth of 5 m daily before feeding events. Temperature, salinity, and dissolved oxygen were measured using a YSI Pro 2030 probe. Ammonia, pH, and nitrate were taken using a YSI 6050000 Proplus Multiparameter Meter (YSI

Incorporated, Yellow Springs, Ohio, USA). Phosphate, silica, and iron were measured from water samples collected at a depth of 5 m and sent off-site to be processed using a LaMotte Smart 3 colorimeter (LaMotte Company, Chestertown, Maryland, USA) at the Mowi office in Campbell River.

2.2.3 Sampling of biofouling on net-patches and zooplankton tow samples

Biofouling was monitored in 5 net-pens at each site with one pen being designated for fish health (Figure 2.2A&B) that was monitored weekly (as per Mowi Canada West practice), starting with smolt stocking of the pens (April/May 2020) until the completion of the study (October 30, 2020). The fish were from the same brood stock origin, the same hatchery, of the same smolt quality (all S1 populations) and exposed to the same management practices.

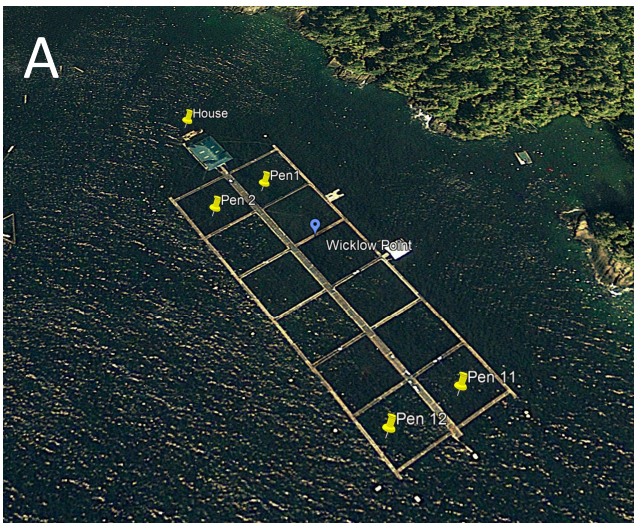

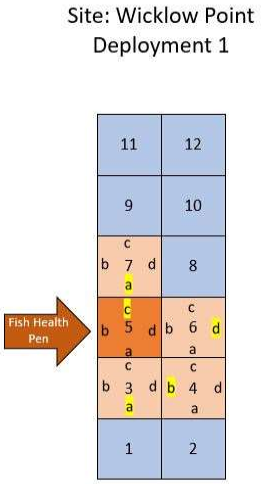

Figure 0.2 A&B: Satellite image (Google Maps) and net diagram (Sandra Hyunh) of Doctor Islets and Wicklow Point farms. Orange denotes study pens; dark orange denotes dedicated fish health net, letters a-d represent a side of the pens, and the yellow highlight indicates which side the net patches were hung on a particular deployment (i.e., here is Wicklow Point deployment 1 and Doctor Islets deployment 3 as examples)

Sample net patches consisting of 30x30 cm net pieces attached to metal frames were suspended on one side of each containment net at 1, 5, 10, 15, and 20 m from the surface by ropes to examine depth-stratified changes in biofouling community structure. They were extracted for biofouling analysis and replaced with clean net patches after each commercial cleaning event (approximately every 1-3 weeks). The net patches with their associated biofouling communities were transported on ice and brought live in individual bags filled with 20-µm filtered seawater on ice to Campbell River, BC for hydroid processing and sample preservation, before being fixed in 3.7% formalin and transported to the Pacific Biological Station in Nanaimo, BC for further biofouling community processing.

Due to the constraints of the on-site processing abilities of the hydroids growing on the

net patches, the species were categorized into four genus groups (*Obelia* spp., *Ectopleura* spp., *Sarsia* spp., and *Clytia* spp.) based on several characteristics. Long smooth stalks with slender cups containing the hydroid polyp and the presence of ridges at the base of the cups and stalks were classified as *Obelia* spp. *Clytia* spp. were similar in appearance, but with the ridges covering more of the stems and distinctive ridged gonopores. *Ectopleura* spp. was characterized by large, fleshy pink polyps and thick stems. Knobby club-like polyps and larger knobby gonopore clumps were characterized as *Sarsia* spp.

In addition, zooplankton samples were taken weekly from 30 m (the maximum net-depth to both sites) to the surface with a tow net (50 cm diameter x 200 cm length, 250 µm mesh) to identify and enumerate stinging plankton species.

2.2.3.1. Sample preservation

After being received at the facility in Campbell River, the net pieces and contents of the shipping bags were immediately placed individually in holding containers (17 x 25 x 25 cm, 5.61 L) with lids and air stones and topped up with 40-µm filtered seawater. Each net was removed from its holding container and tapped gently to remove excess water. The total (net plus biofouling community) wet weight was recorded, and a photograph of the net patch taken before the net was transferred to a MgCl anaesthesia bath (300mL of MgCl crystals dissolved in 3 L of 40-µm filtered seawater). The net patch remained in the bath for at least 3 minutes as per pre-established protocol (R. Greiter-Loerzer, DFO, pers. comm.). Hydroids were removed from the net patch, identified to genus, and their wet weight recorded. All hydroids were collected into a separate container and fixed with 3.7% formalin. The water remaining in the holding container was filtered through a pre-weighed 250 µm sieve to collect anything that had fallen off the net

patch, and the sieve plus biofouling wet weight was recorded.

After approximately 3 minutes in the MgCl solution, the net patch was gently shaken in the bath to dislodge any attached invertebrates and removed to a large bin to be rinsed. The bath water was filtered through a 40 µm sieve and added to the contents of the 250 µm sieve (see above). The MgCl bath water was periodically changed, depending on how much organic debris (e.g., algae, biofilms, etc.) was on the samples. The net was rinsed using a spray hose with fresh tap water and any remaining debris was removed by hand. The cleaned net was tapped gently in the bin to remove excess water and the clean net wet weight was recorded. This weight was subtracted from the net plus biofouling wet weight to give the wet weight of the foulants on the net. The wet weight of the foulants on the net was then added to the weight of the material collected from the holding container (sieve plus biofouling). To obtain the total wet weight of biofoulants the dry weight of the sieve (recorded first thing each morning before sample processing) was subtracted from this total (Figure 2.3).

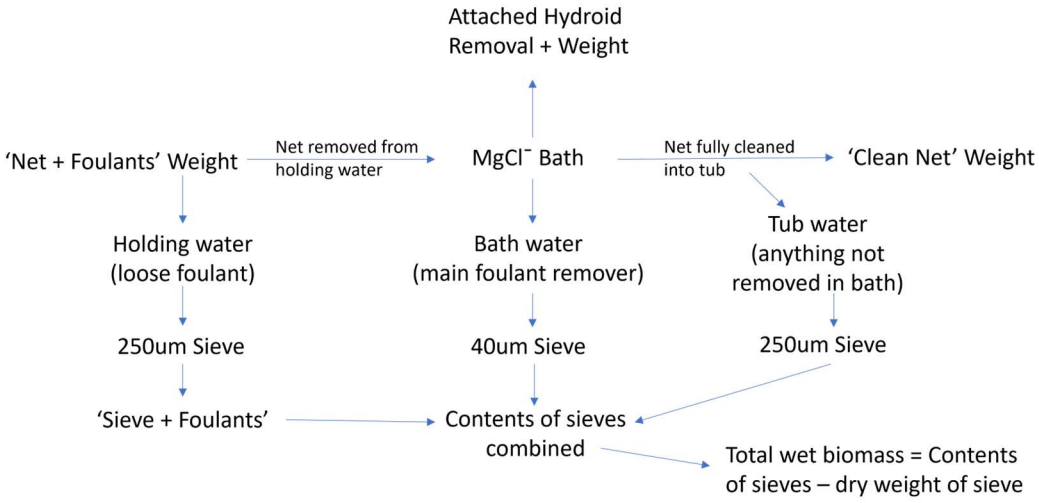

Figure 0.3: Net patch biofoulant collection and cleaning workflow to obtain biofoulant and hydroid wet weights (biomass in grams). Hydroids are collected into a separate container for further processing.

The removed biofoulants were then collected into a 100 mL container. The samples were topped up to an appropriate level with filtered seawater and 37% formalin was added using a bulb pipet in an appropriate amount to dilute to 3.7% (e.g., 20 mL of sample + seawater and 2 mL of formalin).

2.2.3.2 Sample analysis

To analyse the biofouling community structure of the net patches, the preserved contents of the containers were poured through a 60-µm sieve, collecting the formalin into a separate container to be re-added after processing, and the contents were rinsed with fresh water until most or all the formalin was removed. The amount of rinsing depended on how much organic debris (e.g., biofilm, algae, or other organic material) remained in the sample. The cleaned samples were poured into a Bogorov chamber and analyzed under a stereomicroscope with photographs taken of any remaining pieces of hydrozoans or anything else of note. All individuals were identified to the appropriate specificity and enumerated. When counting was completed, samples were poured through a 60-µm sieve again to remove excess fresh water and topped up to the appropriate amount of seawater before re-adding the formalin.

The zooplankton tow samples were cleaned using the same method as the community structure analysis. Species were identified as either present or absent or were individually counted in the case of stinging plankton (i.e., jellyfish, hydroid heads, siphonophores, etc.). Non-stinging species identified as present were not counted due to the lack of evidence that the commonly occurring free-swimming arthropods (mostly copepods or zoea) and other animals (i.e., polychaetes or chaetognaths) present in this study contribute to gill-health related issues directly (via contact) or indirectly (secondary vectors or disease).

In addition, a *post hoc* examination of the collected hydroids was done to identify any cryptic species growing on the net patch samples.

2.2.4. Statistical models

All statistical analyses were implemented in R (R Core Team, 2021). I used generalized linear models (GLMs) and generalized linear mixed models (GLMMs) to examine the effects of the environmental parameters on net-biofoulant counts (grams of hydroid species) and stinging-capable species present in tow samples (counts), using the glmmTMB and MASS packages (Brooks et al., 2017; Venables and Ripley, 2002). The basic structure of a GLM contains three parts: the linear predictor, the error structure, and the link function.

$$\eta_i = \alpha + \beta_1 X_{pi} + \cdots + \beta_p X_{pi}$$

Where η is the linear predictor for each point i of some linear function of the explanatory variables X_{pi}, intercept α, and slope β_p, from 1 to p explanatory variables. The appropriate error structure depends on the type of data of the response variable. In this case, the biofoulant count and tow sample count data use a negative binomial error structure and the mass of hydroids on net samples uses a normal or Gaussian distribution. The link function links the fitted values of the linear predictors to the scale of the original response variable. When using the normal distribution, the identity link is used, meaning predicted values are automatically converted on the original scale of the response variable. When using the negative binomial distribution, the log link is used to ensure the predicted counts are only positive (Buckley, 2015).

GLMMs are like GLMs in basic structure, but they can further handle much more complex models involving both fixed and random predictor variables (hence mixed models). The main downside of GLMMs is their generality and how easy it can be to build an overly complex

model that still indicates plausibility. These models recognize that with groups of collected samples there will be variation within (σ^2_{within}) and among (σ^2_{among}) groups, with the total variation being the sum $\sigma^2_{within} + \sigma^2_{among} = \sigma^2_{total}$. As such, the correlation between any two data points within the same group can be calculated as $\rho = \sqrt{\sigma^2_{among}/\sigma^2_{total}}$. These values are the deviations from the mean of the population for each group and are called random effects (Kain et al., 2015).

Highly correlated variables were identified using correlation plots and removed to prevent issues with collinearity in the models. Factor variables (e.g., depth) and random effects were tested for significance using likelihood ratio testing and further variable selection was done using small-sample corrected Akaike information criterion (AICc) for each of the sets of models for each site. A separate model was developed for each site due to the differences in geography, ecology, and because factors with 5 or less levels (i.e., only two sites were studied here) are not recommended to be used as a random predictor (Kain et al., 2015; Midway, 2022). All environmental data were scaled and centered to a mean of 0 to minimize the variation caused by differing measurement scales.

2.2.4.1 Biofoulant counts (excluding hydroids) on net patches and diversity indices

I developed a GLMM to analyze the effect of environmental parameters on biofoulant species counts growing on each net patch for each site. To account for any variation across each sampling date, I created a grouping variable "Event Day" (starting at day 1 when the first nets were deployed) and this variable was used as a random effect where appropriate. For the Doctor Islets site, I used dissolved oxygen, iron, nitrate levels, pH, phosphate levels, salinity, silica, temperature, and depth (represented as a factor with levels 1, 5, 10, 15, and 20 m). For the

Wicklow Point model, I used dissolved oxygen, iron, nitrate levels, ammonia, salinity, and depth.

To examine the trends of the diversity of the biofouling community on the net patches, the mean Shannon-Weiner index and mean (Gini) Simpson index were calculated for each depth of each sample collection date. The species richness (total number of species recorded each sample date) and total abundance (total individuals for each sample date) were also calculated for each depth and each sample date. The Shannon-Weiner diversity index considers species richness and total abundance to give a metric of species evenness in a sample, with higher values indicating more diversity (Keylock, 2005). The Simpson index (or Gini-Simpson index) is a dominance index that measures the probability that two randomly selected individuals in a sample will belong to different species, giving more weight to common or dominant species than the Shannon-Weiner index (Keylock, 2005).

To examine the relationships between the environmental variables, I built a GLM(M) for each index at each site. For species richness at Doctor Islets, I used pH; at Wicklow Point I used phosphate levels. For total abundance at Doctor Islets, I used depth, phosphate levels, salinity, silica, and temperature. At Wicklow Point I used salinity, ammonia, nitrate levels, phosphate levels, silica, iron, pH, and depth. For the Shannon-Wiener index at Doctor Islets I used depth, ammonia, and nitrate levels; at Wicklow Point I used temperature, dissolved oxygen, silica, and depth. For the Simpson indices at Doctor Islets, the model with the lowest AICc suggested only depth, the Event Day variable, and no continuous variables. At Wicklow Point I used temperature, dissolved oxygen, silica, and depth.

2.2.4.2. Hydroid species on net patches

To examine the effects of environment parameters on the biomass of hydroid species

(*Obelia* sp., *Ectopleura* sp., *Sarsia* sp., and *Clytia* sp.) growing on the net patches, I developed a GLM for the Doctor Islets site and a GLMM for the Wicklow Point site. I investigated continuous variables (dissolved oxygen, iron, ammonia, nitrate levels, pH, phosphate levels salinity, silica, and temperature) and one categorical variable (species: four levels of species identified) in the Doctor Islets model. For Wicklow Point, I used iron, ammonia, nitrate levels, pH, silica, and the species categorical variable.

To examine if any interactions between *Obelia* spp. (the dominant species for the study period) and the other hydroids groups (*Clytia* spp., *Ectopleura* spp., and *Sarsia* spp.), a four-level factor was created for each species. This factor was tested in the same way that depth was tested, and when significant (which was true for both sites), used the intercept of *Obelia* spp. as the reference.

2.2.4.3. Stinging-capable species in tow samples

To assess the effects of environmental parameters on the counts of stinging-capable plankton in the 30 m tow samples I developed a GLMM for both sites. For Doctor Islets ammonia, nitrate levels, and the Event Day variable were used. For Wicklow Point I used ammonia and the Event Day variable.

2.3. Results

2.3.1. Environmental profiles

Average temperatures (Figure 2.4A) were higher at Doctor Islet than Wicklow Point with means of 10.5˚C and 9.66 ˚C, respectively and there was more daily variation at Doctor Islet than Wicklow Point. The dissolved oxygen readings decreased at both sites over the sampling season

(Figure 2.4B) and Wicklow Point had lower levels of dissolved oxygen on average with few exceptions (Table 2.1).

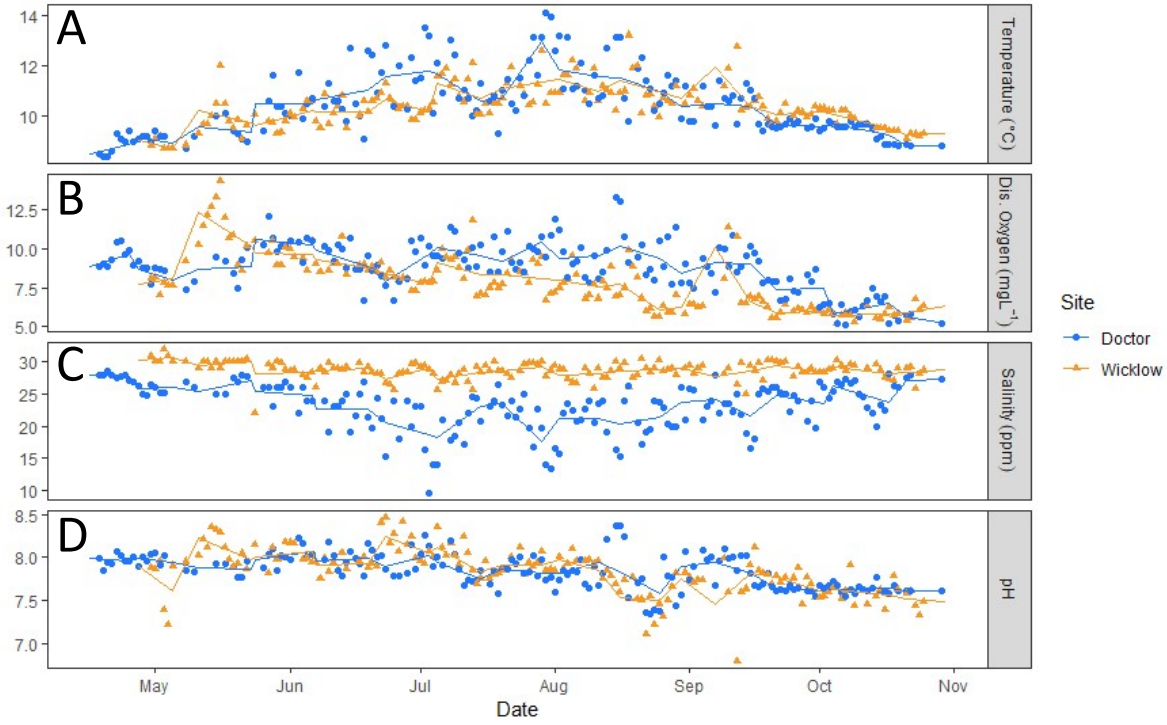

Figure 0.4 A-D: Physical water variables: temperature (˚C), dissolved oxygen (mgL-1), salinity (ppm), and pH of Doctor Islets and Wicklow Point from April 18 to October 29, 2020. Points are individual measurements and lines are weekly averages.

Table 0.1: Environmental profile ranges for Doctor Islets and Wicklow Point of temperature (˚C), dissolved oxygen (mgL^{-1}), salinity (ppm), and pH.

Site	Temperature (˚C)	Dissolved Oxygen (mgL^{-1})	Salinity (ppm)	pH
Doctor Islets	8.4-14.1	5.1-13.3	9.6-28.5	7.5-8.37
Wicklow Point	8.7-13.2	5.2-14.4	22.0-32.0	6.79-8.47

Salinity levels were markedly more stable at Wicklow Point than those at Doctor Islets

(Figure 2.4C; Table 2.1). Salinity levels were lower in the warmer months at Doctor Islet, higher during the cooler months, and a series of higher than usual levels occurred late-July and August. The seasonal pattern of pH was similar at both sites for the duration of the sampling season with both sites experiencing a steady decrease (Figure 2.4D; Table 2.1). The average pH levels were 7.84 at Doctor Islets and 7.32 at Wicklow Point.

Ammonia levels were mostly low for both sites with a sharp drop after October (Figure 2.5A; Table 2.2). The average levels were 0.126 gL^{-1} and 0.100 gL^{-1} at Doctor Islet and Wicklow Point, respectively. The nitrate levels for both sites remained generally stable until July before increasing at a steady rate for the rest of the season (Figure 2.5B; Table 2.2). Phosphate levels varied between the two sites until the end of August before dropping sharply at both sites to near-zero and remaining there with little variation until the end of the sampling periods (Figure 2.5C; Table 2.2). Silica measurements at both sites saw some variation over the sampling season, with a stable average until mid-late September before the levels started to increase for the rest of the season (Figure 2.5D; Table 2.2). The levels of iron measured at both sites show no discernable patterns through the sampling season and varied widely; however, both Doctor Islet and Wicklow Point had several high and low measurements in common (Figure 2.5E; Table 2.2). The average value for Doctor Islet was 2.47 gL^{-1} and 2.59 gL^{-1} for Wicklow Point.

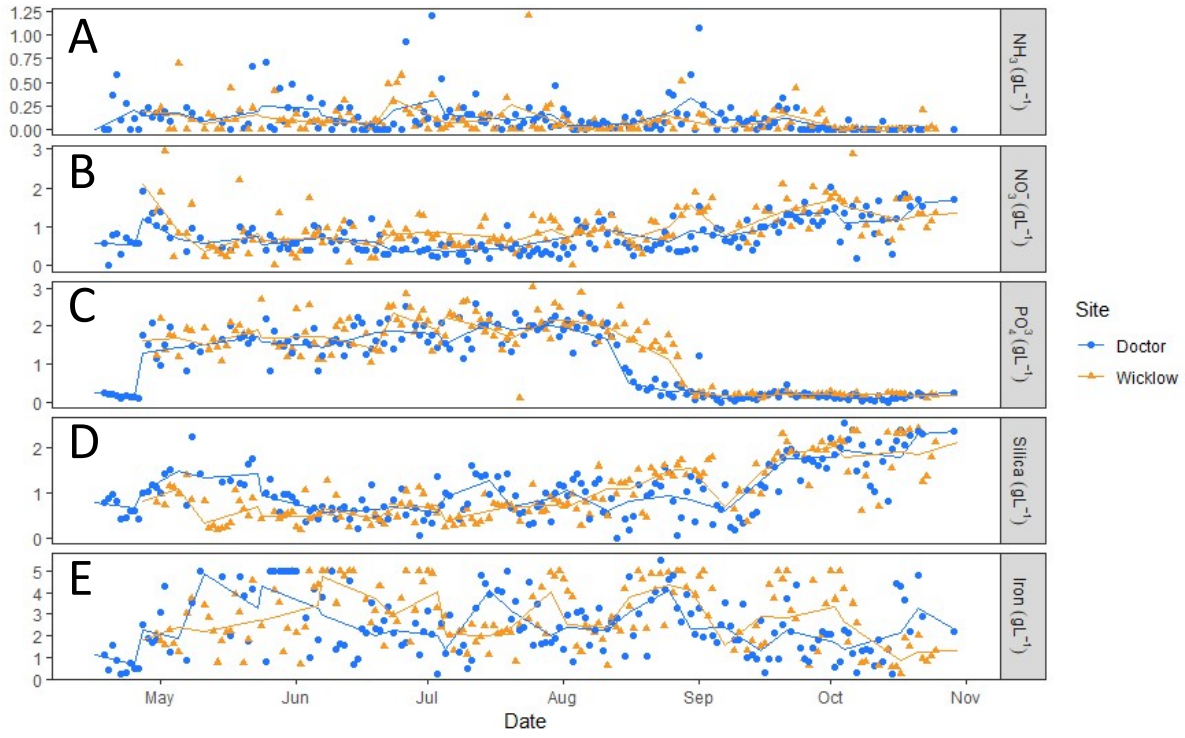

Figure 0.5 A-E: Nutrient water parameters: ammonia (gL^{-1}), nitrate levels (gL^{-1}), phosphate levels (gL^{-1}), silica (gL^{-1}), and iron(gL^{-1}) of Doctor Islets and Wicklow Point from April 18 to October 29, 2020.

Table 0.2: Nutrient profile ranges for Doctor Islets and Wicklow Point of ammonia (NH3 [gL^{-1}]), nitrates (NO-3 [gL^{-1}]), phosphates (PO43 [gL^{-1}]), silica (gL^{-1}), and iron (gL^{-1}).

Site	Ammonia (gL^{-1})	Nitrate (gL^{-1})	Phosphate (gL^{-1})	Silica (gL^{-1})	Iron (gL^{-1})
Doctor Islets	0.000-1.200	0.000-2.024	0.00-2.60	0.18-2.45	0.22-5.54
Wicklow Point	0.000-1.212	0.000-2.948	0.00-3.02	0.00-2.55	0.22-5.03

2.3.2. Biofoulant composition

2.3.2.1 Net patch compositions

Species composition on the net-samples deployed at Doctor Islets (Figure 2.6A) were

largely dominated by Arthropoda and Mollusca, with most deployments showing a general increase in Arthropoda composition with depth. Species composition at Wicklow Point (Figure 2.6B) was largely dominated by Arthropoda at almost all deployments and depths. Wicklow Point had a greater variety of species than Doctor Islets, but unlike Doctor Islets, there was no discernable pattern of composition by depth.

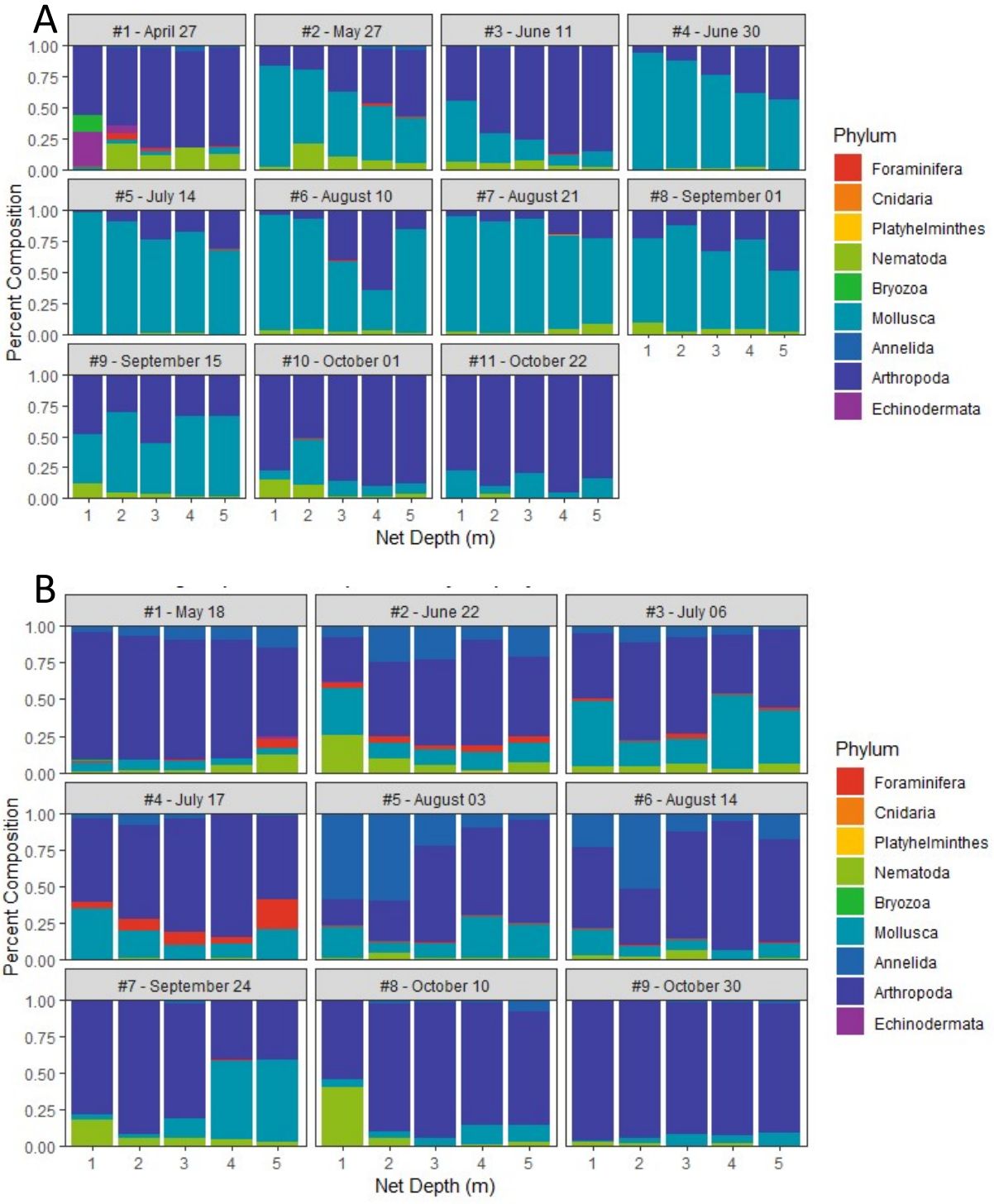

Figure 0.6 A-B: Average species (grouped by phylum) composition of biofouling net patches by depth (1, 5, 10, 15, and 20 m) and sampling date for Doctor Islets (A) and Wicklow Point (B).

To get a broader look at the compositions of the entire sampling seasons, I examined the monthly count summaries of the classes of species found on the net-samples. Doctor Islets (Figure 2.7) had large counts of bivalves (mostly *Mytilus* sp.) for most of the sampling season, tapering off in numbers near the end of the study (September-October). Maxillopoda (copepods, harpactacoids, etc.) and to a lesser extent, Malacostraca (crabs, shrimp, etc.) were both counted in larger numbers for the entire duration of the sampling season. Other classes that were common for the entire duration but in not usually more than a few dozen individuals were Thecostraca (barnacles), Ostracoda (seed shrimp), Gastropoda (snails), and Polychaeta and Nematoda (bristle and round worms). Wicklow Point (Figure 2.7) had similar compositions with high counts of Maxillopoda and Bivalvia that tapered off towards the end of the sampling season. Smaller, but consistent, counts of Ostracoda, Malacostraca, Gastropoda, Polychaeta, and Nematoda were seen, with no definite pattern to numbers of individuals across the months.

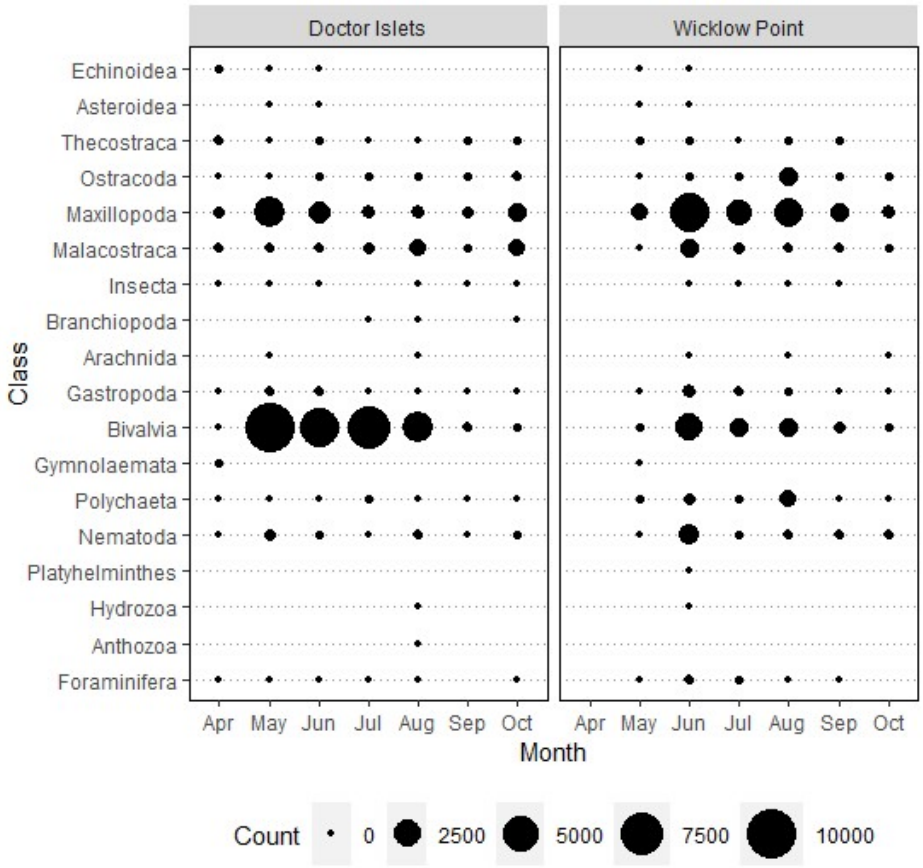

Figure 0.7: Total count summaries of biofouling net patches by month of species (grouped by class) for Doctor Islets and Wicklow Point.

2.3.2.2. Diversity indices

Figures 2.8 and 2.9 show the species richness (A), total abundance (B), mean Shannon-Wiener index value (C), and mean Simpson index value (D) for each depth of each net patch sampling date. Some general trends are similar between the two sites; species richness gradually decreases through the study period with peak richness in late spring (May 22 and June 22 at Doctor Islets and Wicklow Point, respectively), and total abundance at each site also peaked in these samples before decreasing through the study period. All the diversity indices show more

variation between depths at Doctor Islets than at Wicklow Point.

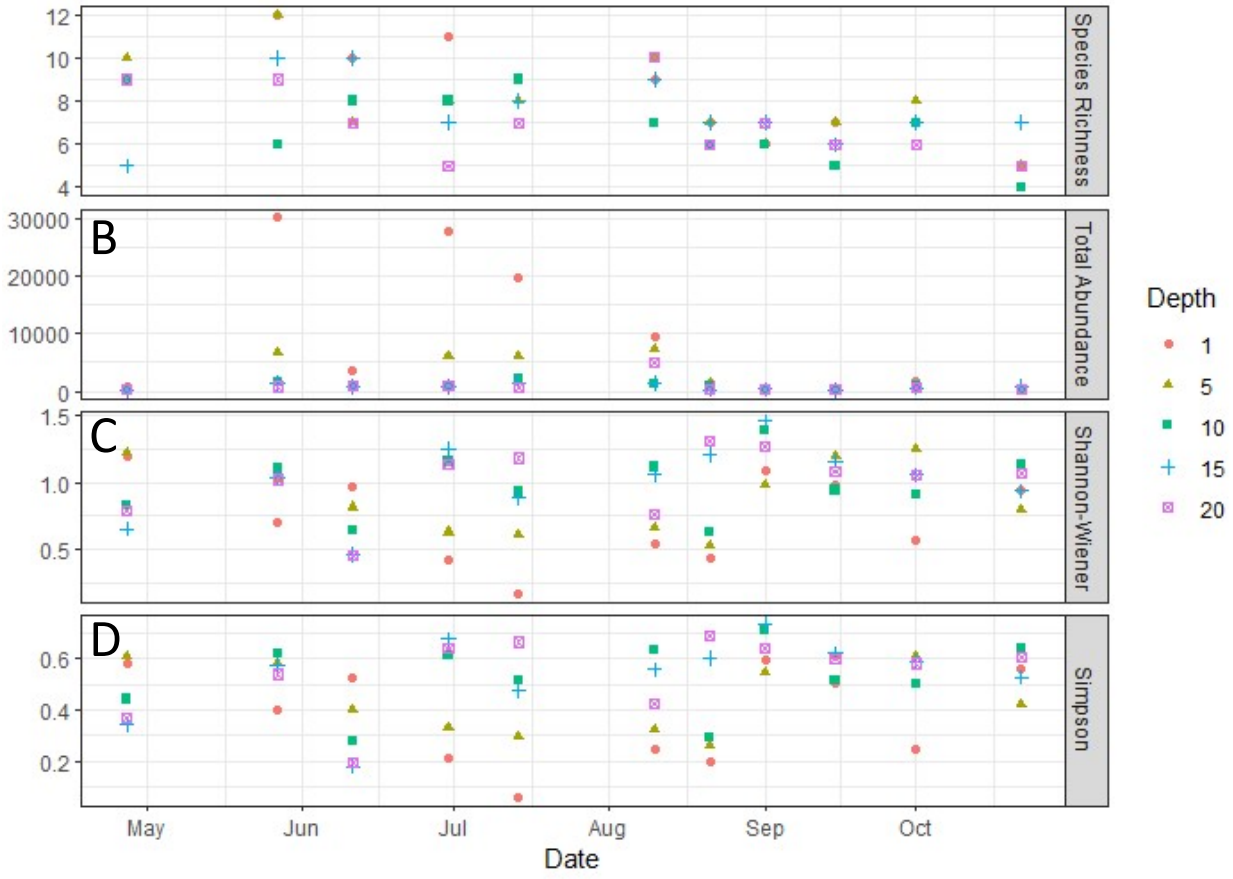

Figure 0.8 A-D: Diversity indices (species richness, total abundance, Shannon-Wiener diversity index, and Simpson index) by depth (1, 5, 10, 15, and 20 m) for each sampling date (denoted by a point) of biofouling counts on net patches for Doctor Islets.

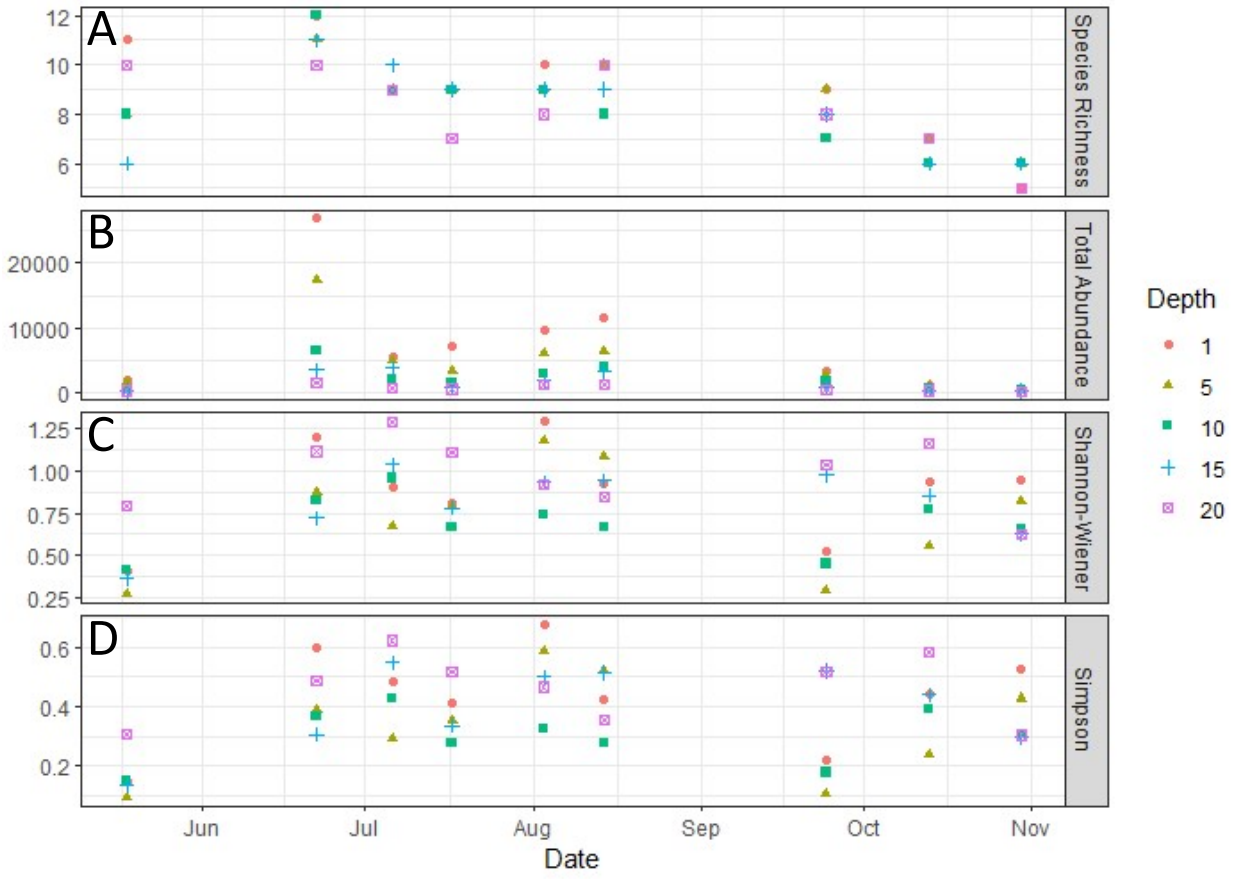

Figure 0.9 A-D: Diversity indices (species richness, total abundance, Shannon-Wiener diversity index, and Simpson index) by depth (1, 5, 10, 15, and 20 m) for each sampling date (denoted by a point) of biofouling counts on net patches for Wicklow Point.

At Doctor Islets there is a lot of variation of species richness between depths, with no gradient or pattern evident. Richness is highest at 1 m until August before it decreases and remains stable with the other depths until the end of the study period. The other depths (5, 10, 15, and 20 m) vary widely in richness between samples throughout the study period until August, before becoming more stable and gradually decreasing until the end of the study period. At Wicklow Point, there is an evident gradient in species richness, with more species at shallower

depths, with few exceptions. Richness is highest for all depths in June, before gradually decreasing. Species richness at 20 m is the exception, with higher richness near the beginning of the study, dipping to a low point in July, increasing again until August and then gradually decreasing until the end of the study.

The total abundance at Doctor Islets is much higher at 1 m for more of the study period than any other depth by several tens of thousands of individuals. The total abundance of all depths drops sharply late-August and remains low for the rest of the study period. At Wicklow Point, there is a much more even gradient with depth. Similar to species richness, there was a peak in total abundance in June before gradually decreasing until the end of the study period.

The Shannon-Wiener diversity index and Simpson index show nearly identical trends to each other at each depth, within each site. At Doctor Islets at 1 m, the indices started high, decreased until late July, and increased again until the end of the study period. The other depths for both indices followed an interesting gradient in that if the index value at 1 m was low, the 5 m value was slightly higher etc. until the highest value, indicating highest evenness and the highest probability that any two individuals would be of two different species was usually from the 15 m or 20 m samples. This was true in the opposite direction as well, where when the 1 m sample value was high, the 5 m was slightly lower, etc. At Wicklow Point, for both the Shannon-Wiener and Simpson indices, 1 m and 20 m had the highest values, periodically switching through the sampling period. The indices showed similar peaks at 5 m, 10 m, and 15 m and dips as the 20 m sample and generally in a gradient from 5 m to 15 m, with some exception to this variation.

2.3.2.3. Hydroids on net patches

Obelia spp. complex was the most common species recorded on the net patches throughout the study period at both Doctor Islets (Figure 2.10A) and Wicklow Point (Figure 2.10B), with no evident distribution pattern by depth or deployment date. *Ectopleura* spp. was only found at Doctor Islets (August 10 & 21, October 01 & 22), *Clytia* spp. was only found at Wicklow Point (July 31), and *Sarsia* spp. was found in small amounts at both sites (September-October at Doctor Islets, and throughout July at Wicklow Point).

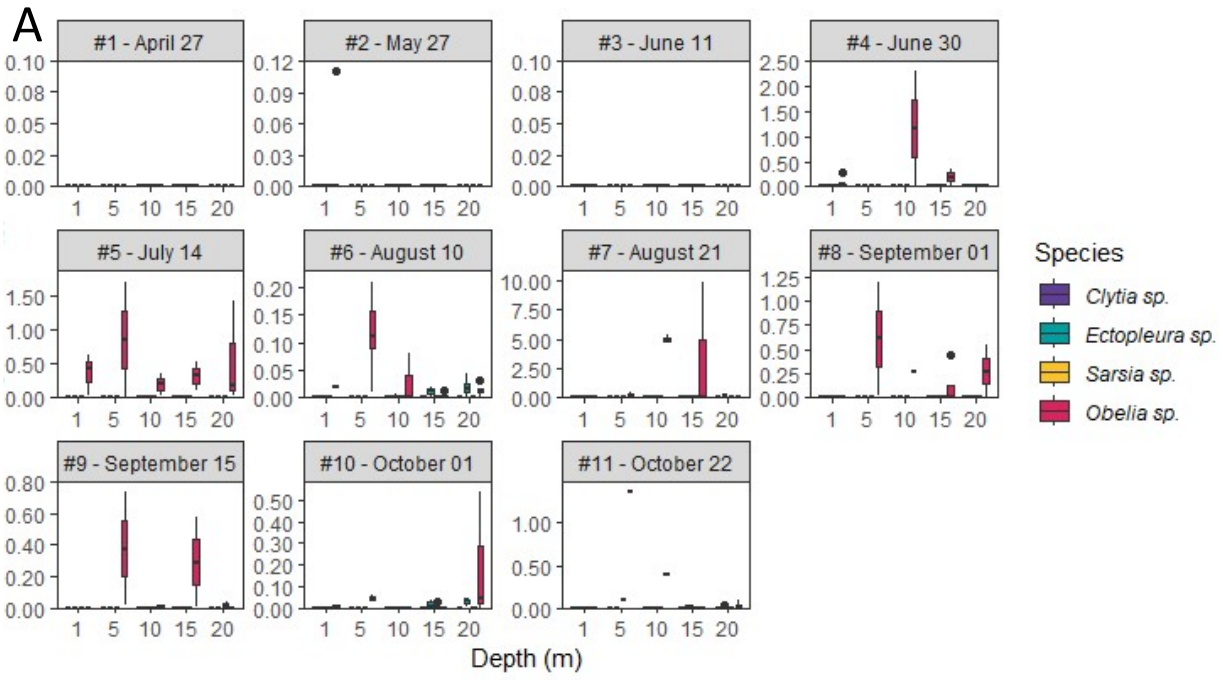

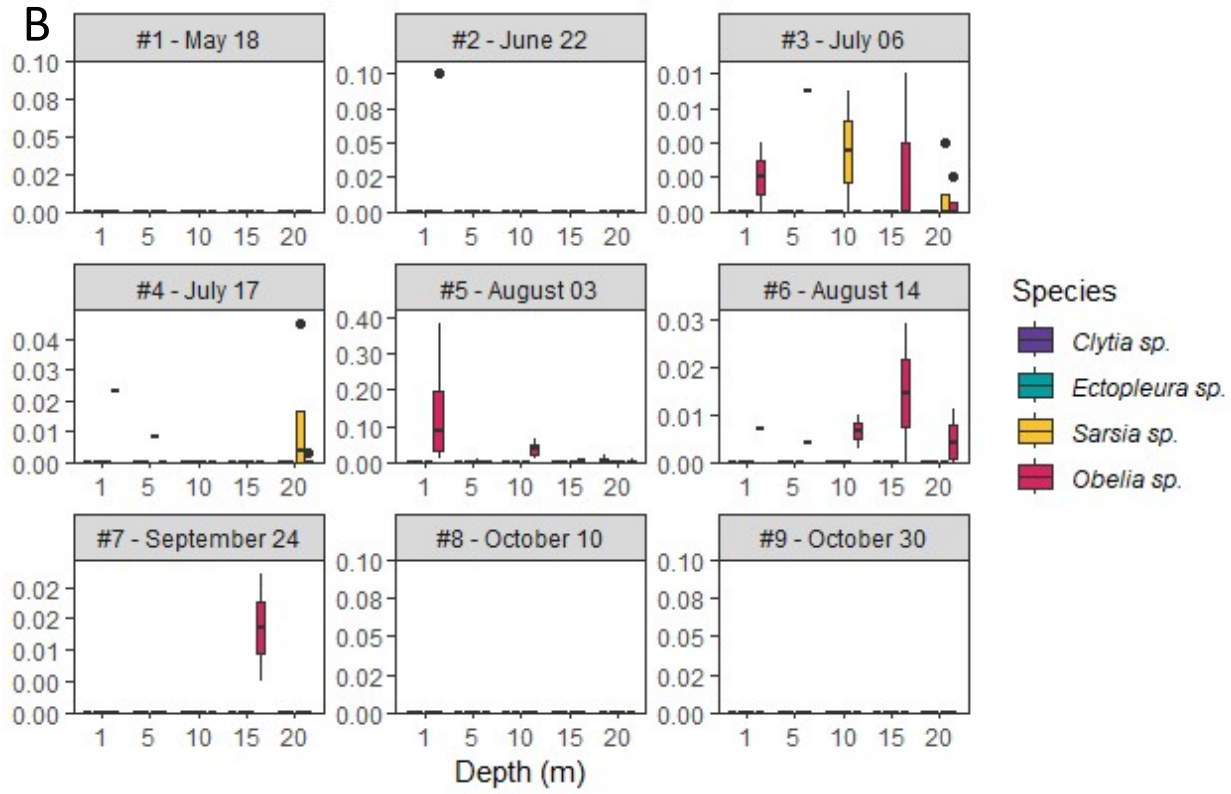

Figure 0.10 A-B: Biomass (g) of hydroid species (grouped by genus) by depth (1, 5, 10, 15, and 20 m) and sampling date for Doctor Islets (A) and Wicklow Point (B).

For the duration of the study *Obelia* species were dominant on the net patches at both sites, sometimes being the only species collected. Both sites had a peak in biomass during August and September. I collected more *Obelia* at Doctor Islets (Figure 2.11A), with a maximum mass of 9.904 g from a single net patch. In contrast, the maximum mass recorded at Wicklow Point (Figure 2.11B) was only 0.382 g. I collected *Sarsia* sp. at both sites in small amounts from September to November (maximum: 0.082 g Doctor Islets), and July-August (maximum: 0.045 g at Wicklow Point). *Ectopleura* sp. was only collected in small amounts at Doctor Islets from August to October with a maximum mass of 0.189 g, and *Clytia* sp. was only collected at Wicklow Point in a single sample in August with a mass of 0.021 g.

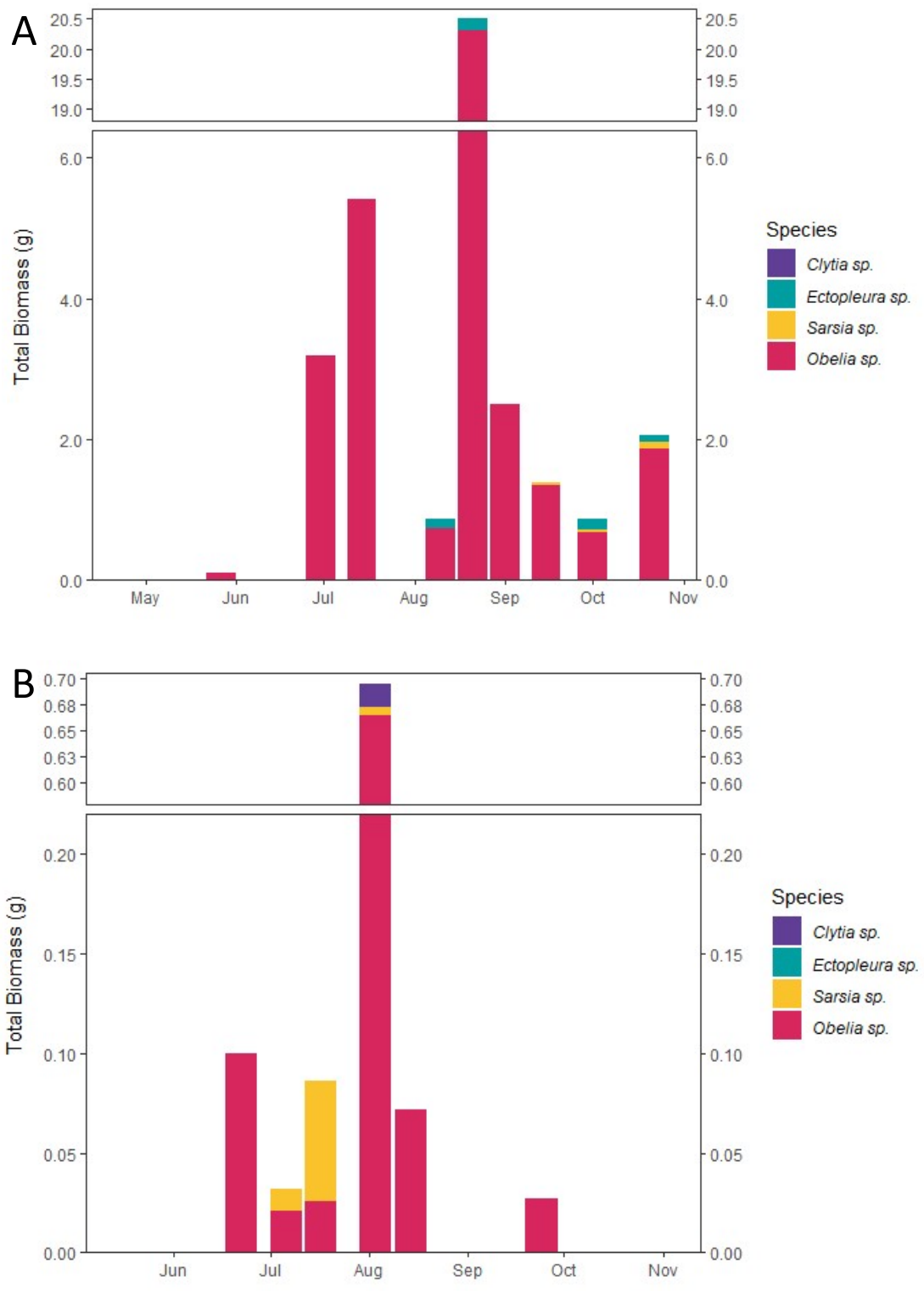

Figure 0.11 A-B: Total biomass (g) of hydroids (grouped by genus) for each sampling date at Doctor Islets (A) and Wicklow Point (B).

2.3.2.4. Stinging-species in tow samples

In the count summary of the stinging-species in the tow samples for both Doctor Islets and Wicklow Point (Figure 2.12) I recorded *Obelia* species (usually free-swimming medusa form) as the most numerous stinging-capable species in the water column for several, but not all months. Other common species seen were Diphydae (usually *Lensia* sp. or *Diphyes* sp.) and *Muggiaea* species (both of class Siphonophora), and *Clytia* species, which were separated into diameter (>10 mm and <10 mm). *Clytia* sp. were separated into diameter for ease of counting and because I noticed that while the two sizes (arbitrarily decided at 10 mm due to the grid size of the Bogorov chamber used to examine and enumerate the samples) were often concurrent, when the species would bloom only one of the two sizes would be present in high numbers. At Doctor Islets I recorded a general trend of larger counts early (May-June) and late (October), and a general trend of larger counts early (May-June) for Wicklow Point, with fewer species and smaller counts near the end of the study.

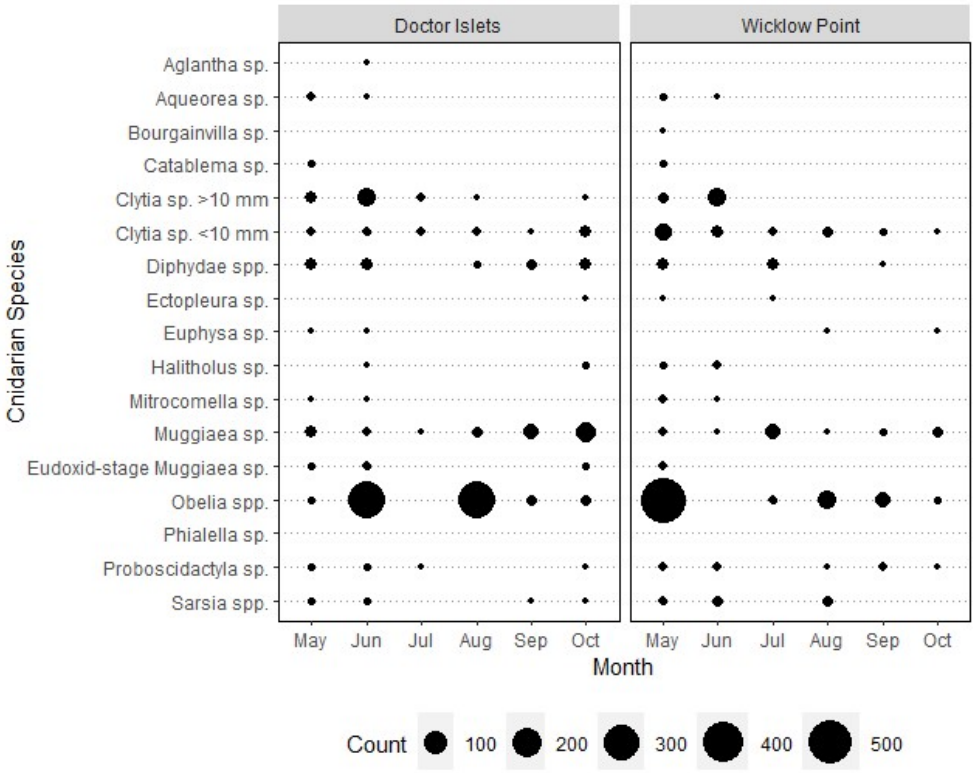

Figure 0.12: Total count summaries of stinging-capable species in tow samples by month at Doctor Islets and Wicklow Point.

2.3.3. Statistical model results

2.3.3.1. Correlation of water parameters with biofoulant counts and diversity indices

Correlation plots used to aid model selection for this section can be found in the appendix (Figures A2.1 and A2.2). For the Doctor Islets model each unit-increase of temperature, dissolved oxygen, salinity, and phosphate levels was associated with an increase of log-expected mean counts (Table 2.3). With each unit increase of nitrate levels, iron, and pH the mean counts were expected to decrease. Silica had the largest effect size of the positive correlations and iron had the largest effect size of the negative correlations. Depth was found to be a significant factor (Table 2.4) and with each increase in depth, the log of expected species counts decreased.

Table 0.3: Regression summary of the models with the lowest AICc examining environmental parameters on net patch biofoulant counts for Doctor Islets and Wicklow Point. S.e. is the standard error and 95% is the confidence interval.

	Doctor Islets	Wicklow Point
Intercept	3.687, s.e.=0.135, 95%=[3.423,3.951]	4.268, s.e.=0.134, 95%=[4.004,4.531]
Temperature	0.978, s.e.=0.182, 95%=[0.621,1.336]	0.203, s.e.=0.173, 95%=[-0.135,0.542]
Dissolved Oxygen	1.492, s.e.=0.352, 95%=[0.803,2.181]	-4.268, s.e.=0.760, 95%=[-5.757,-2.778]
Salinity	1.026, s.e.=0.195, 95%=[0.644,1.408]	0.810, s.e.=0.303, 95%=[0.215,1.405]
Ammonia		-7.927, s.e.=1.413, 95%=[-10.697,-5.156]
Nitrate	-0.539, s.e.=0.132, 95%=[-0.797,-0.281]	5.435, s.e.=0.955, 95%=[3.563,7.307]
Phosphate	1.012, s.e.=0.139, 95%=[0.738,1.285]	
Silica	1.797, s.e.=0.228, 95%=[1.350,2.244]	
Num.Obs.	4788	3384

Table 2.3: Continued.

	Doctor Islets	Wicklow Point
Intercept	3.687, s.e.=0.135, 95%=[3.423,3.951]	4.268, s.e.=0.134, 95%=[4.004,4.531]
Iron	-1.031, s.e.=0.196, 95%=[-1.415,-0.647]	3.493, s.e.=0.667, 95%=[2.186,4.800]
pH	-0.393, s.e.=0.225, 95%=[-0.834,0.049]	7.364, s.e.=1.286, 95%=[4.842,9.885]
Depth 5 m	-0.897, s.e.=0.185, 95%=[-1.259,-0.536]	-0.413, s.e.=0.188, 95%=[-0.782,-0.045]
Depth 10 m	-1.427, s.e.=0.195, 95%=[-1.809,-1.046]	-1.156, s.e.=0.190, 95%=[-1.529,-0.784]
Depth 15 m	-1.572, s.e.=0.196, 95%=[-1.956,-1.188]	-1.467, s.e.=0.192, 95%=[-1.844,-1.089]
Depth 20 m	-1.527, s.e.=0.194, 95%=[-1.906,-1.147]	-2.218, s.e.=0.188, 95%=[-2.588,-1.849]
Num.Obs.	4788	3384

Table 0.4: Model selection using a generalized linear mixed-effects model with a log link function to describe the effect of water parameters on net patch biofoulant counts for Doctor Islets. The model with the lowest AICc used the terms: dissolved oxygen, iron, nitrate levels, pH, phosphate levels, salinity, silica, temperature, and depth which is a 5-level factor representing each depth net patches were collected from (1, 5, 10, 15, and 20 m). The column "Random" represents the presence (+) or absence ( ) of the random grouping effect. NEG.BINOMIAL and POISSON denote the testing of distributions with the full model. In this model the negative binomial distribution was more appropriate.

Model	Random	df	logLik	AICc	delta	weight
Depth+Temp+DOmgL+Salinity+NO3+PO43+Silica+Iron+pH		14	-8,768.35	17,564.78	0.00	0.46
Depth+Temp+DOmgL+Salinity+NO3+PO43+Silica+Iron		13	-8,769.87	17,565.81	1.03	0.28
Depth+Temp+DOmgL+Salinity+NH3+NO3+PO43+Silica+Iron+pH		15	-8,768.21	17,566.51	1.73	0.19
NEG.BINOMIAL EventDay+Depth+Temp+DOmgL+Salinity+NH3+NO3+PO43+Silica+Iron+pH	+	16	-8,768.21	17,568.52	3.74	0.07
Depth+DOmgL+Salinity+NO3+PO43+Silica+Iron		12	-8,793.30	17,610.67	45.89	0.00
Depth+Temp+DOmgL+Salinity+pH		10	-8,813.99	17,648.02	83.24	0.00
EventDay+Temp+DOmgL+Salinity+NH3+NO3+PO43+Silica+Iron+pH		11	-8,816.66	17,655.38	90.60	0.00
Depth		6	-8,883.17	17,778.36	213.58	0.00
POISSON EventDay+Depth+Temp+DOmgL+Salinity+NH3+NO3+PO43+Silica+Iron+pH	+	15	-406,853.43	813,736.96	796,172.18	0.00

For the Wicklow Point site model (Table 2.3) examining the counts of biofouling species, the log-expected mean counts on the sample nets increased with each unit-increase of salinity, nitrate levels, iron, and pH. The log-expected mean counts decreased with each increase of dissolved oxygen and ammonia. Of these variables, pH had the largest positive and total effect size and ammonia had the largest negative effect size. Depth was considered significant (Table 2.5) and had a negative effect that increased in size with each depth.

Table 0.5: Model selection using a generalized linear mixed-effects model with a log link function to describe the effect of water parameters on net patch biofoulant counts for Wicklow Point. The model with the lowest AICc used the terms: dissolved oxygen, iron, ammonia, nitrate levels, pH, salinity, and depth which is a 5-level factor representing each depth net patches were collected from (1, 5, 10, 15, and 20 m). The column "Random" represents the presence (+) or absence ( ) of the random grouping effect. NEG.BINOMIAL and POISSON denote the testing of distributions with the full model. In this model the negative binomial distribution was more appropriate.

Model	Random	df	logLik	AICc	delta	weight
Depth+DOmgL+NH3+NO3+Salinity+Iron+pH		12	-8,166.99	16,358.08	0.00	0.51
Depth+Temp+DOmgL+NH3+NO3+Salinity+Iron+pH		13	-8,166.32	16,358.76	0.68	0.36
NEG.BINOMIAL EventDay+Depth+Temp+DOmgL+NH3+NO3+Salinity+Iron+pH	+	14	-8,166.32	16,360.77	2.70	0.13
Depth+Temp+Salinity+Iron+pH		10	-8,182.84	16,385.74	27.67	0.00
Depth+Temp+DOmgL+NH3+NO3+pH		11	-8,182.56	16,387.20	29.12	0.00
Depth+DOmgL+NH3+NO3+Salinity+Iron+pH		11	-8,184.99	16,392.06	33.98	0.00
Depth		6	-8,238.07	16,488.16	130.08	0.00
EventDay+Temp+DOmgL+NH3+NO3+Salinity+Iron+pH		9	-8,242.78	16,503.61	145.53	0.00
POISSON EventDay+Depth+Temp+DOmgL+NH3+NO3+Salinity+Iron+pH	+	13	-322,976.47	645,979.04	629,620.96	0.00

In addition, the diversity indices of each net patch were examined in relation to water parameters. At Doctor Islets (Table 2.6), only pH was associated with a log-expected increase in species richness. This model is also one of the few in which depth was not a significant variable (Table 2.7). Total abundance was positively associated with temperature, phosphate levels, salinity, and silica, with temperature having the largest effect size. Depth was tested to be significant to the model structure and was negatively associated with the abundance (Table 2.8). For the Shannon-Wiener index values ammonia and nitrate levels were positively associated with higher index values, and no parameters were negatively associated. Depth was tested to be significant and had the largest effect sizes (Table 2.9). For the model examining the Simpson index values, none of the continuous variables were included in the selected model. Depth was tested to be significant and was positively associated with Simpson index values (Table 2.10).

Table 0.6: Regression summary of the models with the lowest AICc used to examine the environmental parameters on the species richness, total abundance, Shannon-Wiener diversity index, and Simpson index values calculated from the net patch biofoulant counts at Doctor Islets. S.e. is the standard error and 95% is the confidence interval.

	Species Richness	Total Abundance	Shannon-Wiener	Simpson Index
Intercept	2.011, s.e.=(0.050), 95%=[1.914,2.108]	8.323, s.e.=(0.205), 95%=[7.922,8.725]	0.730, s.e.=(0.073), 95%=[0.587,0.873]	0.375, s.e.=(0.045), 95%=[0.287,0.463]
Temperature		1.351, s.e.=(0.220), 95%=[0.919,1.783]		
Salinity		0.621, s.e.=(0.209), 95%=[0.211,1.031]		
Ammonia			0.070, s.e.=(0.034), 95%=[0.004,0.135]	
Nitrate			0.061, s.e.=(0.034), 95%=[-0.005,0.126]	
Phosphate		0.928, s.e.=(0.202), 95%=[0.532,1.324]		
Silica		0.887, s.e.=(0.230), 95%=[0.437,1.337]		
pH	0.141, s.e.=(0.049), 95%=[0.045,0.237]			
Depth 5 m		-1.042, s.e.=(0.280), 95%=[-1.591,-0.494]	0.154, s.e.=(0.103), 95%=[-0.048,0.355]	0.077, s.e.=(0.057), 95%=[-0.035,0.190]
Depth 10 m		-1.653, s.e.=(0.291), 95%=[-2.223,-1.083]	0.251, s.e.=(0.103), 95%=[0.050,0.453]	0.148, s.e.=(0.057), 95%=[0.036,0.261]
Depth 15 m		-1.730, s.e.=(0.295), 95%=[-2.309,-1.151]	0.288, s.e.=(0.103), 95%=[0.086,0.489]	0.159, s.e.=(0.057), 95%=[0.046,0.271]
Depth 20 m		-1.610, s.e.=(0.292), 95%=[-2.182,-1.038]	0.284, s.e.=(0.103), 95%=[0.082,0.486]	0.165, s.e.=(0.057), 95%=[0.052,0.277]
Num.Obs.	55	55	55	55

Table 0.7: Model selection using a generalized linear mixed-effects model with a log link function to describe the effect of water parameters on the species richness of the net-patches at Doctor Islets. The model with the lowest AICc used only pH. The column "Random" represents the presence (+) or absence ( ) of the random grouping effect.

Model	Random	df	logLik	AICc	delta	weight
pH		2	-113.88	231.98	0.00	0.69
Salinity+pH		3	-113.69	233.86	1.87	0.27
Salinity+Silica+Iron+pH		5	-113.47	238.16	6.17	0.03
Temp+Salinity+NH3+NO3+PO43+Silica+Iron+pH		9	-111.88	245.76	13.77	0.00
DOmgL+Salinity+NH3+NO3+PO43+Silica+Iron+pH		9	-112.17	246.33	14.35	0.00
Temp+DOmgL+Salinity+NH3+Silica+Iron+pH		9	-112.66	247.33	15.34	0.00
Temp+DOmgL+Salinity+NH3+NO3+PO43+Silica+Iron+pH		10	-111.83	248.66	16.68	0.00
Depth+Temp+DOmgL+Salinity+NH3+NO3+PO43+Silica+Iron+pH		14	-110.59	259.68	27.70	0.00
EventDay+Depth+Temp+DOmgL+Salinity+NH3+NO3+PO43+Silica+Iron+pH	+	15	-110.59	263.49	31.51	0.00

Table 0.8: Model selection using a generalized linear mixed-effects model with a log link function to describe the effect of water parameters on the total abundance of the net-patches at Doctor Islets. The model with the lowest AICc used terms temperature, salinity, phosphate levels, silica, and depth. The column "Random" represents the presence (+) or absence ( ) of the random grouping effect. NEG.BINOMIAL and POISSON denote the testing of distributions with the full model. In this model the negative binomial distribution was more appropriate.

Model	Random	df	logLik	AICc	delta	weight
Depth+Temp+Salinity+PO43+Silica		10	-437.34	899.67	0.00	0.65
Depth+Temp+DOmgL+Salinity+NH3+NO3+PO43+Silica+Iron+pH		15	-429.44	901.19	1.52	0.31
NEG.BINOMIAL EventDay+Depth+Temp+DOmgL+Salinity+NH3+NO3+PO43+Silica+Iron+pH	+	16	-429.44	905.20	5.53	0.04
Depth+Temp+DOmgL+Salinity+NH3+NO3		11	-442.59	913.32	13.64	0.00
Depth+NH3+NO3+PO43+Silica+Iron+pH		12	-442.81	917.05	17.37	0.00
Depth+Temp+DOmgL+Salinity+Silica+Iron+pH		12	-447.97	927.37	27.70	0.00
Temp+DOmgL+Salinity+NH3+NO3+PO43+Silica+Iron+pH		11	-449.73	927.60	27.92	0.00
Depth		6	-465.67	945.09	45.42	0.00
POISSON EventDay+Depth+Temp+DOmgL+Salinity+NH3+NO3+PO43+Silica+Iron+pH	+	15	-15,074.53	30,191.37	29,291.70	0.00

Table 0.9: Model selection using a generalized linear mixed-effects model with a log link function to describe the effect of water parameters on the Shannon-Weiner diversity index of the net-patches at Doctor Islets. The model with the lowest AICc used terms: ammonia, nitrate levels, and depth. The column "Random" represents the presence (+) or absence ( ) of the random grouping effect.

Model	Random	df	logLik	AICc	delta	weight
Depth+NO3+NH3		8	0.16	18.82	0.00	0.78
Depth		6	-4.21	22.17	3.35	0.15
Depth+NH3+NO3+PO43+Silica+Iron+pH		12	3.07	25.29	6.47	0.03
Depth+Temp+DOmgL+Salinity+NH3+NO3+PO43		12	2.80	25.82	7.00	0.02
Temp+DOmgL+Salinity+NH3+NO3+PO43+Silica+Iron+pH		11	0.25	27.63	8.81	0.01
Depth+Temp+DOmgL+Salinity+NH3+NO3+PO43+Silica+Iron+pH		15	6.55	29.20	10.38	0.00
EventDay+Depth+Temp+DOmgL+Salinity+NH3+NO3+PO43+Silica+Iron+pH	+	16	6.55	33.21	14.39	0.00
Depth+Temp+DOmgL+Salinity+Silica+Iron+pH		12	-1.33	34.10	15.28	0.00

Table 0.10: Model selection using a generalized linear mixed-effects model with a log link function to describe the effect of water parameters on the Simpson index of the net-patches at Doctor Islets. The model with the lowest AICc used no continuous variables but did include the depth variable. The column "Random" represents the presence (+) or absence ( ) of the random grouping effect.

Model	Random	df	logLik	AICc	delta	weight
EventDay+Depth		7	28.12	-39.86	0.00	0.53
EventDay+Depth+NO3		8	29.29	-39.45	0.41	0.43
Depth+Temp+DOmgL+Salinity+NH3+NO3+PO43+Silica+Iron+pH		15	37.99	-33.67	6.20	0.02
EventDay+Temp+DOmgL+Salinity+NH3+NO3+PO43+Silica+Iron+pH		12	31.37	-31.30	8.56	0.01
EventDay+Depth+NH3+NO3+PO43+Silica+Iron+pH		13	32.71	-30.54	9.33	0.00
EventDay+Depth+Temp+DOmgL+Salinity+NH3+NO3+PO43		13	32.30	-29.73	10.13	0.00
EventDay+Depth+Temp+DOmgL+Salinity+NH3+NO3+PO43+Silica+Iron+pH	+	16	37.99	-29.66	10.20	0.00
EventDay+Depth+Temp+DOmgL+Salinity+Silica+Iron+pH		13	30.59	-26.31	13.56	0.00

For the Wicklow Point model (Table 2.11), only phosphate was (positively) associated with species richness and depth was not significant (Table 2.12). For total abundance ammonia, phosphate levels, and silica were positively associated with a log-expected increase in abundance, and salinity, nitrate levels, iron, and pH were negatively associated. Depth tested significant (Table 2.13), and each depth was negatively associated with the effect sizes increasing with each depth. Ammonia had the highest positive effect size, and the depths had the highest negative effect sizes. For the Shannon-Wiener index of the net patches, temperature was significantly associated with an increase in index values, and dissolved oxygen and silica were negatively associated. Depth was significant (Table 2.14) and each depth except 20 m was negatively associated. Of the negatively associated variables, most of the depths had the highest effect sizes. Similarly, for the Simpson index, only temperature was positively associated, and dissolved oxygen and silica were negatively associated. Depth tested significant (Table 2.15), and each depth except 20 m was negatively associated.

Table 0.11: Regression summary of the models used to examine the environmental parameters on the species richness, total abundance, Shannon-Wiener diversity index, and Simpson index values calculated from the net patch biofoulant counts at Wicklow Point. S.e. is the standard error and 95% is the confidence interval.

	Species Richness	Total Abundance	Shannon-Wiener	Simpson Index
Intercept	2.174, 95%=(0.053), c.i.=[2.069,2.279]	8.650, 95%=(0.091), c.i.=[8.472,8.828]	0.876, 95%=(0.060), c.i.=[0.758,0.993]	0.426, 95%=(0.035), c.i.=[0.358,0.494]
Temperature			0.115, 95%=(0.032), c.i.=[0.052,0.179]	0.073, 95%=(0.019), c.i.=[0.036,0.110]
Dissolved Oxygen			-0.138, 95%=(0.036), c.i.=[-0.209,-0.066]	-0.083, 95%=(0.021), c.i.=[-0.124,-0.041]
Salinity		-0.388, 95%=(0.123), c.i.=[-0.630,-0.146]		
Ammonia		1.189, 95%=(0.151), c.i.=[0.892,1.486]		
Nitrate		-1.066, 95%=(0.228), c.i.=[-1.513,-0.620]		
Phosphate	0.116, 95%=(0.057), c.i.=[0.004,0.228]	1.141, 95%=(0.105), c.i.=[0.936,1.346]		
Silica		0.819, 95%=(0.175), c.i.=[0.475,1.163]	-0.107, 95%=(0.041), c.i.=[-0.187,-0.027]	-0.051, 95%=(0.024), c.i.=[-0.097,-0.004]
Iron		-0.812, 95%=(0.273), c.i.=[-1.346,-0.278]		
pH		-0.184, 95%=(0.297), c.i.=[-0.766,0.398]		
Depth 5 m		-0.373, 95%=(0.128), c.i.=[-0.624,-0.123]	-0.160, 95%=(0.084), c.i.=[-0.326,0.005]	-0.105, 95%=(0.049), c.i.=[-0.201,-0.009]
Depth 10 m		-1.169, 95%=(0.128), c.i.=[-1.421,-0.918]	-0.188, 95%=(0.084), c.i.=[-0.354,-0.022]	-0.127, 95%=(0.049), c.i.=[-0.224,-0.031]
Depth 15 m		-1.471, 95%=(0.130), c.i.=[-1.726,-1.216]	-0.049, 95%=(0.084), c.i.=[-0.215,0.116]	-0.014, 95%=(0.049), c.i.=[-0.110,0.083]
Depth 20 m		-2.151, 95%=(0.129), c.i.=[-2.404,-1.898]	0.158, 95%=(0.084), c.i.=[-0.008,0.323]	0.057, 95%=(0.049), c.i.=[-0.040,0.153]
Num.Obs.	40	40	40	40

Table 0.12: Model selection using a generalized linear mixed-effects model with a log link function to describe the effect of water parameters on the species richness of the net-patches at Wicklow Point. The model with the lowest AICc used only phosphate levels. The column "Random" represents the presence (+) or absence ( ) of the random grouping effect.

Model	Random	df	logLik	AICc	delta	weight
PO43		2	-83.42	171.17	0.00	0.70
Salinity+PO43		3	-83.37	173.40	2.23	0.23
Salinity+NH3+NO3+PO43		5	-82.37	176.51	5.34	0.05
NO3+PO43+Silica+Iron+pH		6	-82.48	179.50	8.32	0.01
Salinity+NH3+Silica+Iron+pH		6	-82.83	180.21	9.03	0.01
Salinity+NH3+NO3+PO43+Silica+Iron+pH		8	-82.27	185.19	14.02	0.00
Depth+Salinity+NH3+NO3+PO43+Silica+Iron+pH		12	-81.86	199.28	28.11	0.00
EventDay+Depth+Salinity+NH3+NO3+PO43+Silica+Iron+pH	+	13	-81.86	203.72	32.55	0.00

Table 0.13: Model selection using a generalized linear mixed-effects model with a log link function to describe the effect of water parameters on the total abundance of the net-patches at Wicklow Point. The model with the lowest AICc used terms: salinity, ammonia, nitrate levels, phosphate levels, silica, iron, pH, and depth. The column "Random" represents the presence (+) or absence ( ) of the random grouping effect. NEG.BINOMIAL and POISSON denote the testing of distributions with the full model. In this model the negative binomial distribution was more appropriate.

Model	Random	df	logLik	AICc	delta	weight
Depth+Salinity+NH3+NO3+PO43+Silica+Iron+pH		13	-306.08	652.15	0.00	0.83
Depth+NH3+NO3+PO43+Silica+Iron+pH		11	-312.55	656.52	4.37	0.09
NEG.BINOMIAL EventDay+Depth+Salinity+NH3+NO3+PO43+Silica+Iron+pH	+	14	-306.08	656.95	4.80	0.08
Depth+Salinity+NH3+NO3+PO43+Silica		11	-317.07	665.57	13.42	0.00
Depth+PO43+Silica+Iron+pH		10	-331.63	690.85	38.70	0.00
Depth+Salinity+NH3+NO3+Iron+pH		11	-334.81	701.05	48.90	0.00
Depth		6	-354.07	722.69	70.54	0.00
Salinity+NH3+NO3+PO43+Silica+Iron+pH		9	-352.06	728.12	75.97	0.00
POISSON EventDay+Depth+Salinity+NH3+NO3+PO43+Silica+Iron+pH	+	13	-3,276.32	6,592.64	5,940.49	0.00

Table 0.14: Model selection using a generalized linear mixed-effects model with a log link function to describe the effect of water parameters on the Shannon-Wiener diversity index of the net-patches at Wicklow Point. The model with the lowest AICc used terms: temperature, dissolved oxygen, silica, and depth. The column "Random" represents the presence (+) or absence ( ) of the random grouping effect.

Model	Random	df	logLik	AICc	delta	weight
Depth+Temp+DOmgL+Silica		9	14.37	-4.74	0.00	0.76
Depth+Temp+DOmgL		8	11.20	-1.76	2.98	0.17
Depth+Temp+DOmgL+Silica+Iron+pH		11	14.94	1.56	6.30	0.03
Depth+Temp+DOmgL+Salinity+NH3		10	12.72	2.15	6.90	0.02
Depth+Temp+DOmgL+Salinity+NH3+Silica+Iron+pH		13	18.33	3.33	8.07	0.01
Temp+DOmgL+Salinity+NH3+Silica+Iron+pH		9	8.25	7.51	12.25	0.00
EventDay+Depth+Temp+DOmgL+Salinity+NH3+Silica+Iron+pH	+	14	18.33	8.13	12.87	0.00
Depth		6	1.53	11.48	16.22	0.00
Depth+Salinity+NH3+Silica+Iron+pH		11	9.87	11.69	16.43	0.00

Table 0.15: Model selection using a generalized linear mixed-effects model with a log link function to describe the effect of water parameters on the Simpson index of the net-patches at Wicklow Point. The model with the lowest AICc used terms: temperature, dissolved oxygen, silica, and depth. The column "Random" represents the presence (+) or absence ( ) of the random grouping effect.

Model	Random	df	logLik	AICc	delta	weight
Depth+Temp+DOmgL+Silica		9	35.99	-47.97	0.00	0.58
Depth+Temp+DOmgL		8	33.81	-46.97	1.00	0.35
Depth+Temp+DOmgL+Silica+Iron+pH		11	36.77	-42.12	5.86	0.03
Depth+Temp+DOmgL+Salinity+NH3+Silica		11	36.56	-41.70	6.28	0.03
Depth+Temp+DOmgL+Salinity+NH3+Silica+Iron+pH		13	39.51	-39.02	8.95	0.01
Temp+DOmgL+Salinity+NH3+Silica+Iron+pH		9	30.37	-36.73	11.24	0.00
EventDay+Depth+Temp+DOmgL+Salinity+NH3+Silica+Iron+pH	+	14	39.51	-34.22	13.75	0.00
Depth		6	23.14	-31.74	16.23	0.00
Depth+Salinity+NH3+Silica+Iron+pH		11	31.40	-31.36	16.61	0.00

2.3.3.2. Correlation of water parameters with hydroid biomass on net-patches

Correlation plots used to aid model selection for this section can be found in the appendix (Figures A2.1 and A2.2) and are the same as the correlation plots for the biofouling species counts. For the model examining the mass of hydroids (in grams) growing on the net-patches at Doctor Islets, I found temperature, nitrate levels, pH, and iron were positively associated, with iron having the largest effect size (Table 2.16). Dissolved oxygen, salinity, ammonia, phosphate levels and silica were negatively associated, with dissolved oxygen having the largest (and largest overall) effect size. The species variable is a factor with four levels with one species

(*Obelia* spp.) used as a reference species. The species variable was significant (Table 2.17), and it was found that with each increase in grams of *Obelia* spp., the grams of *Sarsia* sp. and *Ectopleura* sp. (*Clytia* sp. was not identified at Doctor Islets) were expected to decrease.

At Wicklow Point, I found that no continuous variables were associated with hydroid growth (Table 2.16). The species variable tested significant and of the individual hydroid genus, an increase of *Obelia* spp. was associated with a decrease in grams of *Sarsia* sp., and *Clytia* sp. (*Ectopleura* sp. was not identified at this site) (Table 2.18). In addition, the depth variable was tested to be significant and with each depth the grams of hydroids was expected to decrease.

Table 0.16: Regression summary of the models used to examine the environmental parameters on the hydroid biomass from the net patch biofoulant counts at Doctor Islets and Wicklow Point. S.e. is the standard error and 95% is the confidence interval.

	Doctor Islets	Wicklow Point
Intercept	0.285, s.e.=0.054, 95%=[0.179,0.390]	0.021, s.e.=0.004, 95%=[0.013,0.030]
Temperature	0.254, s.e.=0.103, 95%=[0.051,0.456]	
Dissolved Oxygen	-1.243, s.e.=0.395, 95%=[-2.018,-0.469]	
Salinity	-0.225, s.e.=0.114, 95%=[-0.449,-0.002]	
Ammonia	-0.242, s.e.=0.080, 95%=[-0.399,-0.086]	
Nitrate	0.338, s.e.=0.118, 95%=[0.108,0.569]	
Phosphate	-0.204, s.e.=0.078, 95%=[-0.357,-0.052]	
Silica	-0.967, s.e.=0.283, 95%=[-1.521,-0.413]	
Iron	0.841, s.e.=0.237, 95%=[0.377,1.306]	
pH	0.262, s.e.=0.159, 95%=[-0.049,0.573]	
Num.Obs.	381	255

Table 2.16: Continued.

	Doctor Islets	Wicklow Point
Intercept	0.285, s.e.=0.054, 95%=[0.179,0.390]	0.021, s.e.=0.004, 95%=[0.013,0.030]
Species - Sarsia	-0.283, s.e.=0.076, 95%=[-0.433,-0.134]	-0.010, s.e.=0.004, 95%=[-0.018,-0.002]
Species - Clytia		-0.010, s.e.=0.004, 95%=[-0.018,-0.003]
Species - Ectopleura	-0.280, s.e.=0.076, 95%=[-0.430,-0.131]	
Depth 5 m		-0.014, s.e.=0.006, 95%=[-0.025,-0.003]
Depth 10 m		-0.012, s.e.=0.005, 95%=[-0.023,-0.002]
Depth 15 m		-0.013, s.e.=0.005, 95%=[-0.023,-0.003]
Depth 20 m		-0.013, s.e.=0.005, 95%=[-0.022,-0.003]
Num.Obs.	381	255

Table 0.17: Model selection using a generalized linear mixed-effects model with a log link function to describe the effect of water parameters on hydroid biomass (g) on net patches for Doctor Islets. The model with the lowest AICc used terms: temperature, dissolved oxygen, salinity, ammonia, nitrate levels, phosphate levels, silica, iron, pH, and species which is a 4-level factor representing the four species groups (Obelia sp., Sarsia sp., Ectopleura sp., and Clytia sp.). The column "Random" represents the presence (+) or absence ( ) of the random grouping effect.

Model	Random	df	logLik	AICc	delta	weight
Species+Temp+DOmgL+Salinity+NH3+NO3+PO43+Silica+Iron+pH		13	-350.78	728.55	0.00	0.81
Species+NH3+NO3+PO43+Silica+Iron+pH		10	-356.24	733.07	4.52	0.08
Depth+Species+Temp+DOmgL+Salinity+NH3+NO3+PO43+Silica+Iron+pH		17	-349.23	734.15	5.59	0.05
Species+Temperature+DOmgL+Salinity+Silica+Iron+pH		10	-356.91	734.41	5.85	0.04
EventDay+Depth+Species+Temp+DOmgL+Salinity+NH3+NO3+PO43+Silica+Iron+pH	+	18	-349.23	736.35	7.80	0.02
Species+Temperature+DOmgL+Salinity		7	-363.17	740.64	12.09	0.00
Species		4	-368.19	744.49	15.93	0.00
Temp+DOmgL+Salinity+NH3+NO3+PO43+Silica+Iron+pH		15	-358.20	747.72	19.16	0.00

Table 0.18: Model selection using a generalized linear mixed-effects model with a log link function to describe the effect of water parameters on hydroid biomass (g) on net patches for Wicklow Point. The model with the lowest AICc used the terms species, which is a 4 level factor representing the four species groups (Obelia sp., Sarsia sp., Ectopleura sp., and Clytia sp., and depth (1, 5, 10, 15, and 20 m). The column "Random" represents the presence (+) or absence ( ) of the random grouping effect.

Model	Random	df	logLik	AICc	delta	weight
Depth+Species		8	572.02	-1,127.45	0.00	0.35
Depth+Species+NH3+NO3+Silica+Iron+pH		13	576.91	-1,126.30	1.15	0.20
Depth+Species+Temp+DOmgL+Salinity+Iron+pH		13	576.84	-1,126.17	1.28	0.18
Depth+Species+Temp		9	572.45	-1,126.16	1.30	0.18
Depth+Species+Temp+DOmgL+Salinity+NH3+NO3+Silica		14	576.99	-1,124.23	3.22	0.07
Species+Temp+DOmgL+Salinity+NH3+NO3+PO43+Silica+Iron+pH		12	572.64	-1,119.99	7.46	0.01
Depth+Species+Temp+DOmgL+Salinity+NH3+NO3+PO43+Silica+Iron+pH		16	577.04	-1,119.80	7.65	0.01
Depth+Temp+DOmgL+Salinity+NH3+NO3+PO43+Silica+Iron+pH		14	572.52	-1,115.29	12.16	0.00
EventDay+Depth+Species+Temp+DOmgL+Salinity+NH3+NO3+PO43+Silica+Iron+pH	+	18	577.04	-1,115.19	12.27	0.00

2.3.3.3. Correlation of water parameters and stinging-capable species

Correlation plots used to aid model selection for this section can be found in the appendix (Figures A2.3 and A2.4). I found that for the tow samples from Doctor Islets, each unit-increase of ammonia and nitrate levels increased the log-expected counts of stinging-capable individuals with nitrate levels having the larger effect size (Table 2.19). No variables were significantly negatively associated with individual counts. The Event Day variable was significant (Table 2.20) and explained a considerable amount of variation in this model.

For the Wicklow Point model each unit-increase in ammonia showed an increase in the log-expected individual counts of the stinging-capable species in tow samples (Table 2.19). No variables were associated with a decrease. Similar to Doctor Islets, the Event Day variable was significant (Table 2.21) and the variance between samples that were explained by the Event Day variable was large.

Table 0.19: Regression summary of the models used to examine the environmental parameters on the counts of stinging-capable species in the tow samples at Doctor Islets and Wicklow Point. S.e. is the standard error and 95% is the confidence interval.

	Doctor Islets	Wicklow Point
Intercept	-0.663, s.e.=0.405, 95%=[-1.456,0.130]	-1.121, s.e.=0.485, 95%=[-2.072,-0.169]
Ammonia	0.959, s.e.=0.354, 95%=[0.264,1.654]	0.799, s.e.=0.411, 95%=[-0.006,1.604]
Nitrate	1.145, s.e.=0.481, 95%=[0.203,2.087]	
Num.Obs.	578	510

Table 0.20: Model selection using a generalized linear mixed-effects model with a log link function to describe the effect of water parameters on the counts of stinging-capable species in the tow samples for Doctor Islets. The model with the lowest AICc used terms: ammonia, nitrate levels, temperature, dissolved oxygen, and the Event Day variable. The column "Random" represents the presence (+) or absence ( ) of the random grouping effect. NEG.BINOMIAL and POISSON denote the testing of distributions with the full model. In this model the negative binomial distribution was more appropriate.

Model	Random	df	logLik	AICc	delta	weight
EventDay+Temp+DOmgL+NH3+NO3	+	7	-528.38	1,070.96	0.00	0.52
EventDay	+	3	-533.40	1,072.84	1.87	0.20
EventDay+Temp+DOmgL+NH3+NO3+PO43+Silica	+	9	-527.55	1,073.42	2.46	0.15
EventDay+NH3+NO3+PO43+Silica+Salinity+Iron+pH	+	10	-527.31	1,075.01	4.04	0.07
EventDay+Temp+DOmgL	+	5	-533.02	1,076.14	5.17	0.04
NEG.BINOMIAL EventDay+Temp+DOmgL+NH3+NO3+PO43+Silica+Salinity+Iron+pH	+	12	-526.92	1,078.39	7.43	0.01
EventDay+Temp+DOmgL+Silica+Salinity+Iron+pH	+	9	-531.82	1,081.96	10.99	0.00
Temp+DOmgL+NH3+NO3+PO43+Silica+Salinity+Iron+pH		11	-531.76	1,086.00	15.03	0.00
POISSON EventDay+Temp+DOmgL+NH3+NO3+PO43+Silica+Salinity+Iron+pH	+	11	-3,619.84	7,262.15	6,191.19	0.00

Table 0.21: Model selection using a generalized linear mixed-effects model with a log link function to describe the effect of water parameters on the counts of stinging-capable species in the tow samples for Doctor Islets. The model with the lowest AICc used terms ammonia and the Event Day variable. The column "Random" represents the presence (+) or absence ( ) of the random grouping effect. NEG.BINOMIAL and POISSON denote the testing of distributions with the full model. In this model the negative binomial distribution was more appropriate.

Model	Random	df	logLik	AICc	delta	weight
EventDay+NH3	+	4	-418.46	844.99	0.00	0.60
EventDay	+	3	-420.27	846.58	1.59	0.27
EventDay+NH3+NO3+PO43+Silica+Salinity+Iron+pH	+	10	-414.41	849.26	4.26	0.07
EventDay+Temp+DOmgL+Silica+Salinity+Iron+pH	+	9	-416.38	851.11	6.12	0.03
EventDay+Temp+DOmgL+NH3+NO3+PO43	+	8	-417.45	851.18	6.18	0.03
NEG.BINOMIAL EventDay+Temp+DOmgL+NH3+NO3+PO43+Silica+Salinity+Iron+pH	+	12	-414.38	853.38	8.39	0.01
Temp+DOmgL+NH3+NO3+PO43+Silica+Salinity+Iron+pH		11	-419.95	862.43	17.44	0.00
POISSON EventDay+Temp+DOmgL+NH3+NO3+PO43+Silica+Salinity+Iron+pH	+	11	-2,492.10	5,006.72	4,161.73	0.00

2.4. Discussion

2.4.1 Biofoulant community on net patches and diversity indices

In finfish aquaculture, the growth of biofouling on net-pens and other structures can cause damages due to increased drag, reduced water flow leading to low dissolved oxygen and accumulation of waste, and potentially injure fish via stinging-species or transmission of diseases (Bosch-Belmar et al., 2020; Cornejo et al., 2020). The interactions of biofouling organisms and farmed fish have been studied extensively globally but have largely focused on stinging capable species such as *Ectopleura larynx* due to its involvement in several mass mortalities and other ongoing health issues in Europe and the Mediterranean Sea (Bosch-Belmar et al., 2019; Gansel et al., 2015; Martell et al., 2018). Studies examining how environmental parameters might affect counts of each individual species in a biofouling assemblage and the corresponding diversity indices are scarce, and to my knowledge, non-existent in British Columbia and the surrounding area.

Species composition varied widely depending on deployment date, site, and depth (Figure 2.6A-B). Arthropods (mostly Harpacticoids) and bivalves (mostly *Mytilus* sp. <10 mm) were the dominant species at both sites. *Mytilus* sp. dominated the compositions during late spring until late summer at Doctor Islets which roughly corresponds to when temperatures were above 10˚ C (to a max of 14.1˚ C) and salinity was below 25 ppt (Figure 2.4). Some studies have shown that optimal growing conditions for *Mytilus* sp. seem to be temperatures lower than 20˚ C and salinity around 20 ppt (Almada-villela, 1984; Almada-Villela et al., 1982); however, most studies focus on extreme values well beyond what was recorded at either site. In addition, the period where *Mytilus* sp. was dominant on the samples was during the "spatfall" season in which free-swimming larvae undergo metamorphosis into their sessile stage (FAO, 2003). This is likely

a major contributor to the large counts of small individuals (<10 mm) that were observed.

Descriptions or studies of the compositions of zooplankton assemblages in British Columbia is sparse. Tommasi (et al., 2013) described the seasonal and interannual variation in assemblages in the central-coast area of British Columbia; however, this assemblage was obtained via tow samples, which are considerably different from benthic or biofouling assemblages. Some other factors that could contribute to the compositions of each site that were not explicitly examined is tidal flow.

Doctor Islets lies in Knight Inlet and is exposed to a greater amount of freshwater, as well as deeper upwelling currents from two sources: directly into Knight Inlet from the Queen Charlotte Strait and from Tribune Channel. Conversely, Wicklow Point is in a small bay in Fife Sound in between the mouth of Tribune Channel and the Queen Chalotte Strait. It has much less freshwater input and a longer circulation time, leading to greater exposure to local conditions (Foreman et al., 2006; B. Vornicu, pers. comm.).

In addition to species composition, I examined several diversity indices (Shannon-Wiener index, Simpson index, species richness, and total abundance). It is important to look at more than just one measure of diversity (e.g., species richness is commonly the only measurement analyzed), especially when examining trends. Dominance, rarity, and identity of individual species play large parts in how communities and assemblages are structured and function over time (Hillebrand et al., 2018). As an example, Hillebrand states: the decline of a long-lived foundational species and the subsequent replacement with short lived “weedier” species doesn’t change the species richness, but changes the dominance, evenness, and foundational traits associated with the assemblage. This is especially evident when examining non-indigenous species which can invade and dominate or predate on local species, weakening species richness

or evenness by overshadowing or removing rarer species (Winfree et al., 2015).

The species richness was calculated by counting the total unique species that occurred on each net patch at each depth for a sampling date. After each sample collection, the net patches were replaced with clean ones, and as such the species richness values (and other index values) here represent a snapshot of what was in the water column during the 1–3-week immersion period. It is interesting to note that the species richness decreases at all depths over the study period at both sites (Figure 2.8A and 2.9A). A possible reason for the decreasing trend is seasonality. Spring is a common spawning time for many organisms, and as such the recruitment ability may be reduced in later months. In addition to seasonality, depth plays a part in species richness at both sites. At Doctor Islets, shallower depths (1 m and 5 m) usually had the highest richness, although this was much more varied at Doctor Islets than Wicklow Point. In contrast, at Wicklow Point, the species richness follows a gradient, from more richness at shallow depths to less at deeper depths, except for 20 m, which tended to have a higher richness index.

The total abundance is the total counts of all individuals of all species at each depth by sampling date. At Doctor Islets (Figure 2.8B), total abundance was lower at deeper depths, and all depths drop off sharply in individual counts in the August 21 sample and remain low for the remainder of the study period. Interestingly, this sharp drop in individual counts overlaps with a sharp drop in phosphate levels (Figure 2.5C). Phosphate is a key limiting nutrient in aquatic algae growth, which is a major food source for many biofoulant organisms, including *Mytilus* spat (Ngatia et al., 2019). The total abundance at Wicklow Point follows a defined gradient with much less variation than Doctor Islets (Figure 2.8B). There was a spring-time peak in individuals counted, but larger counts and more even spread at each depth indicates that Wicklow Point may have better water column mixing abilities or a more favourable set of environmental parameters

throughout.

The Shannon-Wiener index of diversity is a measurement of species evenness in a population, using both species richness and total abundance in its calculation. The higher the index value, the higher the diversity. The Simpson index is a calculation that gives the probability that any two individual species selected at random in a sample do not belong to the same species. It is more sensitive to changes in evenness of common species and less sensitive to changes in rare species. As both indices measure evenness in someway, they are intrinsically similar in trends. I found at Doctor Islets (Figure 2.8C&D) that at 1 m the evenness is higher in spring and fall, and low during summer. At lower depths I generally saw higher values if the 1 m value was low, and vice versa, with the inflection point being around 0.75 (Shannon-Wiener index) and 0.5 (Simpson index). This difference in the patterns between 1 m and the other depths can be explained by the trends seen in the species richness and especially the total abundance graphs. Since these indices measure evenness, the presence of large counts and the decreasing species richness indicated that the samples at 1 m were being dominated by a single species (*Mytilus* sp.). This was especially evident in the July and August samples, when evenness and the probability that two individuals are different were the lowest. At other depths, I saw that the evenness and diversity generally increased with deeper depths, although total abundance did not. This supports the idea that without the presence of a dominating species, other groups of species can be more evenly dispersed and contribute to these values.

At Wicklow Point (Figure 2.9C&D), I found that the Shannon-Wiener and Simpson index generally showed a gradient of high to low index values as depth increased, except for 20 m, which showed high, sometimes higher than 1 m, index values. Unlike Doctor Islets, the peak of species richness and total abundance corresponded to a peak in the Shannon-Wiener and

Simpson values. Figure 2.6B gives some insight – this peak (which occurred on June 22) saw a more varied composition at each depth than most of the other sampling dates and saw low compositions of Mollusca (mostly *Mytilus* sp.) which indicated that more species were able to settle and grow rather than be out-competed. Interestingly, the 20 m samples recorded higher species richness, Shannon-Wiener index, and Simpson indices. The phylum composition (Figure 2.6B) of 20 m on the June 22 sample was similar to the other depths of that sample, which likely indicates that the higher index values were caused by a greater species-level variety and evenness of counts between species.

2.4.2 Hydroid growth on net patches

To gain a better understanding of what cryptic species were present at these sites, a *post hoc* examination of the collected hydroids with a more powerful microscope revealed several additional species. At Doctor Islets I identified six species: *Obelia longissima*, *O. dichotoma* (the latter being more common), *Phialella* sp., *Sarsia* sp., *Ectopleura crocea*, and *Garvei* sp. At Wicklow Point I identified seven species; *O. longissima, O.dichotoma* (in roughly equal amounts), *Sarsia* sp., *Ectopleura crocea*, *Garvei* sp., *Clytia hemisphearica*, and *Plumularia lagenifera*.

The compositions of hydroids growing on the net patches was largely the *Obelia* spp. group at both sites and at all depths, which was to be expected based on past observations (B. Vornicu, pers. comm.). Total amounts were much greater at Doctor Islets than Wicklow Point, which is contrary to observations in past years in which Wicklow Point experienced a greater mass growing on the net pens (B. Vornicu, pers. comm). *Ectopleura* spp. and *Sarsia* spp. appeared to prefer deeper depths at their respective sites, however, this may have more to do

with competition with *Obelia* sp. and other shallow biofoulers such as *Mytlius* sp.

Ectopleura spp. have been extensively studied in Europe in relation to the health of farmed fish, especially in context of gill pathologies and biofouling (Bosch-Belmar et al., 2017; Fitridge and Keough, 2013; Gansel et al., 2015; Mitchell et al., 2011). *E. larynx* is the most studied species; however, the range of the species is limited to the North Atlantic Ocean, Northern Europe, and the Mediterranean Sea (Fofonoff et al., 2020). *Ectopleura crocea*, which is the likely species identified in this study, is a common species in the North and South Pacific and is a common nuisance species in shellfish aquaculture in Australia (Fitridge and Keough, 2013). No evidence exists of it causing harm in finfish aquaculture, but the potential remains.

Obelia species are common and ubiquitous, save the Artic and Antarctic region, and mostly observed in the colonial hydroid stage in fouling communities (Piraino et al., 1996). Several species, including the two identified in this study, *Obelia dichotoma* and *O. longissima*, have been identified as causing injuries and mortalities in finfish aquaculture facilities in the Mediterranean Sea (Bosch-Belmar et al., 2019, 2017; Martell et al., 2018) the Northeastern Pacific (Edwards et al., 2015; Gartner et al., 2016), the North Atlantic (Martell et al., 2018), and New Zealand (Floerl et al., 2016).

No evidence exists that the other common species identified in this study, *Sarsia* spp. and *Clytia hemisphaerica*, pose any threat to fin or shellfish aquaculture. However, they are cnidarians with stinging-capable cnidocytes and as such the potential for harm remains, especially during net-cleaning events when power-washing debris can be blown into the water column.

2.4.3. Stinging-species in tow samples

A total of 15 genus and species of stinging-capable cnidarians and siphonophores were found during the study period, with 14 species found at Doctor Islets and 14 species at Wicklow Point. Figure 10A and B shows the summary of the counts for each month of each of these species, with some extra divisions for size (*Clytia gregaria* was separated into >10 mm and <10 mm) and for life stage. Several of these species have been documented as harmful to the aquaculture industry.

Muggiaea atlantica is a calycophoran siphonophore, which are a class of colonial cnidarian whose life cycle is characterized by alternating between polygastric (feeding) stage and eudoxid (sexual) stage (Mackie et al., 1987). Both stages can reproduce (asexually and sexually, respectively), increasing the potential for simultaneously blooming. *Muggiaea* species, including *M. atlantica* have implicated in several mass mortalities at fish farms in the Ireland and Scotland (Baxter et al., 2011; Fitridge and Keough, 2013; Purcell et al., 2013).

In addition to a sessile hydroid stage, *Obelia* species also have a free-swimming medusa stage that has the potential to form harmful blooms. Both species identified in this study, *O. dichotoma* and *O. longissima*, have been among those implicit in several harmful bloom events, causing or being associated with mortalities in Atlantic salmon farms in Scotland and Ireland (Baxter et al., 2011; Kintner and Brierley, 2019) and in Sea Bass in Spain (Bosch-Belmar et al., 2014).

Other jellyfish that have been implicated in harmful events that have been identified in this study are *Catablema* sp., which was involved in several incidents of Atlantic salmon mortalities in Scotland (Purcell et al., 2007), and *Phialella quadrata*, which, in addition to typical stinging-related injuries and mortalities, has been shown to cause mortalities due to secondary transmission of the bacteria *Tenacibaculum maritimum* which causes Tenacibaculosis

in Irish fish farms (Baxter et al., 2011; Ferguson et al., 2010).

Not implicit in fish farm mortalities, but species of note that were identified in this study are *Proboscidactyla flaviccirata*, *Aqueorea victoria*, and *Sarsia tubulosa* (among other *Sarsia* species). These species are commonly found around British Columbia and have been shown to predate on herring roe and larvae, which is an important fisheries industry (Purcell and Grover, 1990). Finally, other species of class Diphydae (largely *Lensia* sp. and *Diphyes* sp. in this study), have no records of harm but are very similar to *Muggiaea atlantica* (also of class Diphydae) in appearance and stinging ability at all life-stages.

2.4.4. Biofoulant counts and diversity indices with water parameters

Comparing the results of the models for Doctor Islets and Wicklow Point show that each site is vastly different from each other in both effect size and directionality of each coefficient, which, in conjunction with the general rule to not use variables with less than five levels as a random effect (Kain et al., 2015; Midway, 2022), validates my decision to separate the models by site. Only salinity and depth shared a directional coefficient and the coefficients calculated for Wicklow Point are much higher. On this last point lies an issue with the Wicklow Point model (and a common issue with GLM(M)s), however, that may affect the prediction capabilities. In these GLM(M)s, the coefficients are reported in the log (link function) of the units of the response variable (count of species) indicating strength (effect) and directionality (negative or positive). To get the per-variable unit-increase in counts one must exponentiate the regression estimates. As an example, Doctor Islets reports that for each unit increase of temperature, the coefficient estimate is 0.978, and thus $e^{0.978} = 2.66$ times the expected counts per sample, when all other variables are held at a constant mean (Table 2.3). The model for Wicklow Point (and all

models) were selected for using AICc values, and the lowest value of the combinations of variables usually indicates the best fit for the data. In this case, the values of some of the estimates are relatively high which is likely due to collinearity-related errors remaining after variable and model selection. As an example, the pH estimate is 7.609, and thus $e^{7.609} = 2016.26$ times the expected count per sample, which is possible, but unlikely due to the scaling and centering of the environmental variables. When pH was removed the estimates were similar in effect size to what had been expected; however, the AICc value increased by more than 19 points, well over the general "rule-of-thumb" of ≤2 points and indicate that the pH-removed model combination is not appropriate (Burnham and Anderson, 2004).

The variable with the largest effect size for the biofoulant counts at Doctor Islets was silica. We can see on Figure 2.5D that silica was higher in late-spring, lower and stable during the warmer months, before rising again to higher levels during September. Total abundance at Doctor Islets (Figure 2.8B) is also highest in late spring. Silica is an essential nutrient required for the cell wall structure of diatoms, a major primary producer and food source for many of the biofoulants counted on the net patches. Excluding depth, the variable with the largest negative effect size was iron. This is interesting in the context of diatom production, as iron limitation restricts diatom growth, among other functions (Greene et al., 1991). There is some use for the inclusion of iron in reverse osmosis membranes to prevent the formation of bio films (Armendáriz-Ontiveros et al., 2019); however, historically iron does not inhibit the growth rates of foulants. When the British Navy started using iron-hulled ships instead of wood, the ships became so fouled that by the mid-19th century they considered abandoning or selling the entire fleet (Field, 1981).

At Wicklow Point, the variable with the largest (negative) effect size for biofouling

counts was ammonia. Ammonia is produced via excretion from fish and invertebrates, as well as the breakdown of fish feed and detritus. Ammonia levels at Wicklow Point were low for most of the sampling season, with a few instances of higher levels being recorded randomly through the study (Figure 2.5A). The toxicity of ammonia increases with lower pH levels and decreases with higher salinity (Miller et al., 1990; Sampaio et al., 2002), and Wicklow Point experienced a drop in pH in late August and early September (Figure 2.4D), whereas salinity was stable for the duration of the study (Figure 2.4C). During this time, all the diversity indices for Wicklow Point started to gradually decrease (and did for the rest of the study), but there are no sharp increases or decreases in any of the indices (Figure 2.9). Miller and Sampaio (1990;2002) both noted in their respectively studies that the effect of ammonia toxicity varies between species, but that fishes are more sensitive than invertebrates, generally.

Similar trends exist between sites between the diversity index models (Figs 2.6, 2.11). The species richness models at both sites indicated that one (pH at Doctor Islets and phosphate levels at Wicklow Point) environmental variable was significant, whereas nearly all variables were associated with total abundance. At Doctor Islets, the environmental variables associated with the Shannon-Wiener and Simpson indices were fewer (ammonia and nitrate levels in the Shannon-Wiener index and none in the Simpson index) than at Wicklow Point, and the effect sizes were smaller, indicating that these variables might have less explanatory power than those at Wicklow Point. However, this is opposite with the depth variables, with each depth at Doctor Islets having a larger effect size than at Wicklow Point. This can be visualized on Figures 2.8 and 2.9, where I found that Wicklow Point experiences a more stable gradient of decreasing diversity with depth, versus the variation at Doctor Islets. Because depth has less explanatory power at Wicklow Point, this may indicate that the trends I saw in the biofoulant counts were better

explained by favourable water parameters, rather than a better mixing ability.

Another variable that likely has some impact on the compositions of the tow samples, especially of free-swimming jellyfish and other buoyant zooplankton would be the currents of the area. This has been discussed previously (section 2.4.1) and Krkošek et al. (2005) wrote an excellent article on the transmission dynamics of sea lice in this area.

2.4.5. Hydroid biomass with water parameters

All continuous variables measured for this study were associated with hydroid biomass at Doctor Islets, however, in contrast, none of these variables were associated with hydroid biomass at Wicklow Point. In addition, as another contrast, while depth was not significant at Doctor Islets, it was at Wicklow Point. Both sites indicated that the species variable was significant, and I found that the effect size at Doctor Islets was much larger than at Wicklow Point, which could indicate that the species variable at Doctor Islets had a much stronger explanatory power in the trends of the grams of hydroids collected. However, as Doctor Islets also had a much higher biomass of hydroids than Wicklow Point, it is possible that this is influencing the effect sizes.

All species, when recorded, were impacted negatively with each increasing gram of *Obelia* spp. The effect sizes were higher at Doctor Islets; however, this might be because the total biomass recorded at this site was much higher (Fig 2.11A). Interactions between hydroids and other biofoulant species in succession has been studied (Bloecher et al., 2013; Guenther et al., 2010; Martell et al., 2018), but information on the interactions between hydroids species is sparse. Many factors may be at play as to why *Obelia* spp. dominate and out-compete other species, such as growth rate, recruitment ability, food availability, favourable water parameters, etc.

2.4.6. Stinging-capable species with water parameters

In addition to biofouling growing on net patches, weekly tow samples were taken at each site to count and identify stinging-capable species present in the water column. Both sites were similar in that I only found one (Doctor Islets, ammonia) or two (Wicklow Point, ammonia and nitrate levels) variables that were considered associated with counts (Table 2.19). All zooplankton excrete ammonia and small amounts of nitrates and nitrites which can contribute significantly to the available nutrients for primary production. Jellyfish especially have been shown to contribute large percentages, with their presence often resulting in algal blooms. This effect was also noted to be exemplified in shallow, inshore, and coastal regions where fish farms are typically situated (Hubot et al., 2021; Jawed, 1973).

While many factors may be involved in the distribution and abundance of jellyfish, in literature, temperature is considered to be the main driver. This is seen especially as the abundance, intensity and duration of blooms, and expansion of spatial distributions have increased in recent decades due to rising ocean temperatures (Purcell, 2005). In addition, the Event Day random variable was significant at both sites and the variance was large, indicating that much of the variation seen in the counts from sample-to-sample could be explained by seasonality, rather than the existing variables.

2.5. Conclusion

Chapter 2 explored whether correlations exist between the environmental variables and the biofouling community. For the biofoulant species counts on the net-patches, the models indicated that most of the environmental variables examined were associated either positively or

negatively with an increase in the counts of each species, with silica and iron having the largest positive and negative effect sizes, respectively, at Doctor Islets and pH and ammonia having the largest positive and negative effect sizes, respectively, at Wicklow Point.

Four groups of hydroid species (*Obelia* spp., *Sarsia* spp., *Ectopleura* sp., and *Clytia* sp.) were identified growing on the net patches, with *Ectopleura* sp. only found at Doctor Islets and *Clytia* sp. only found at Wicklow Point. *Obelia* spp. was dominant at both sites for the duration of the study with no discernable pattern by depth or sampling date. Additionally, *Obelia* spp. was found in much greater amounts at Doctor Islets, contrary to previous years where the reverse was true. All environmental variables were associated with the grams of hydroids at Doctor Islets (iron and dissolved oxygen having the largest positive and negative effects, respectively), while none were associated at Wicklow Point. In addition, I examined species interactions between the four hydroid groups at both sites, and I found that at each site with each increase in grams of *Obelia* spp., the expected grams of all the other species decreased.

The models examining the environmental parameters and counts of the stinging-species in the tows indicated that ammonia at both sites, and nitrate levels at Doctor Islets all were positively associated with an increase in counts.

As such, correlations do exist between the various water parameters examined in this study and the biofouling community at these sites. However, correlation does not equal causation and given that the range of measured environmental variables were decidedly uneventful for the areas coupled with only a single year of data collection, it cannot be said for certain whether any of the variables were directly responsible for the associations found.

Chapter 3 **Linking the environment to the gill health of Atlantic salmon**

3.1. Gill Health in Aquaculture

In aquaculture settings, finfish are particularly vulnerable to external factors as their gills are in direct contact with the environment. Mechanical damage from algae and zooplankton blooms, water parameter fluctuations, and infectious organisms and diseases that target gill tissues are examples of these factors (Herrero et al., 2018). Gill disease in farmed salmon typically use seven types of "actiology-based" categories: amoebic gill disease (AGD), parasitic gill disease, viral gill disease, bacterial gill disease, zooplankton (usually cnidarian) associated gill disease, harmful algae gill disease, and chemical or toxin-associated gill disease (Rodger, 2007). When more than one, or all, of these types are observed it is referred to as complex proliferative gill disease (CPG) or proliferative gill disease (PGD), with the usage of each term often overlapping (Boerlage et al., 2020).

Some of the common or important pathogens and parasites that affect the gill health of Atlantic salmon are; *Neoparamoeba peruruans*, the amoeba responsible for AGD (Herrero et al., 2018), *Desmozoon lepeoptherii*, a microsporidian parasite known to spread from sea lice, infecting several tissue types as well as gills (Freeman and Sommerville, 2009), Salmon gill poxvirus (SGPV), an important virus in Norwegian salmon farms (Gjessing et al., 2015), and bacterial infections of *Candidatus Branchiomonas cisticola* and *Chlamydiae* causing epitheliocystis of gill tissues (Toenshoff et al., 2012).

Harmful algal bloom species (HABs), like diatoms *Chaetoceros concavicorne* and *C. convolutus*, have long spines that can cause irritation and mechanical damage to gills, triggering the production of mucus as an attempt to clear the gill filaments. This excess production can result in necrosis, hyperplasia, and respiratory dysfunction that can directly cause mortality or

increase the susceptibility to secondary infections (Rensel and Whyte, 2003). As well as mechanical damages, HABs can be toxin-producing, like the haptophyte *Prymnesium parvum* which produces a toxin that destroys the selective permeability of gills and has caused mass mortalities in Norway. In addition, *Prymnesium parvum* has been known to settle in biofilms on fish farm nets and structures (Johnsen et al., 2010).

3.1.1. Water parameters and gill health

In addition to providing a first line of defense against the immediate environment, gills are also involved in the osmotic, ionic, acid-base regulation, and nitrogenous waste excretion processes. The disruption of these processes via environmental changes can lead to increased susceptibility and facilitation of injury and infection (Cabillon and Lazado, 2019).

Water temperature is widely studied in relation to fish, not only because of the relations to disease and immune response, but because of the associations with behaviour, growth, and reproduction. In addition to the direct affect on fish, temperature is also a driver of change in other physiochemical parameters (Cabillon and Lazado, 2019). Fish exposed to higher temperatures increase oxygen consumption which increases the production of reactive-oxygen species (ROS) as a by-product and can result in oxidative stress (Cao et al., 2017). As an example of this, Parihar et al. (1997) recorded elevated levels of superoxide dismutase (an oxidative stress marker) in the gills of Asian stinging catfish (*Heteropneustes fossilis*), which resulted in lower levels of an antioxidant involved in oxidative stress regulation. This interaction was also recorded in Antarctic fishes exposed to higher temperatures and suggests that the gills of many fishes are unable to upregulate antioxidants after a heat-stress event (Klein et al., 2017).

In addition to direct effects on the metabolisms of fish, higher water temperatures have

been associated with an increase in severity of diseases especially AGD in Atlantic salmon. The first reports of this disease in areas often came when the water temperatures were reported as above average, suggesting temperature as either a trigger for the spread of AGD, or contributing to the increased susceptibility of the fish (Rozas-Serri, 2019). Also, a common treatment for AGD, sea lice, and several other ailments is hydrogen peroxide baths which are made toxic and possibly lethal when temperatures are over 13.5˚ C especially when fish are experiencing gill dysfunctions (Karlsbakk et al., 2013).

Dissolved oxygen is important for most cellular functions in an organism and is a major limiting factor in aquaculture systems (Cabillon and Lazado, 2019). It can directly affect the development, growth, reproduction, and survival of fish, and is inversely related to water temperatures (e.g., as temperatures increase, the threshold for 100% saturation decreases) (Mota et al., 2020).

Salmonids are generally adapted to cooler waters with high oxygen contents, and as such are especially vulnerable to low dissolved oxygen events (Krasnov et al., 2021). In a study, post-smolts exposed to a cyclical low oxygen regime showed reduced appetite and growth, increased cortisol levels, and up to 5% mortality when compared to a control (Remen et al., 2012). In addition to the various immunological and physical effects, Atlantic salmon exposed to low dissolved oxygen levels and the AGD causing amoeba, *Neoparamoeba perurans*, showed an acceleration of the progression of the diseases as well as higher amoeba counts and fish mortality (Oldham et al., 2020). Bowden et al. (2022) also demonstrated that due to the increase in energy requirements when infected with AGD, Atlantic salmon smolts experience a decreased tolerance for low dissolved oxygen conditions. This has led to numerous fish farms to supersaturate the water inside the net-pens to improve growth, increased pathogen resistance, and increase

stocking density. However, a study by Person-Le Ruyet et al. (2002) was unable to determine the effectiveness of this strategy and poorly controlled supersaturation can result in gas bubble disease when the pressure of the gases becomes higher than ambient atmosphere (Espmark et al., 2010).

Interestingly, hypoxia induced gill adaptions can be seen in some species of carp (Matey et al., 2008; Sollid et al., 2003) in which the lamellae of the gills protrude, increasing surface area after hypoxia exposure, and completely recover to normoxia condition after a period of time. It has been theorized that this is an adaption for the migration and overwintering into ice-covered ponds. This effect has also been recorded in reverse in some carp species, where the lamellae withdraw to decrease surface area in hyperoxia conditions (Tzaneva et al., 2011). In general, however, suboptimal levels of dissolved oxygen (both too high or too low) compromise mucosal barrier functions and induce molecular changes. This can directly result in mortality or result in an increased susceptibility to pathogens and infection (Cabillon and Lazado, 2019).

Salmon, as part of their life history are anadromous and migrate from freshwater to saltwater. Subsequently they have a parr-smolt transformation that consists of behaviour, morphological, and physiological changes to enable the survival of this journey. One of the most important parts of this transformation is the increase in an ability for the ion regulation of seawater (Vargas-Chacoff et al., 2018). Gills play a crucial role in ion regulation via specialized cells called ionocytes. These cells are involved in chloride and sodium secretion and uptake, among other functions (Hiroi and McCormick, 2012). Some studies have shown that in salmon specifically, ionocytes have different distributions depending on the salinity of the water. In freshwater, ionocytes were distributed on both the gill filaments and lamellae, whereas in saltwater the ionocytes were enlarged on the filaments and completely absent on the lamellae

(Pelis et al., 2001). Another study showed that temperature can affect this process as well, especially during the smoltification process, reducing the ion regulation ability and causing the fish to be more sensitive to salinity changes (Vargas-Chacoff et al., 2018).

Freshwater has become a standard to treat AGD since it was first used in Australia in the 1980s, and relatively recently, has also become a large-scale treatment option for sea lice as well. Fish are typically held in freshwater with supersaturation levels of dissolved oxygen for 2-4 hours with the expectation that the AGD-causing amoeba or sea lice will detach from the host fish (Powell et al., 2015). In this review by Powell (2015), it was noted that the combination of soft water and the addition of dissolved organic carbon sources were the most effective at treating AGD and provided the longest intervals between reinfection to treatment-required levels. Additionally, in another study examining the effects of differing salinity levels on the gill health of salmon infected with AGD, it was found that with increasing salinity, the probability of finding more severe gill injuries increased, whereas there were no significant relationships in the control AGD-negative fish (Jones and Price, 2022).

Responses to CO_2 in fish are highly variable, with some studies recording strongly negative effects, no effects, and even some positive effects, depending on the species, CO_2 concentration, and exposure time (Cattano et al., 2018). These responses can vary between populations, such as in populations with large spatial distributions (Frommel et al., 2012), and even between individuals in the same populations (Murray et al., 2014). Adult fish are better able to self-regulate CO_2 by controlling the acid-base balance generally via bicarbonate buffering across the gills, but early life stages with larger surface area to volume ratios or underdeveloped bicarbonate buffering are not able to do so and thus are at the most risk (Frommel et al., 2012).

In general, changes to CO_2 are less of a problem to teleost fish than other marine

organisms, especially those that calcify such as bivalves or gastropods, but are of special concern in recirculating aquaculture systems or semi-closed systems. However, these systems primarily deal with pre-smolts and as such data on the effects of CO_2 on adult Atlantic salmon specifically are lacking in some areas (Gil Martens et al., 2006). Some studies have shown that exposure to high CO_2 and lower pH levels found that growth was stunted in Atlantic salmon, although exposures under certain temperature thresholds were found to be recoverable or not statistically significant (Fivelstad et al., 1998). Another study found that in adult Coho salmon (*Onchorhyncus kisutch*) exposure to medium and high levels of CO_2 impaired the olfactory systems, making the fish less able to detect prey or avoid predator scents in lab settings, which has implications for other functions such as natal stream migration (Williams et al., 2019). Gil Martens et al. (2006) also showed that higher CO_2 levels increases the toxicity of aluminum, which can cause hypertrophy and hyperplasia of the gill tissue. However, like most other water parameters, the impacts on Atlantic salmon seem to depend on life stage, production method, and other concurrent water parameters (Mota et al., 2020).

3.1.2. Biofoulants and gill health

Hydroids and jellyfish, with their stinging capable cells (cnidocytes), are the primary species known to cause direct harm to animals in finfish aquaculture and have been extensively reviewed. Hydroids are key pioneering components of fouling communities, colonizing early and quickly, often crowding out or providing a secondary substrate for other foulants to settle (Martell et al., 2018). Rising ocean temperatures are a contributing factor for recent jellyfish blooms and the increased recruitment and survival of both native and invasive (Bosch-Belmar et al., 2020).

Hydroids cause injuries via skin lesions from contact envenomation, gill pathologies, and secondary infections (Baxter et al., 2012). Fish in aquaculture settings are especially at risk during and after in situ cleaning events as hydroids and other biofoulants can be washed into the water column and potentially come into contact with fish skin, breathed through gills, or swallowed causing mouth and digestive injuries (Baxter et al., 2012).

Species in the genus *Ectopleura* in the family Tubilariidae are the most common hydroid in scientific research due to a long history of biofoulant-aquaculture interactions in the Mediterranean Sea and Northern Europe (Bosch-Belmar et al., 2019; Gansel et al., 2015; Martell et al., 2018). Recently, however, more species such as *Obelia*, which have a cosmopolitan distribution, have been identified as potentially causing injuries, mortalities, or increasing susceptibility to secondary infections (Bosch-Belmar et al., 2019, 2017; Martell et al., 2018).

Like hydroids, jellyfish can harm fish via contact envenomation. Skin, gill, and mouth injuries are common, and several species have been implicit in mass mortalities in Asia, Australia, North and South America, and Europe (Bosch-Belmar et al., 2017; Palma et al., 2007; Wiox et al., 2008). Some of the more common problem species are *Aurelia aurita*, which is responsible for mass mortalities in Ireland (Baxter et al., 2011), *Pelagica noctiluca*, which is responsible for mass mortalities in Ireland and the Mediterranean Sea (Baxter et al., 2011; Bosch-Belmar et al., 2017; Marcos-López et al., 2016), and *Muggiea atlantica*, a small siphonophore responsible for many harmful stinging events in Europe and the Mediterranean Sea (Bosch-Belmar et al., 2017; Baxter et al., 2011). In addition to the bloom forming capabilities of jellyfish, large jellyfish such as *Cyanea capillata* are vulnerable to breaking apart due to wave action against the mesh of fish farm nets. These small pieces still contain stinging-capable cnidocytes that can potentially come into contact with the skin and gills of fish (Powell et al.,

2018). Hydroids and jellyfish are also known vectors to a variety of pathogens that affect farmed fish, such as *Tenacibaculum maritimum* (Ferguson et al., 2010), *Neoparamoeba peruruans*, the causative organism of AGD (Downes et al., 2018; Hellebø et al., 2017), and *Vibrio* and *Pseudomonas* bacterial infections (Clinton et al., 2020).

There is scarce to no data in the literature that other species commonly found in biofouling assemblages are directly harmful to finfish, either before, during, or after in situ cleaning events. However, there is some interest in examining if species with the capability of producing sharp edges after in situ cleaning (e.g., *Mytilus* sp., which are a very common biofoulant species) are affecting the gills when debris is breathed in (S. Cross, pers. comm.). A study by Østevik (et al., 2021) saw an increase in gill health injuries and severity of injuries directly after in situ cleaning events, despite the absence of any hydroids, although it was short lived. This could possibly indicate that in situ cleaning events irritate gills at the very least, regardless of the presence of hydroids.

As such, I aim to determine if any relationships exist between individual biofoulant species (hydroid and otherwise) and gill health severity scores at two Atlantic salmon farms off the coast of Vancouver Island, British Columbia. I also examine relationships between free swimming stinging capable species and gill health, as well as various water parameters.

3.2. Methods and materials

See Chapter 2 for a detailed explanation of the study sites and methods pertaining to the collection of environmental parameters and biofouling samples.

3.2.1. Gill health scoring

Both sites had one designated net pen (Figure 2.2A&B) that was monitored weekly for

fish health (as per Mowi Canada West . practice), starting with the population of the pens with hatchery reared S1 Atlantic salmon smolts until the completion of the study. We minimized variation in the fish health assessment by choosing fish that were from the same brood stock origin, the same hatchery, of the same smolt quality (all S1 populations) and exposed to the same management practices. Fish gill health was examined by single trained farm employee to minimize observational bias approximately weekly through non-lethal gill scoring on 20 randomly sampled fish from the designated net pen and 1 or 2 other net-pens depending on the week at each site for the duration of the experimental period. Scores ranged from 0 (no damage) to 5 (severe damage) (Table 3.1) in accordance with standard operating procedures for Mowi salmon farms.

Table 0.1: Damage criteria used to assign gill scores to farmed Atlantic salmon.

Score	Definition
0	None - Mild lesions on **one** arch, some thickening of filaments
1	Mild lesions and filament thickening on multiple arches, >75% healthy tissue
2	Moderate lesions and filament thickening on multiple arches, >75% healthy tissue
3	Moderate - severe lesions and filament thickening on multiple arches, 50-75% healthy tissue
4	Severe lesions, filaments extensively thickened and shortened/necrotic, 25-50% healthy tissue
5	Severe lesions, filaments thickened and shortened/necrotic on **all** arches, <25% healthy tissue

3.3.2. Statistical models

To examine the response of fish gill health to the various explanatory factors I built statistical models using the Ordinal package in R (Christensen, 2018; R Core Team, 2021). This package enables the implementation of ordinal categorical variables as a response (i.e., gill health was scored from 0-5 in terms of severity [“no damage – severe damage”] rather than a continuous or integer value) by using cumulative link mixed models (CLMMs). These models

are also known as ordered regression models and proportional odds models. The main assumption for these models is that for each term, the slope between each pair of response levels is assumed to be the same, regardless of level. The basic cumulative link model defines cumulative probabilities as:

$$\gamma_{ij} = P(Y_i \leq j) = \pi_{i1} + \cdots + \pi_{ij}$$

Where Y_i is the ordinal response variable in $j = 1,..., J$ categories and follows a multinomial distribution with the parameter π. π_{ij} denotes the probability that the ith observation falls in the category j. Further, the models I built use the logit link function, of which the cumulative logits can be defined as:

$$\text{logit}(\gamma_{ij}) = \text{logit}(P(Y_i \leq j)) = \log \frac{P(Y_i \leq j)}{1 - P(Y_i \leq j)} \quad j = 1, \ldots, J$$

The cumulative logit model, therefore, is defined as:

$$\text{logit}(\gamma_{ij}) = \theta_j - x_i^T \beta$$

Where x_i are the explanatory variables for the ith observation and β are the regression parameters. The parameters θ_j are each cumulative logit for each j with each having its own intercept. With $x_i^T \beta$ being independent of j meaning β has the same effect for each of the J-1 cumulative logits (Christensen, 2018).

Model variables were selected similarly to the models used in Chapter 2, where highly correlated variables were identified using correlation plots and removed to prevent issues with collinearity in the models, and further variable selection was done using small-sample corrected Akaike information criterion (AICc) for each set of models for each site. All environmental data has been scaled and centered to a mean of 0, and the species counts of the biofoulant net-patches were scaled, but not centered. This is to minimize the variance due to the differing scales of

measurements between each environmental predictor variable, and to reduce the effect of extremely large counts from the biofouling count predictors (Schielzeth, 2010).

3.2.2.1. Environmental variables

I developed models to determine the effect of environmental variables on gill health severity scores at the Doctor Islets site. Variables included were iron, nitrate levels, pH, and the Event Day variable (as a random effect to examine the variance of all data recorded between each sampling date). For Wicklow Point, I used pH, temperature, dissolved oxygen and the Event Day variable in the model. As previously mentioned in Chapter 2, the Event Day variable is an integer value starting at 1 indicating the first day of the project when the first sample nets were deployed.

3.2.2.2. Biofoulant counts on net patches

In the Doctor Islets model that I used to explore relationships between the biofoulant species counts on the net patches, I found that models containing no counts of any of the species were considered most appropriate. The Doctor Islets model used the depth variable (a 5-leveled factor; 1, 5, 10, 15, and 20 m), the Event Week variable, and the Delta Day variable. Event Week was used as a random effect and is similar to the Event Day variable (numbered week starting at 1 from first week of deployment), and Delta Day consists of three levels (“Before”, “On”, “After”) that signified if the gill health scores were recorded before, on the exact date, or after the biofoulant samples were collected with the time limit used to calculate this variable being constrained to the Event Week number. As an example: a net-sample was collected on July 14/2020 (Event Week = 14) and during this week the gill scores were also recorded on July

14/2020 so the Delta Day for this set of scores would be “ON”. Another example would be for a net-patch collection on September 15/2020 (Event Week = 23) and during this week gill scores were recorded on September 18/2020 so the Delta Day for this set of scores would be “AFTER”.

Similar to Doctor Islets, the Wicklow Point model did not use any of the counts of the biofoulant species as variables. I used depth, the Event Week variable, and the Delta Day variable.

3.3.2.3. Hydroids on net patches

For both Doctor Islets and Wicklow Point, the models I developed to examine the relationship between the grams of any of four hydroid species groups (*Obelia* spp., *Ectopleura* spp., *Clytia* spp., and *Sarsia* spp.) did not include the mass of any hydroid species. Model selection for these models indicated only the Delta Day variable was appropriate, however, as these hydroid samples are collected from the biofoulant net patches, and thus share the same Delta Day variable and its influence on gill health, I determined a regression was unnecessary here.

3.3.2.4. Stinging-capable species in tow samples

To assess the effects of stinging-capable species identified in the tow samples from Doctor Islets on the gill health scores, I used only the Delta Day and Event Week variable as none of the species counts were appropriate for this model. For the Wicklow Point model, I used *Clytia* sp. (>10 mm), Diphydae sp., *Sarsia* sp., *Bourgainvilla* sp., and the Delta Day and Event Week variables.

3.3. Results

3.3.1 Gill health score profiles

Figures 3.1A-B show the individual scores given to each fish sampled for gill health at each sampling event from May-December 2020 (note that the net-patch study only ran until October 31). Scores range from 0 (no damage) to 5 (severe damage), with a maximum score of 4 recorded for both sites, however, most of the scores were 0 or 1 for both sites. The highest scores were recorded at Doctor Islet in the July 21 and November 20 samples, and at Wicklow Point in the July 23, October 14, and October 26 samples.

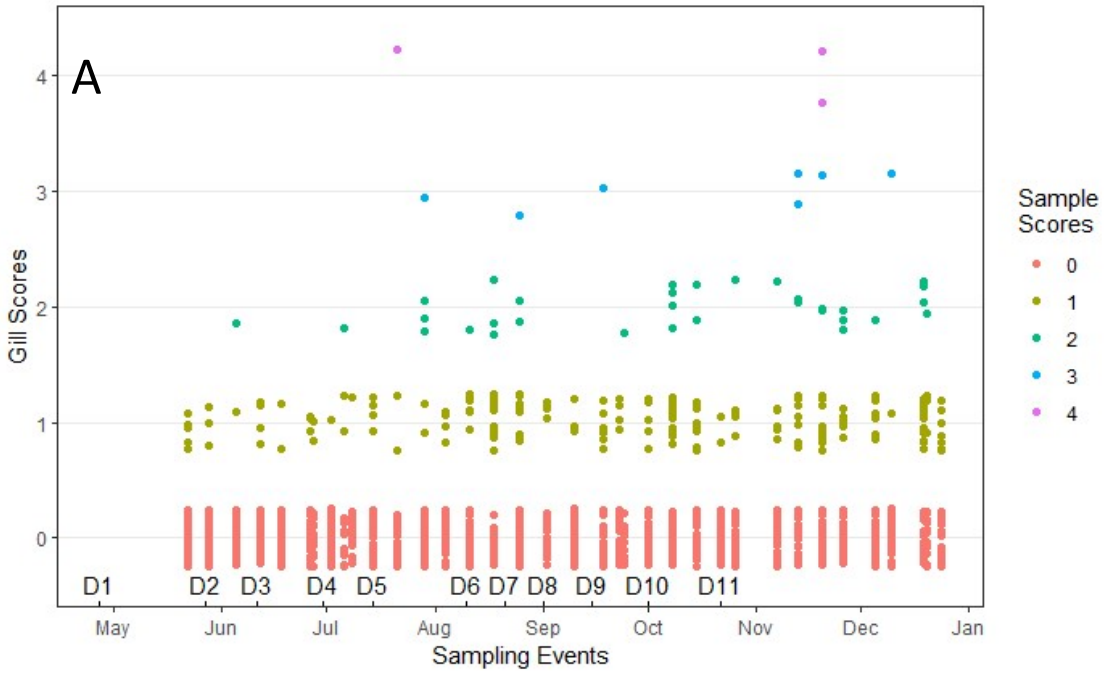

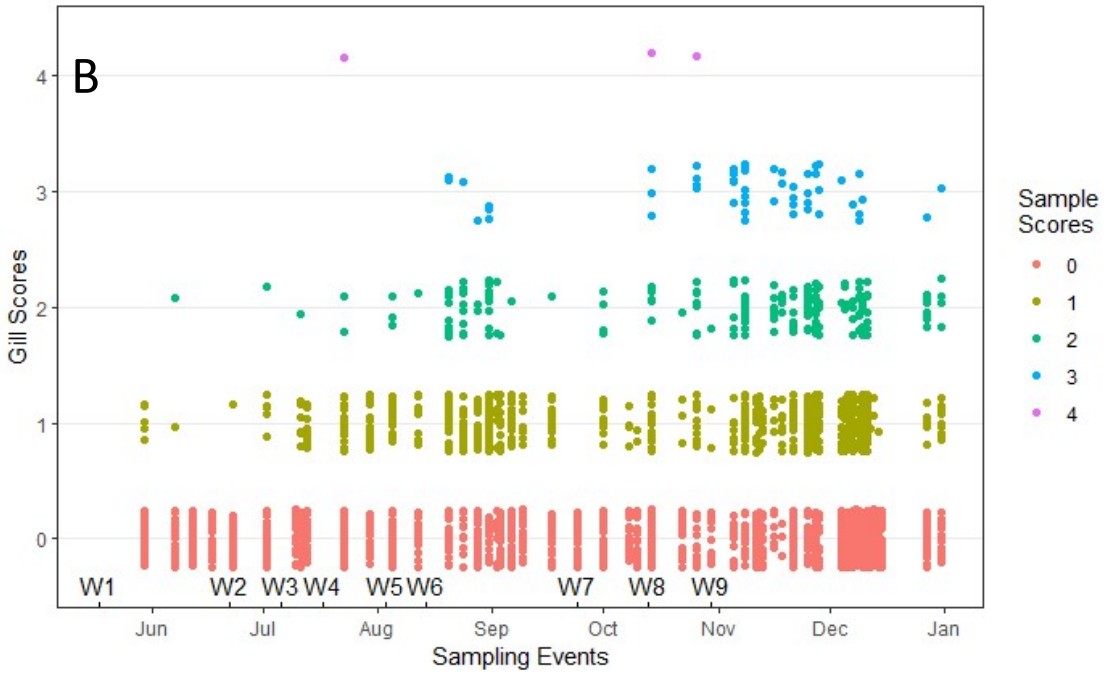

Figure 0.1 A-B: Individual gill health severity scores (0 = no damage – 5 = severe damage) for Doctor Islets (A) and Wicklow Point (B). Scores are jittered vertically to show density of each score for each sampling event. Labelled marks on axis (e.g., D4, W6, etc.) denote dates of biofouling net-patch collection. Note that the study period ends in late October, but gill scores were sampled until late December at both sites.

3.3.2. Statistical model results

3.3.2.1. Environmental parameters

Correlation plots used to aid model selection for this section can be found in the appendix (Figures A3.1 and A3.2). The model selected for Doctor Islets indicated that for each unit increase of iron, nitrate levels, and pH, the cumulative probability or log-odds of a more severe health score decreased (the odds of finding scores higher than 0), with pH having the largest effect size (Table 3.2). No measurements were positively contributing to the cumulative

probability of a more severe health score being sampled. Depth was tested and found to be not significant (Table 3.3). For Wicklow Point, the model I selected (Table 3.4) indicated that for each unit increase in temperature the cumulative probability of a more severe health score increased, and for each unit increase in pH and dissolved oxygen the cumulative probability decreased, and for each unit increase in temperature the cumulative probability increased (Table 3.2). Of the variables that negatively contributed to the model, dissolved oxygen had the larger effect size, and temperature had the largest total effect size.

Table 0.2: Regression summary for water parameters and gill health scores for Doctor Islets and Wicklow Point. Each intercept represents the tau cuts between each category of gill health score. S.e. is the standard error and 95% is the confidence interval.

	Doctor Islets	Wicklow Point
Intercept 0|1	2.214, s.e.=0.131, 95%=[1.956,2.471]	1.200, s.e.=0.198, 95%=[0.813,1.588]
Intercept 1|2	4.263, s.e.=0.239, 95%=[3.794,4.732]	3.534, s.e.=0.234, 95%=[3.076,3.992]
Intercept 2|3	5.998, s.e.=0.512, 95%=[4.994,7.001]	5.447, s.e.=0.362, 95%=[4.737,6.157]
Intercept 3|4	7.387, s.e.=1.006, 95%=[5.415,9.359]	7.868, s.e.=1.020, 95%=[5.868,9.867]
Iron	-0.289, s.e.=0.123, 95%=[-0.531,-0.047]	
Nitrates	-0.248, s.e.=0.124, 95%=[-0.491,-0.004]	
pH	-0.715, s.e.=0.135, 95%=[-0.980,-0.449]	-0.645, s.e.=0.234, 95%=[-1.103,-0.187]
Temperature		0.872, s.e.=0.232, 95%=[0.417,1.327]
Dissolved Oxygen		-0.715, s.e.=0.256, 95%=[-1.218,-0.213]
Num.Obs.	1160	1100

Table 0.3: Model selection using a cumulative link mixed-effects model with a logit link function to describe the effect of water parameters on the log-odds of recording gill health scores greater than 0 for Doctor Islets. The model with the lowest AICc used terms: iron, nitrate levels, pH, and the Event Day variable. The Random column represents the presence (+) or absence ( ) of the random grouping effect.

Model	Random	df	logLik	AICc	delta	weight
NO3+Iron+pH+EventDay	+	8	-466.90	949.92	0.00	0.77
DOmgL+NH3+NO3+PO43+Iron+pH+EventDay	+	11	-465.92	954.06	4.14	0.10
DOmgL+NH3+NO3+PO43+Iron+pH+Silica+EventDay	+	12	-465.15	954.58	4.66	0.08
Temp+DOmgL+NH3+NO3+PO43+Iron+pH+Silica+EventDay	+	13	-465.11	956.53	6.61	0.03
Temp+DOmgL+NH3+NO3+PO43+Iron+pH+Silica		12	-466.53	957.34	7.42	0.02
DOmgL+NH3+NO3+PO43+Iron+Silica+EventDay	+	11	-469.56	961.35	11.42	0.00
DOmgL+NH3+NO3+PO43+Iron+EventDay	+	10	-471.81	963.81	13.89	0.00
EventDay	+	5	-476.93	963.92	13.99	0.00
DOmgL+NH3+PO43+Iron+EventDay	+	9	-473.39	964.93	15.01	0.00

Table 0.4: Model selection using a cumulative link mixed-effects model with a logit link function to describe the effect of water parameters on the log-odds of recording gill health scores greater than 0 for Wicklow Point. The model with the lowest AICc used terms: dissolved oxygen, pH, temperature, and the Event Day variable. The column Random represents the presence (+) or absence ( ) of the random grouping effect.

Model	Random	df	logLik	AICc	delta	weight
Temp+DOmgL+pH+EventDay	+	8	-754.57	1,525.28	0.00	0.90
Temp+DOmgL+Salinity+NH3+NO3+Iron+pH+EventDay	+	12	-753.35	1,530.99	5.71	0.05
Temp+DOmgL+Salinity+NH3+NO3+Iron+pH+PO43+EventDay	+	13	-753.29	1,532.92	7.64	0.02
Temp+DOmgL+Salinity+NH3+NO3+Iron+pH+Silica+EventDay	+	13	-753.32	1,532.97	7.69	0.02
Temp+DOmgL+Salinity+NH3+NO3+Iron+pH+Silica+PO43+EventDay	+	14	-753.25	1,534.88	9.60	0.01
DOmgL+Salinity+NH3+NO3+Iron+pH+EventDay	+	11	-757.20	1,536.63	11.35	0.00
DOmgL+Salinity+NH3+NO3+Iron+pH+Silica+PO43+EventDay	+	13	-756.89	1,540.11	14.83	0.00
EventDay	+	5	-765.60	1,541.25	15.97	0.00
Temp+DOmgL+Salinity+NH3+NO3+Iron+pH+Silica+PO43		13	-780.82	1,587.98	62.70	0.00

3.3.2.2. Biofoulant counts on net patches

Correlation plots used to aid model selection for this section can be found in the appendix (Figures A3.3. and A3.4). The model I selected for Doctor Islets indicated that none of the counts are positively or negatively associated with higher gill health scores. In comparison to health scores recorded “after” (in which the intercept is used as a reference) the biofoulant sampling, the health scores recorded from both “before” and “on” are associated with lower gill health scores (Table 3.5). In addition, the biomass of the biofoulants (in grams) was tested and not found to be significant for this model (Table 3.6).

Table 0.5: Regression summary for net-patch biofoulant counts and gill health scores for Doctor Islets and Wicklow Point. Each intercept represents the tau cuts between each category of gill health score. S.e. is the standard error and 95% is the confidence interval.

	Doctor Islets	Wicklow Point
Intercept 0|1	0.164, s.e.=0.698, 95%=[-1.204,1.531]	1.390, s.e.=1.063, 95%=[-0.693,3.473]
Intercept 1|2	2.863, s.e.=0.703, 95%=[1.486,4.240]	3.403, s.e.=1.063, 95%=[1.319,5.487]
Intercept 2|3	4.496, s.e.=0.725, 95%=[3.075,5.917]	4.695, s.e.=1.065, 95%=[2.608,6.782]
Intercept 3|4		6.245, s.e.=1.072, 95%=[4.143,8.346]
Biomass (g)		0.000, s.e.=0.008, 95%=[-0.015,0.014]
Depth 5 m	0.001, s.e.=0.096, 95%=[-0.188,0.189]	-0.001, s.e.=0.081, 95%=[-0.160,0.157]
Depth 10 m	0.000, s.e.=0.096, 95%=[-0.189,0.189]	-0.002, s.e.=0.085, 95%=[-0.168,0.164]
Depth 15 m	0.001, s.e.=0.096, 95%=[-0.187,0.188]	-0.002, s.e.=0.085, 95%=[-0.168,0.164]
Depth 20 m	0.000, s.e.=0.095, 95%=[-0.187,0.187]	-0.002, s.e.=0.084, 95%=[-0.167,0.163]
Delta Day - BEFORE	-2.224, s.e.=0.749, 95%=[-3.693,-0.755]	-0.135, s.e.=1.426, 95%=[-2.930,2.661]
Delta Day - ON	-2.493, s.e.=0.801, 95%=[-4.062,-0.924]	-2.465, s.e.=0.144, 95%=[-2.748,-2.182]
Num.Obs.	11700	10260

Similar to Doctor Islets, no biofoulant counts were associated with higher gill health scores at Wicklow Point. In comparison to scores recorded “after” a sample collection, scores recorded “before” and “on” were negatively associated (Table 3.5). Biomass was tested and found to be significant (Table 3.7)

Table 0.6: Model selection using a cumulative link mixed-effects model with a logit link function to describe the effects of biofoulant counts on the log-odds of recording gill health scores greater than 0 for Doctor Islets. The model with the lowest AICc used terms: depth, which is a five-leveled factor (1, 5, 10, 15, and 20 m), DeltaDay which is a three-leveled factor ('before', 'on', 'after') that indicates if the gill scores were recorded before, on, or after a sample collection, and Event Week. The column Random represents the presence (+) or absence ( ) of the random grouping effect.

Model	Random	df	logLik	AICc	delta	weight
EventWeek+Depth+DeltaDays	+	10	-4,185.03	8,390.08	0.00	0.95
EventWeek+Depth+DeltaDays+Biv+Max+Pol	+	13	-4,185.02	8,396.06	5.98	0.05
EventWeek+Depth+DeltaDays+Biv+Gas+Mal+Ost+The	+	15	-4,185.00	8,400.04	9.96	0.01
EventWeek+Depth+DeltaDays+Ara+Ast+Col+Biv+Bra+Ech+For+Hyd+Ins+Max+Nem	+	19	-4,188.62	8,415.30	25.22	0.00
EventWeek+Biomass+DeltaDays+Ara+Ast+Col+Biv+Bra+Ech+For+Gas+Hyd+Ins+Mal+Max+Nem+Ost+Pol+The	+	23	-4,184.99	8,416.06	25.99	0.00
EventWeek+Depth+DeltaDays+Ara+Ast+Biv+Bra+Ech+Gas+Hyd+Ins+Mal+Nem+Ost+Pol+The	+	23	-4,184.99	8,416.07	25.99	0.00
EventWeek+Depth+DeltaDays+Ara+Ast+Col+Biv+Bra+Ech+For+Gas+Hyd+Ins+Mal+Max+Nem+Ost+Pol+The	+	26	-4,184.98	8,422.09	32.01	0.00
EventWeek+Depth+Biomass+DeltaDays+Ara+Ast+Col+Biv+Bra+Ech+For+Gas+Hyd+Ins+Mal+Max+Nem+Ost+Pol+The	+	27	-4,184.98	8,424.09	34.01	0.00
Depth+Biomass+DeltaDays+Ara+Ast+Col+Biv+Bra+Ech+For+Gas+Hyd+Ins+Mal+Max+Nem+Ost+Pol+The		26	-4,281.24	8,614.60	224.52	0.00

Ara= Arachnida, Ast=Asteroidea, Biv=Bivalvia, Bra=Branchipoda, Col=Collembola, Ech=Echinoidea, For=Foraminifera, Gas=Gastropoda, Hyd=Hydrozoa, Ins=Insecta, Mal=Malacostraca, Max=Maxillopoda, Nem=Nemotoda, Ost=Ostrocoda, Pol=Polychaeta, The=Thecostraca

Table 0.7: Model selection using a cumulative link mixed-effects model with a logit link function to describe the effects of biofoulant counts on the log-odds of recording gill health scores greater than 0 for Wicklow Point. The model with the lowest AICc used terms: depth, which is a five-leveled factor (1, 5, 10, 15, and 20 m), DeltaDay which is a three-leveled factor ('before', 'on', 'after') that indicates if the gill scores were recorded before, on, or after a sample collection, biomass (in grams), and Event Week were included. The column Random represents the presence (+) or absence ( ) of the random grouping effect.

Model	Random	df	logLik	AICc	delta	weight
EventWeek+Depth+Biomass+DeltaDays	+	12	-6,907.34	13,838.71	0.00	0.73
EventWeek+Depth+Biomass+DeltaDays+Biv	+	13	-6,907.34	13,840.72	2.01	0.27
EventWeek+Depth+Biomass+DeltaDays+Ast+Biv+For+Gas+Ins+Mal+Max	+	19	-6,907.34	13,852.75	14.04	0.00
EventWeek+Depth+Biomass+DeltaDays+Biv+Ech+Hyd+Nem+Ost+Pla+Pol+The	+	20	-6,907.33	13,854.75	16.04	0.00
EventWeek+Biomass+DeltaDays+Ast+Biv+Ech+For+Gas+Hyd+Ins+Mal+Max+Nem+Ost+Pla+Pol+The	+	22	-6,907.33	13,858.76	20.04	0.00
EventWeek+Depth+Biomass+DeltaDays+Ast+Biv+Ech+Hyd+Ins+Mal+Max+Nem+Ost+Pla+Pol+The	+	23	-6,907.33	13,860.77	22.06	0.00
EventWeek+Depth+DeltaDays+Ast+Biv+Ech+For+Gas+Hyd+Ins+Mal+Max+Nem+Ost+Pla+Pol+The	+	25	-6,907.33	13,864.78	26.07	0.00
EventWeek+Depth+Biomass+DeltaDays+Ast+Biv+Ech+For+Gas+Hyd+Ins+Mal+Max+Nem+Ost+Pla+Pol+The	+	26	-6,907.33	13,866.79	28.08	0.00
Depth+Biomass+DeltaDays+Ast+Biv+Ech+For+Gas+Hyd+Ins+Mal+Max+Nem+Ost+Pla+Pol+The		25	-7,281.47	14,613.06	774.35	0.00

Ast=Asteroidea, Biv=Bivalvia, Ech=Echinoidea, For=Foraminifera, Gas=Gastropoda, Hyd=Hydrozoa, Ins=Insecta, Mal=Malacostraca, Max=Maxillopoda, Nem=Nemotoda, Ost=Ostrocoda, Pla=Plathyhelminthes, The=Thecostraca

3.3.2.3. Hydroid species on net patches

For both Doctor Islets and Wicklow Point, no measured variables were associated with an increase in the cumulative probability of recording a higher gill health score (Table 3.8, 3.9). Model selection included the terms Delta Day and the Event Week variables for both sites, however, because the hydroid samples were collected from the same net patches as the biofoulant count samples, the influences of these variables on gill health scores was the same and thus no regression was done.

Table 0.8: Model selection using a cumulative link mixed-effects model with a logit link function to describe the effects of biomass of net-patch hydroids on the log-odds of recording gill health scores greater than 0 for Doctor Islets. The model with the lowest AICc used terms: DeltaDay which is a three-leveled factor ('before', 'on', 'after') that indicates if the gill scores were recorded before, on, or after a sample collection and Event Week. The column Random represents the presence (+) or absence ( ) of the random grouping effect.

Model	Random	df	logLik	AICc	delta	weight
EventWeek+DeltaDays	+	6	-1,960.54	3,933.09	0.00	0.39
EventWeek+Ectopleura+DeltaDays	+	7	-1,960.54	3,935.09	2.00	0.14
EventWeek+Obelia+DeltaDays	+	7	-1,960.54	3,935.09	2.00	0.14
EventWeek+Sarsia+DeltaDays	+	7	-1,960.54	3,935.09	2.00	0.14
EventWeek+Obelia+Ectopleura+DeltaDays	+	8	-1,960.54	3,937.10	4.01	0.05
EventWeek+Sarsia+Ectopleura+DeltaDays	+	8	-1,960.54	3,937.10	4.01	0.05
EventWeek+Obelia+Sarsia+DeltaDays	+	8	-1,960.54	3,937.10	4.01	0.05
EventWeek+Obelia+Ectopleura+DeltaDays	+	9	-1,960.54	3,939.10	6.02	0.02
EventWeek+Depth+Obelia+Sarsia+Ectopleura+DeltaDays	+	13	-1,960.53	3,947.12	14.03	0.00
Depth+Obelia+Sarsia+Ectopleura+DeltaDays		12	-2,023.84	4,071.74	138.65	0.00

Table 0.9: Model selection using a cumulative link mixed-effects model with a logit link function to describe the effects of biomass of net-patch hydroids on the log-odds of recording gill health scores greater than 0 for Wicklow Point The model with the lowest AICc used terms: DeltaDay which is a three-leveled factor ('before', 'on', 'after') that indicates if the gill scores were recorded before, on, or after a sample collection and Event Week. The column Random represents the presence (+) or absence ( ) of the random grouping effect.

Model	Random	df	logLik	AICc	delta	weight
EventWeek+DeltaDays	+	7	-2,178.28	4,370.58	0.00	0.39
EventWeek+Sarsia+DeltaDays	+	8	-2,178.28	4,372.59	2.01	0.14
EventWeek+Obelia+DeltaDays	+	8	-2,178.28	4,372.59	2.01	0.14
EventWeek+Clytia+DeltaDays	+	8	-2,178.28	4,372.59	2.01	0.14
EventWeek+Obelia+Sarsia+DeltaDays	+	9	-2,178.28	4,374.60	4.01	0.05
EventWeek+Obelia+Clytia+DeltaDays	+	9	-2,178.28	4,374.60	4.01	0.05
EventWeek+Sarsia+Clytia+DeltaDays	+	9	-2,178.28	4,374.60	4.01	0.05
EventWeek+Obelia+Sarsia+Clytia+DeltaDays	+	10	-2,178.28	4,376.61	6.02	0.02
EventWeek+Depth+Obelia+Sarsia+Clytia+DeltaDays	+	14	-2,178.28	4,384.65	14.07	0.00
Depth+Obelia+Sarsia+Clytia+DeltaDays		13	-2,567.35	5,160.78	790.20	0.00

3.3.2.4. Stinging-capable species in tow samples

Correlation plots used to aid model selection for this section can be found in the appendix (Figures A3.5 and A3.6). For Doctor Islets, I found that no counts of stinging-species collected in tows were associated with gill health scores (Table 3.10). The Delta Day variable tested significant (Table 3.11) and, in comparison to scores sampled "after" tow sample collection, I found that scores sampled "before" and "on" a tow sample collection were negatively associated.

Table 0.10: Regression summary for counts of stinging-capable species in tow samples and gill health scores for Doctor Islets and Wicklow Point. Each intercept represents the tau cuts between each category of gill health score. S.e. is the standard error and 95% is the confidence interval.

	Doctor Islets	Wicklow Point
Intercept 0|1	2.049, s.e.=0.300, 95%=[1.460,2.638]	0.188, s.e.=0.350, 95%=[-0.498,0.874]
Intercept 1|2	4.359, s.e.=0.352, 95%=[3.670,5.049]	2.218, s.e.=0.356, 95%=[1.521,2.915]
Intercept 2|3	6.117, s.e.=0.537, 95%=[5.065,7.169]	3.763, s.e.=0.388, 95%=[3.004,4.523]
Intercept 3|4	6.340, s.e.=0.582, 95%=[5.200,7.480]	5.623, s.e.=0.563, 95%=[4.518,6.727]
Bourgainvilla		-1.714, s.e.=1.438, 95%=[-4.533,1.105]
Clytia >10 mm		-0.451, s.e.=0.123, 95%=[-0.693,-0.209]
Diphydae		-0.004, s.e.=0.029, 95%=[-0.062,0.053]
Sarsia		0.179, s.e.=0.051, 95%=[0.080,0.278]
Delta Day - BEFORE	-0.264, s.e.=0.321, 95%=[-0.893,0.364]	-1.307, s.e.=0.214, 95%=[-1.727,-0.887]
Delta Day - ON	-0.383, s.e.=0.380, 95%=[-1.129,0.362]	-1.164, s.e.=0.273, 95%=[-1.699,-0.629]
Num.Obs.	1820	1960

Table 0.11: Model selection using a cumulative link mixed-effects model with a logit link function to describe the effects of counts of stinging-capable species in tow samples on the log-odds of recording gill health scores greater than 0 for Doctor Islets. The model with the lowest AICc used terms: DeltaDay which is a three-leveled factor ('before', 'on', 'after') that indicates if the gill scores were recorded before, on, or after a sample collection and Event Week. The column Random represents the presence (+) or absence ( ) of the random grouping effect.

Model	Random	df	logLik	AICc	delta	weight
EventWeek+DeltaDay	+	7	-686.19	1,386.44	0.00	0.50
EventWeek+Eup+DeltaDay	+	8	-685.86	1,387.81	1.36	0.25
EventWeek+Sarsia+Eup+DeltaDay	+	9	-685.38	1,388.85	2.41	0.15
EventWeek+Sarsia+Pro+Eup+DeltaDay	+	10	-685.37	1,390.86	4.42	0.06
EventWeek+Dip+Sar+Pro+Eup+DeltaDay	+	11	-684.70	1,391.54	5.10	0.04
EventWeek+C10+Cly+Ect+Mit+Eup+Agl+DeltaDay	+	13	-685.40	1,397.00	10.56	0.00
EventWeek+Eud+Dip+Ect+Sar+Hal+Pro+Bou+Aqu+Cat+Mit+Eup+Agl+DeltaDay	+	17	-683.45	1,401.24	14.80	0.00
EventWeek+Obe+Mug+Eud+Dip+Sar+Phi+Hal+Pro+Bou+Aqu+Cat+Eup+DeltaDay	+	18	-682.87	1,402.13	15.69	0.00
EventWeek+C10+Cly+Obe+Mug+Eud+Dip+Ect+Sar+Phi+Hal+Pro+Bou+Aqu+Cat+Mit+Eup+Agl+DeltaDay	+	22	-682.05	1,408.67	22.23	0.00
EventWeek+C10+Cly+Obe+Mug+Eud+Dip+Ect+Sar+Phi+Hal+Pro+Aqu+Cat+Mit+Eup+DeltaDay	+	22	-682.05	1,408.67	22.23	0.00
C10+Cly+Obe+Mug+Eud+Dip+Ect+Sar+Phi+Hal+Pro+Bou+Aqu+Cat+Mit+Eup+Agl+DeltaDay		21	-694.44	1,431.40	44.96	0.00

C10=Clytia >10 mm, Cly=Clytia <10 mm, Obe=Obelia, Mug=Muggiaea, Eud=Muggiaea Eudoxid, Dip=Diphydae, Ect=Ectopleura, Sar=Sarsia, Phi=Phiallela, Hal=Halotholus, Pro=Proboscidactyla, Bou=Bourgainvilla, Aqu=Aqueorea, Cat=Catablema, Mit=Mitrocomella, Eup=Euphysa, Agl=Aglantha

For Wicklow Point, with each increase in counts of *Bourgainvilla* sp., *Clytia* sp. (>10 mm), and Diphydae spp. the cumulative probability of recording a higher gill score decreased, and for each count increase of *Sarsia* spp., the probability increased (Table 3.10). In addition, I tested the Delta Day variable and found it to be significant (Table 3.12). The Delta Day variable indicates that in comparison to health scores sampled "after" a tow sample collection, those scored "before" or "on" the same date indicated a lower probability of recording higher health scores.

Table 0.12: Model selection using a cumulative link mixed-effects model with a logit link function to describe the effects of counts of stinging-capable species in tow samples on the log-odds of recording gill health scores greater than 0 for Wicklow Point. The model with the lowest AICc used terms: Bourgainvilla, Clytia <10 mm, Diphydae, and Sarsia. In addition, Delta Day which is a three-leveled factor ('before', 'on', 'after') that indicates if the gill scores were recorded before, on, or after a sample collection and Event Week were included. The column Random represents the presence (+) or absence ( ) of the random grouping effect.

Model	Random	df	logLik	AICc	delta	weight
EventWeek+C10+Dip+Sar+Bou+DeltaDay	+	12	-1,347.33	2,718.82	0.00	0.48
EventWeek+C10+Dip+Sar+Ect+Bou+Aqu+Cat+Mit+DeltaDay	+	13	-1,346.37	2,718.92	0.10	0.46
EventWeek+C10+Cly+Eud+Dip+Ect+Sar+Phi+Hal+Pro+Bou+Aqu+Cat+Mit+Eup+Agl+DeltaDay	+	19	-1,342.86	2,724.11	5.29	0.03
EventWeek+C10+Cly+Obe+Mug+Eud+Dip+Sar+Phi+Hal+Pro+Bou+Aqu+Cat+Eup+Agl+DeltaDay	+	19	-1,343.91	2,726.21	7.39	0.01
EventWeek+C10+Dip+DeltaDay	+	9	-1,354.56	2,727.22	8.40	0.01
EventWeek+C10+Cly+Obe+Mug+Eud+Dip+Ect+Sar+Phi+Hal+Pro+Bou+Aqu+Cat+Mit+Eup+Agl+DeltaDay	+	21	-1,342.55	2,727.58	8.76	0.01
EventWeek+Ect+Mit+DeltaDay	+	9	-1,355.38	2,728.86	10.04	0.00
EventWeek+Ect+DeltaDay	+	9	-1,355.38	2,728.86	10.04	0.00
EventWeek+DeltaDay	+	7	-1,358.58	2,731.21	12.40	0.00
C10+Cly+Obe+Mug+Eud+Dip+Ect+Sar+Phi+Hal+Pro+Bou+Aqu+Cat+Mit+Eup+Agl+DeltaDay		20	-1,423.71	2,887.85	169.03	0.00

C10=Clytia >10 mm, Cly=Clytia <10 mm, Obe=Obelia, Mug=Muggiaea, Eud=Muggiaea Eudoxid, Dip=Diphydae, Ect=Ectopleura, Sar=Sarsia, Phi=Phiallela, Hal=Halotholus, Pro=Proboscidactyla, Bou=Bourgainvilla, Aqu=Aqueorea, Cat=Catablema, Mit=Mitrocomella, Eup=Euphysa, Agl=Aglantha

3.4. Discussion

3.4.1. Gill health scores

The gill health of farmed finfish, and salmonids especially, is a significant challenge for aquaculture globally (Rodger, 2007). Gills are especially vulnerable to external factors and are involved in many body processes beyond respiration. Gill disorders are the largest cause of marine aquaculture loss, both due to mortality, reduced growth rates, and treatment and disposal costs (Rodger, 2007). The causes of gill disorders can be broadly grouped into seven aetiologies of gill diseases: amoebic, parasites, viral, bacterial, zooplankton, algal, and chemical or toxin related. These can be observed singly or combined, which is referred to as proliferative or complex proliferative gill disease (PGD, CPG) with each term overlapping in use (Boerlage et al., 2020; Rodger, 2007).

Gills were non-lethally scored every week from one, two, or three nets, depending on the week. Some weeks were sampled more than three times if scores were higher than expected, or during treatments for issues unrelated to gill health. One net was designated the “fish health pen” which was sampled every week, and the other scores were sampled randomly from the study pens every two or three weeks. Figures 3.1A and B show the individual scores from each sample at each site and there are several similarities between Doctor Islets and Wicklow Point. Both sites largely recorded a score of 0 or 1, with only a few individuals scoring 2 or higher to a maximum score of 4 (Figure 3.1A-B), and both sites saw a peak in scores in early-August and early or late November at Doctor Islets and Wicklow Point, respectively.

3.4.2. Water parameters with gill scores

Variables pH, nitrate levels, and iron were negatively associated with the odds of finding

a score higher than 0 at Doctor Islets, with pH having the largest effect size (Table 3.4). There were no peaks or dips in pH levels recorded at Doctor Islets when the gill scores were high, but the pH steadily decreases over the season and the lowest levels were recorded right before higher gill scores were recorded (Figure 2.4D). This is speculation, however, because environmental parameter monitoring stopped at the end of October while gill health sampling continued until the end of December at both sites. Some studies have shown that exposure to low pH stunted growth in Atlantic salmon, although this seemed to be recoverable or not statistically significant within certain temperature thresholds (Fivelstad et al., 1998).

For a better visualization, I created graphs to represent the predicted probability of each gill score for the span of measurements for each water parameter in the model for Doctor Islets (Figure 3.2). Typically, on these farm sites, a score of 3 or higher (orange/red) is considered cause for concern, with a score of 2 (yellow) cause for closer monitoring, and a score of 0 or 1 (blue) considered non-issues (B. Vornicu, pers. comm.). The prediction graph for pH shows a relatively steep curve towards higher scores at lower pH values. However, in this study the probability of a score being recorded as 3 or higher is still very small.

Iron measurements were sporadic during the study period at both sites, but during August when the gill scores were highest, iron levels were on the lower side of what was recorded. The prediction graph showed that scores tended to be higher as iron levels approached zero, but the probability of a score being in a concerning category was miniscule. The prediction graph for nitrate levels shows a similar distribution of probabilities as iron, with a trend towards higher probabilities as nitrate levels approached zero. Nitrate levels were stable at Doctor Islets until the end of August when the levels start to increase for the rest of the season. The highest gill scores recorded for Doctor Islets were during August when nitrate levels were low, although as

with Iron, the probabilities of being in a concerning category was minimal at any nitrate measurement.

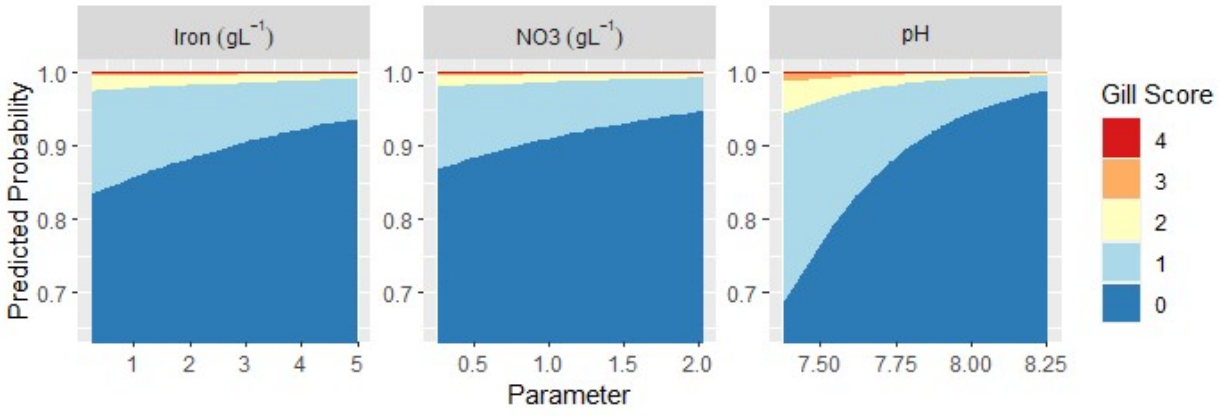

Figure 0.2: The predicted probability of each gill health score for each water parameter, iron, nitrate levels, and pH for Doctor Islets. Blue indicates no concern, yellow indicates caution, and orange/red indicates scores of concern.

At Wicklow Point, temperature had the largest effect size and was positively associated. On Figure 2.4A, we can see that temperatures recorded at Wicklow Point were within normal ranges, being higher in the summer and lower in spring and fall. No peaks or dips were observed during times when gill scores were high, and daily variation was minimal. On the prediction graphs (Figure 3.3) we see that there was a relatively large probability of a non-zero score being recorded (~60%) as temperatures increased, but, as with all the variables, the probability of a concerning score was very small. Dissolved oxygen was negatively associated with scores at Wicklow Point and on Figure 2.4B, we do see a general decrease through the study period. On the prediction graph we can see that gill health scores increase as dissolved oxygen decreases, but the probabilities are low in comparison to the other parameters. There was also effectively no probability that a score of 4 would be recorded at any of the oxygen concentration levels.

Salmonids are generally adapted to cool waters with a high oxygen content, and exposure to low levels can affect appetite, growth, increase cortisol levels, and interfere with immune responses (Krasnov et al., 2021; Oldham et al., 2020; Remen et al., 2012).

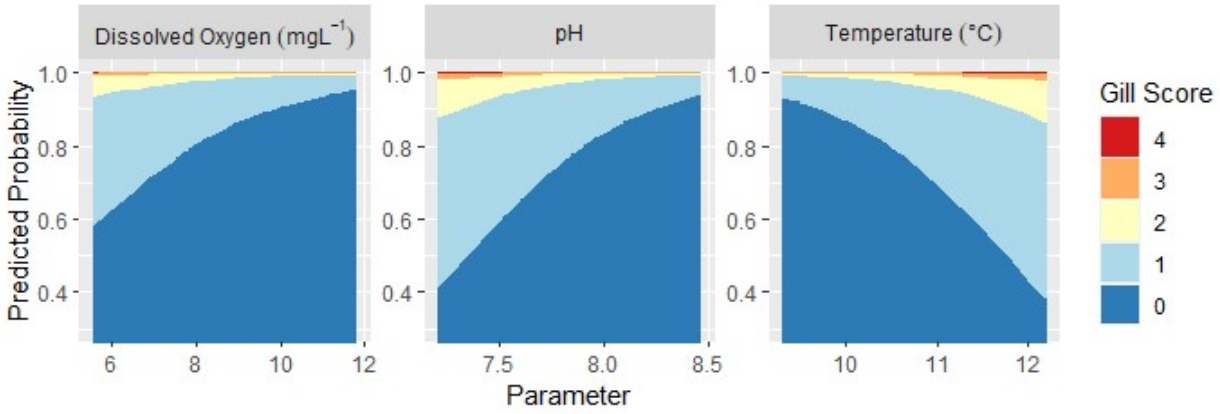

Figure 0.3: The predicted probability of each gill health score for each water parameter, dissolved oxygen, pH, and temperature for Wicklow Point. Blue indicates no concern, yellow indicates caution, and orange/red indicates scores of concern.

Like Doctor Islets, the pH at Wicklow Point was negatively associated with gill scores, and we do see on Figure 2.4D that pH decreases slightly over the season. The period where Wicklow Point experience several higher scores (August); however, the pH was stable and within a normal range. There was a dip in pH around September, and we can see on Figure 3.1B that not only was there an increased sampling effort, but there were also several individuals with gill scores of 3, indicating a cause for concern. This is supported by the prediction graph (Figure 3.3) as we see that the probabilities of scores higher than 0 are highest when pH is around the values recorded during the dip (~7.25).

3.4.3. Biofoulant counts on net patches with gill health scores

Model selection was extensive and for both Doctor Islets and Wicklow Point (Table 3.3, 3.4), but I eventually determined that no counts of any of the biofoulant species were associated with the gill health scores, positively or negatively. In addition, the total wet-weight biomass of the samples were tested as well and was only considered significant at Wicklow Point, however the effect size is so small it is negligible. This is similar to what I found for the depth variables at each site as well, in that the effect sizes are very small. This indicates that most of the explanatory power in the trends of the gill health scores lies with the Event Week random effect variable, and the Delta Day variable.

The Delta Day variable is a three-leveled factor that indicates when the gill health scores were sampled in relation to the net-patch collection. Generally, the fish net pens were cleaned via *in situ* power-washing on either the same day, or early the next day after the patches were collected (B. Vornicu, pers. comm.), but the gill health scoring followed a separate schedule and would often be sampled up to several days before or after a collection, and sometimes several times over consecutive days. Hence, I created the Delta Day variable by taking the difference in the sample collection dates and the gill score sampling dates for each week; if the difference was negative, the gill scores had been sampled "before" the collection, a zero indicated the gills were scored "on" the same date, and a positive number indicated the gills were scored "after" a collection. The coefficient generated by the model uses the intercept of "after" as a reference.

Table 3.7 showed that at Doctor Islets the effect sizes were relatively large in comparison to the effects of the depth variable, and they were similar to each other, with the effect size of the "on" level being slightly larger. At Wicklow Point the "on" level was relatively large in comparison to the depth variable and was much larger than the "before" level. This is visualized

in Figure 3.4 which shows the probability calculated from these models of each gill score for each site based on collection status. Both sites showed that gill scores sampled after a net patch collection had a much higher probability of scoring higher in severity, with Doctor Islets having over a 50% probability of recording a score higher than 0. While none of the biofoulants were associated with the gill scores recorded in this study, Figure 3.4 supports the hypothesis of this thesis that *in-situ* power washing of net pens may be impacting the gill health of Atlantic salmon.

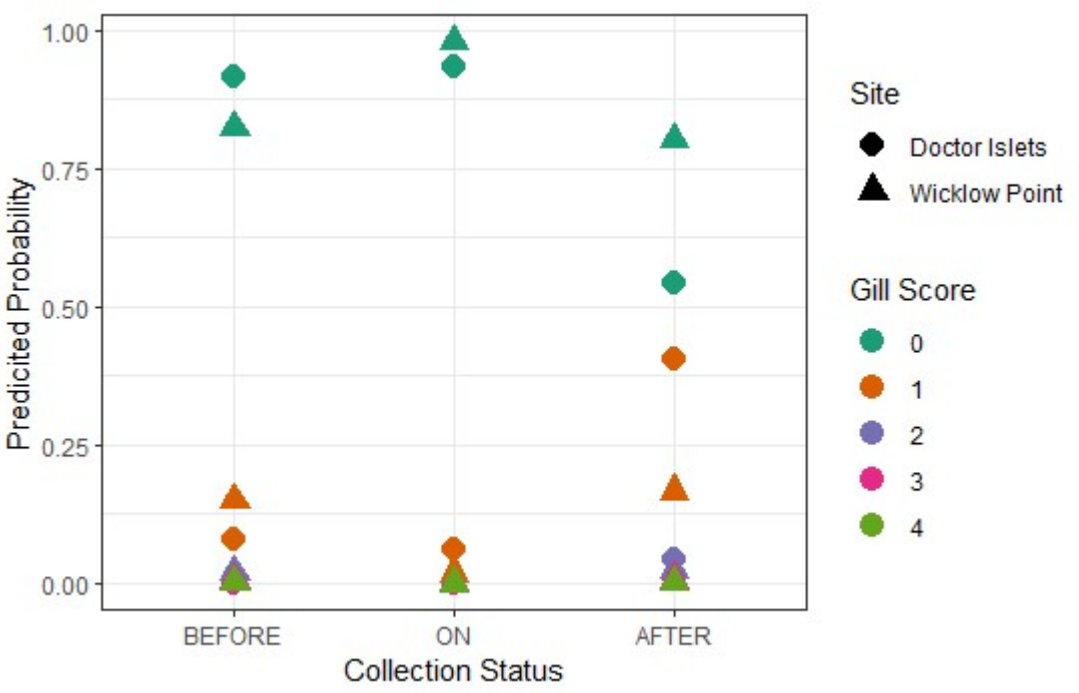

Figure 0.4: The predicted probabilities of each gill health score based on collection status of net patches constrained to the "Event Week". "Before" indicates the gill health scores were sample before the net patches were collected, "On" indicates the same day, and "After" indicates the gill scores were sampled after the tow samples were collected.

3.4.4. Hydroid biomass on net patches with gill scores

The hydroid composition of the biofouling community has been involved in several harmful incidents in finfish aquaculture in the Mediterranean Sea and Northern Europe (Bosch-Belmar et al., 2019; Gansel et al., 2015; Martell et al., 2018). The focus of most of these studies on members of the genus *Ectopleura* (Baxter et al., 2011; Bosch-Belmar et al., 2017; Fitridge and Keough, 2013) and *Obelia* (Bosch-Belmar et al., 2017; Floerl et al., 2016; Gartner et al., 2016; Martell et al., 2018). In addition, large amounts of *Obelia* spp. hydroids were identified in the biofouling community on the net-pens of several Atlantic salmon farms in British Columbia during periods where fish experienced mortalities and gill and mouth injuries typical of contact envenomation (J. Pudota, pers. comm.).

The model selection results show that none of the hydroid species (*Obelia* spp., *Sarsia* sp., *Ectopleura* sp., and *Clytia* sp.) that occurred at each site were associated with the gill health scores (Table 3.8, 3.9). The Delta Day and Event Week variable has the same affect on gill scores as the biofoulant model because the biofoulants and hydroids were collected from the same net-patches as detailed in the methods section of Chapter 2. Thus, a regression model was unnecessary. It is worth reiterating the Event Week variance (as it is in the biofoulant count models as well) is large and likely indicates that the majority of the variation across each sampling date could be contributed by the Event Week (representing the time of year) rather than the mass of hydroids present.

3.4.5. Stinging-capable species in tow samples with gill scores

In addition to the challenges associated with hydroid growth in aquaculture settings, free-swimming jellyfish also present an issue that comes with its own problems. Unlike hydroids, which are mainly of concern when cleaning the net-pens, jellyfish are capable of swimming or

being carried by currents into the nets where fish can suffer injuries related to contact envenomation such as skin gill and mouth injuries. Several species, including some identified in this study, have been implicit in mass mortalities globally (Bosch-Belmar et al.,2017; Bosch-Belmar et al., 2019; Gansel et al., 2015; Martell et al., 2018).

For Doctor Islets, I determined that no counts of stinging-capable species from the tow samples were associated with gill health, however, for Wicklow Point, *Bourgainvilla* sp., *Clytia gregaria* >10 mm, Diphydae spp., and *Sarsia* spp. were all associated with gill scores. *Sarsia* spp. was positively associated, and the rest were negatively associated. Figure 3.5 and Table 3.10 show that *Bourgainvilla* sp., *Clytia gregaria,* and Diphydae spp. are negatively associated with gill scores, meaning that in samples when more of these species are counted, gill health scores tend to be less severe. *Bourgainvilla* spp, *Clytia gregaria,* and Diphydae are not known nuisance species to aquaculture. It is possible that something these species are preying on affects the gill health of fish either directly or indirectly and as such, with each increase in individuals, the harmful zooplankton populations decrease. Another possibility is that they crowd out or are in some way allelopathic to other species which may have more ability to harm the gills of Atlantic salmon.

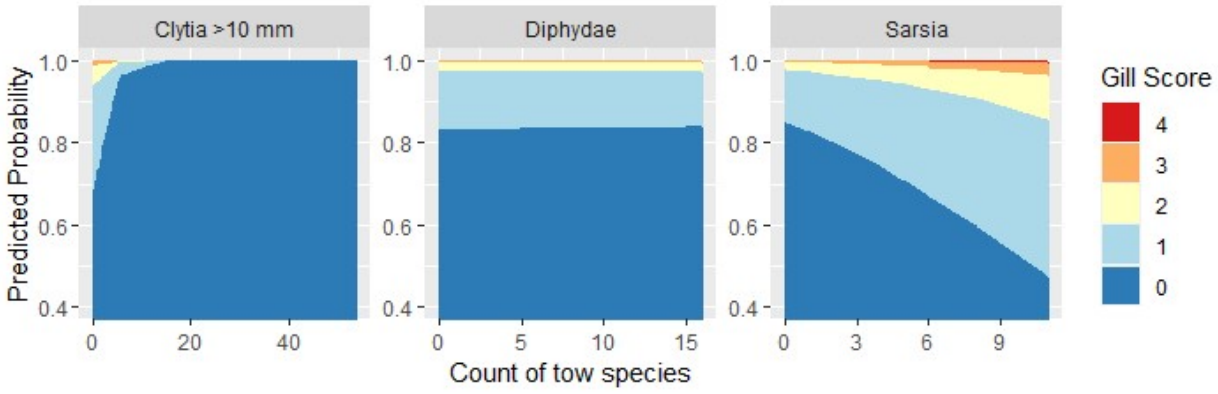

Figure 0.5: The predicted probability of each gill health score for each count of Clytia sp. (>10 mm), Diphydae spp., and Sarsia spp. in tow samples for Wicklow Point. Bourgainvilla sp. is not shown due only having a maximum count of 1 individual. Blue indicates no concern, yellow indicates caution, and orange/red indicates scores of concern.

Sarsia sp. was only present in a few months (May, June, and August; Figure 2.12), and the prediction plot (Figure 3.6) shows that with each individual counted in a sample, the probability of a score greater than 0 increases sharply, at one point reaching a greater than 50% chance that a gill score will be greater than 0, and a greater than 10% chance that a gill score will be in the caution/concerning range (≥2). Like the other species *Sarsia* spp. are not known as either a hydroid or in the free-swimming medusa form to be a nuisance species to either fin or shellfish aquaculture, although *Sarsia tubulosa*, which was one of the *Sarsia* species I identified in this study, is known to prey on herring roe and larvae (Purcell and Grover, 1990). It is important to note, however, that no study to my knowledge has examined the ability of hydroids or jellyfish to harm Atlantic salmon in British Columbia which has its own unique geography, water chemistry, and ecology. All cnidarians have cnidocytes that are capable of stinging, and as such have the potential to cause harm.

Like the models for the net patch samples, the collection status of gill health scores based on tow sample collection was examined. I found that the predictions look similar to the biofoulant collection status graph (Figure 3.4) with gill scores collected after a tow sample predicted to have a greater probability of higher gill scores.

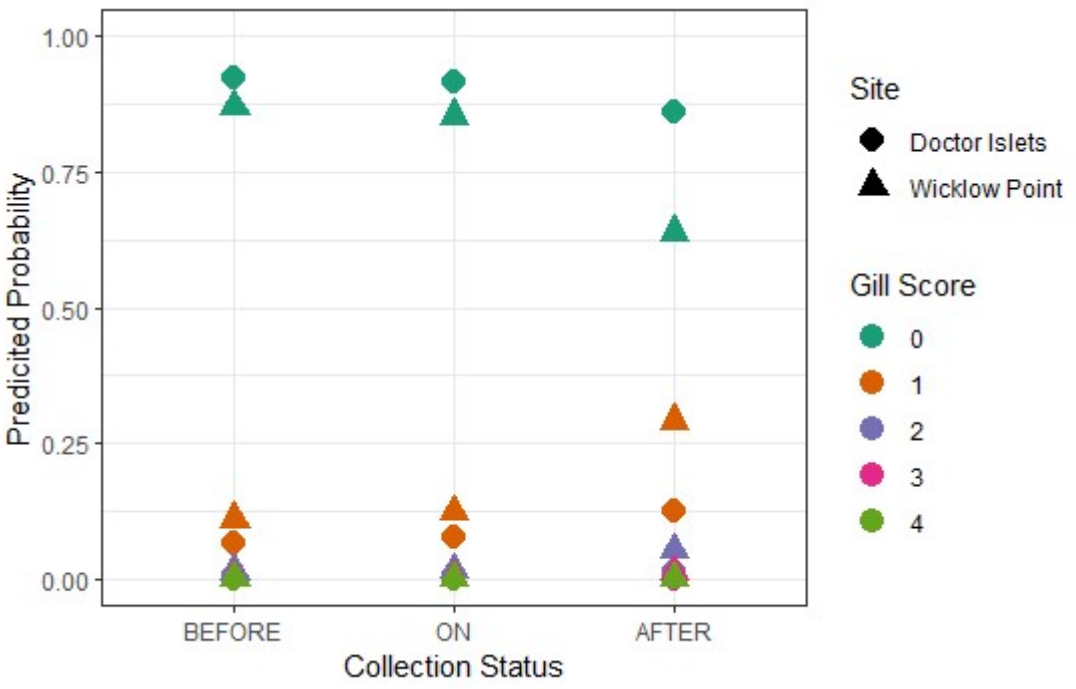

Figure 0.6: The predicted probabilities of each gill health score based on collection status of the tow samples constrained to the "Event Week". "Before" indicates the gill health scores were sample before the tow samples were collected, "On" indicates the same day, and "After" indicates the gill scores were sampled after the tow samples were collected.

While this result was relatively clear for the net-patch study as it had been hypothesized that net cleaning was a potential cause for injuries to gill health, why gill scores would be predicted to be higher after a tow sample collection is not as clear as nothing is being disturbed or distributed into the water column. It's entirely possible that several of the gill scores were sampled after blooms of stinging species, although we saw from Table 3.13 that Doctor Islets indicated no association with any of the stinging species. Another possible, and more probable, reason for this may be that these results are coincidental in the timing of when higher scores were recorded. This latter reason may be supported by the high variance in the Event Week variables at each site, indicating that much of the sample-to-sample variation is due to

seasonality.

As with the biofoulant community in Chapter 2, there are other variables that I did not examine that may play a part in the gill health of the Atlantic salmon at these farms. One of these variables can be seen on Figure 3.1B, in which there was a long period in between sampling dates (W6 and W7) because of a net change. One can see from the figure that directly after the change (which occurred on August 14) there was a cluster of higher gill scores.

An additional variable that had not been accounted for in the duration of the study was the effect of crowding during the grow-out season. Atlantic salmon are stocked as smolts weighing 100-250 grams and typically harvested after 2 years weighing approximate 3-6 kg ("Salmon Farming Industry Handbook", 2023). After 6 months, which was the duration of the study, the stocked smolts would have considerably less room to maneuver. Several studies have examined the effects of high stocking densities, with results such as high densities having a significant impact on the survival rate of AGD affected salmon and high densities impairing immune system functions by chronically stressing the fish (Crosbie et al., 2010; Sundh et al., 2019).

3.5. Conclusion

The first question Chapter 3 sought to explore was the correlation between the water parameters and gill health. Several water parameters were significantly associated with higher gill scores at each site. At Doctor Islets, pH, nitrate levels, and iron were negatively and significantly associated with gill scores. At Wicklow Point, temperature was positively associated with gill scores, and dissolved oxygen and pH were negatively associated. As with Chapter 2, no individual parameters stood out as being atypical. In addition, the gill health

scores for the duration of this study were unproblematic and the farms suffered no unusual illnesses or mortalities.

The second question dealt with how the biofouling community – the net-patch biofoulant counts, hydroid mass, and tow counts – were correlated with gill health. The net patch biofoulant count models revealed that no species in this study were significantly associated with the gill scores recorded. However, the Delta Day variable, created to predict the probability of a gill score when sampled before, on, or after a net sample collection (and thus a net-pen cleaning event) revealed that when gills were scored after a cleaning event, the probability of a higher gill score increased. This supports the hypothesis of this thesis that in situ cleaning of net-pens via power-washing may be impacting the gill health of Atlantic salmon.

The models built to examine the mass of hydroids on the net patches and the gill health scores revealed that none of the four species groups (*Obelia* sp., *Sarsia* sp., *Ectopleura* sp., and *Clytia* sp.) were significantly associated at either site. The random effect (Event Week) variance for these models was high, indicating that the variation in the data that these models examined was better explained by sample-to-sample variation than any of the hydroid species.

None of the stinging-capable species counted in the tow samples at Doctor Islets was associated with gill scores, however, four species were significantly associated with gill scores at Wicklow Point: *Bourgainvilla* spp., *Clytia gregaria*, and Diphydae were positively associated, and *Sarsia* spp. was negatively associated with gill scores. None of these species are considered a nuisance species to aquaculture, and it is interesting that three of the species are positively associated as this indicates that with the presence of more individuals, the probability of a higher gill score being recorded decreases.

Like the Delta Day variable for the net patch samples, the same variable was created for

the tow samples. This showed that, like the net-patch samples, when gills were scored after a tow sample was collected, the probability of a higher score increased. The reason for this is unclear as unlike the net-patch collection in which a cleaning event happens at around the same time, nothing is disturbed or distributed into the water column. The Event Week random effect for these models was high, which indicated that despite several species being significantly associated, a large part of the variation seen sample-to-sample is likely variance caused by seasonality, rather than anything direct.

No parameter or biofoulant stood out in this study, and during the study period at these sites, the severity of the challenges was considered relatively unproblematic compared to the previous year class regarding proliferative gill disorders (PGD) (B. Vornicu, pers. comm.). The mortalities and injuries were much more numerous and severe in the previous year class, and as such the predictive power of these models for use in mitigation is limited. Continued sampling at these sites and others will increase our understanding of possible triggers or contributors to PGD in these areas, which can lead to better mitigation and management to reduce loss.

Chapter 4 **Conclusions, gaps in knowledge, and future directions**

4.1. Summary

In Chapter 2, I explored the question of if any correlations existed between the environmental variables, the biofoulant species, and the free-swimming sting-capable species. I found that most water parameters, with few exceptions, were associated with the individual counts of species of biofoulants on the net patches. Silica had the largest effect size at Doctor Islets and ammonia had the largest effect size at Wicklow Point. Most water parameters were associated with grams of hydroids growing on the net patches, with fewer parameters associated at Wicklow Point. Dissolved oxygen had the largest effect at Doctor Islets and nitrate levels had the largest effect at Wicklow Point. The effect sizes at Wicklow Point were much smaller than Doctor Islets, indicating they have less explanatory power to the trends in hydroid growth. Only ammonia and nitrate levels, and ammonia at Doctor Islets and Wicklow Point, respectively, were associated with the counts of stinging-capable species in the tow samples. The random effect used as a grouping variable to account for seasonality was large and likely accounted for much of the trends in the counts.

In Chapter 3, I explored the questions of if any correlations existed between environmental variables and gill health severity scores. In addition, I also explored if any correlations existed between the biofoulant species, free-swimming sting-capable species, and gill health severity scores. I found that only a few variables (three for each site) were associated with gill health. Temperature and pH had the largest effect sizes for Wicklow Point and Doctor Islets, respectively. I found that for both Doctor Islets and Wicklow Point, no counts of any of the biofoulant species recorded on the net patches, nor grams of any of the hydroid species collected were associated with gill health. The depth of each set of net patches were associated, but the

effect sizes for both sites were very small. The Delta Day variable, which indicated when in relation to a sample collection that gill health scores were taken, indicated that when gills were scored after a sample collection, the scores had a higher probability of scoring above 0. This supports the hypothesis that *in-situ* power washing of nets may impact the gill health of Atlantic salmon. No stinging-capable species identified and counted in the tow samples at Doctor Islets were associated with gill health. Four species, *Bourgainvilla* spp., *Clytia gregaria*, Diphydae spp., and *Sarsia* spp., were all associated (*Sarsia* spp. negatively, the rest positively) with gill health scores. None of these species are known to aquaculture or literature as being harmful or a nuisance species. In addition, the Delta Day variable indicated a similar result as in the biofouling models, in which after a sample collection, there was a higher probability that a gill health score higher than 0 would be recorded. The reason for this is not as obvious as nothing is disturbed or distributed during sampling, however the random effect used as a grouping variable to account for seasonality was relatively large and likely accounted for some of this result.

4.2. Gaps in knowledge

Suggesting biofouling organisms as detrimental to aquaculture and the role of hydroids in the causation or aggravation of gill injuries in finfish aquaculture, Atlantic salmon frequently included, is not new. However, nearly all the literature comes from Northern Europe, the Mediterranean Sea, and Australia (Rodger2011, Fitridge 2012, Bloecher 2021). Hydroids are a common biofoulant on fish farms in British Columbia (J. Pudota), but next to no information exists on their local distributions, how environmental parameters affect growth and settlement rates, or how the hydroids may affect the health, gill or otherwise, of fish despite several of the species known to cause mortalities in Europe existing here (e.g., *Obelia longissima* and *O.*

dichotoma). This gap in knowledge is likely due to the lack of past incidents or the inability to recognize these incidents, however, I expect this will be addressed in the future as climate change continues to disturb the local environments.

In addition to hydroids there are a host of other species growing on fish farm nets, however, literature on the compositions of these communities is scarce globally, and I have been unable to find any study that examines individual count data. Instead, it seems that the only study I located that examined any sort of relationship between non-hydroid biofoulants and gill health used a rating system of "clean" to "heavy fouling" (Østevik, 2021).

4.3. Future directions

There are many ways one could continue this project, especially in a way that address the gaps in knowledge I identified previously. Some of the areas of interest I have identified from literature and from this study would be in the development of a predictive model for use in monitoring and mitigation *in situ*. The identification of individual variables and their likelihood of contributing to or causing events in which higher gill health severity scores were recorded was a goal for this study and may have been possible with a multiyear study or more study sites. Unfortunately, although fortunately for the fish farms in this study, the severity of the challenges was considered unproblematic compared to the previous year regarding PGD.

Some other areas of this project I believe would benefit from more research would be in a closer examination of the hydroid species growing on the fish farm nets. In this study, a post hoc examination of the hydroids collected revealed several cryptic species. There is no information on the differences in stinging-ability or strength of venom in hydroids, and as such is it impossible to know if this has any effect on gill (or other organ) health. In addition, similar to

Østevik et al. (2021), a study examining the delay in immune response would likely provide some valuable insight, especially if combined with a closer examination of the biofouling communities. In conclusion, continued monitoring at these sites will improve the understanding of the interactions of the environment, the biofoulant communities, and gill health, ultimately leading to better mitigation and management strategies.

Literature Cited

Almada-villela, P.C., 1984. The Effects of Reduced Salinity on the Shell Growth of Small Mytilus edulis. J. Mar. Biol. Assoc. U.K. 64, 171–182.

Almada-Villela, P.C., Davenport, J., Gruffydd, L.D., 1982. The effects of temperature on the shell growth of young mytilus edulis L. J. Exp. Mar. Bio. Ecol. 59, 275–288. https://doi.org/10.1016/0022-0981(82)90121-6

Armendáriz-Ontiveros, M.M., García García, A., de los Santos Villalobos, S., Fimbres Weihs, G.A., 2019. Biofouling performance of RO membranes coated with Iron NPs on graphene oxide. Desalination 451, 45–58. https://doi.org/10.1016/j.desal.2018.07.005

Baxter, E., Sturt, M., Ruane, N., Doyle, T., McAllen, R., Rodger, H., 2012. Biofouling of the hydroid Ectopleura larynx on aquaculture nets in Ireland: implications for finfish health. Fish Vet. J. 18–30.

Baxter, E.J., Rodger, H.D., McAllen, R., Doyle, T.K., 2011. Gill disorders in marine-farmed salmon: Investigating the role of hydrozoan jellyfish. Aquac. Environ. Interact. 1, 245–257. https://doi.org/10.3354/aei00024

Birkeland, K., 1996. Consequences of premature return by sea trout (Salmo trutta) infested with the salmon louse (Lepeophtheirus salmonis Kroyer): migration, growth, and mortality. Can. J. Fish. Aquat. Sci. 53, 2808–2813. https://doi.org/10.1139/f96-231

Bloecher, N., Floerl, O., 2021. Towards cost-effective biofouling management in salmon aquaculture: a strategic outlook. Rev. Aquac. 13, 783–795. https://doi.org/10.1111/raq.12498

Bloecher, N., Olsen, Y., Guenther, J., 2013. Variability of biofouling communities on fish cage nets: A 1-year field study at a Norwegian salmon farm. Aquaculture 416–417, 302–309. https://doi.org/10.1016/j.aquaculture.2013.09.025

Boerlage, A.S., Ashby, A., Herrero, A., Reeves, A., Gunn, G.J., Rodger, H.D., 2020. Epidemiology of marine gill diseases in Atlantic salmon (Salmo salar) aquaculture: a review. Rev. Aquac. 12, 2140–2159. https://doi.org/10.1111/raq.12426

Boero, F., Brotz, L., Gibbons, M.J., Piraino, S. and Zampardi, S., 2016. Ocean Warming 3.10 Impacts and effects of ocean warming on jellyfish. Explain. Ocean Warm. Causes, scale, Eff. consequences 213–237.

Bosch-Belmar, M., Escurriola, A., Milisenda, G., Fuentes, V.L., Piraino, S., 2019. Harmful fouling communities on fish farms in the SW mediterranean sea: Composition, growth and reproductive periods. J. Mar. Sci. Eng. 7, 1–17. https://doi.org/10.3390/jmse7090288

Bosch-Belmar, M., Isern, M.M., Taurisano, V., Milisenda, G., Piraino, S., López, M., Fuentes, V., 2014. Potential impacts of fouling and planktonic cnidarians on farmed sea bass in the Western Mediterranean Sea. ICES Annu. Sci. Conf. 3–4.

Bosch-Belmar, M., Milisenda, G., Basso, L., Doyle, T.K., Leone, A., Piraino, S., 2020. Jellyfish Impacts on Marine Aquaculture and Fisheries. Rev. Fish. Sci. Aquac. 0, 1–18. https://doi.org/10.1080/23308249.2020.1806201

Bosch-Belmar, M., Milisenda, G., Girons, A., Taurisano, V., Accoroni, S., Totti, C., Piraino, S., Fuentes, V., 2017. Consequences of stinging plankton blooms on finfish mariculture in the Mediterranean sea. Front. Mar. Sci. 4, 1–11. https://doi.org/10.3389/fmars.2017.00240

Bosch-Belmar, M., Piraino, S., Sarà, G., 2022. Predictive Metabolic Suitability Maps for the Thermophilic Invasive Hydroid Pennaria disticha Under Future Warming Mediterranean Sea Scenarios. Front. Mar. Sci. 9. https://doi.org/10.3389/fmars.2022.810555

Bowden, A.J., Adams, M.B., Andrewartha, S.J., Elliott, N.G., Frappell, P.B., Clark, T.D., 2022. Amoebic gill disease increases energy requirements and decreases hypoxia tolerance in Atlantic salmon (Salmo salar) smolts. Comp. Biochem. Physiol. -Part A Mol. Integr. Physiol. 265. https://doi.org/10.1016/j.cbpa.2021.111128

Brooks, M., Kristensen, K., van Benthem, K., Magnusson, A., Berg, C., Nielsen, A., Skaug, H., Maechler, M., Bolker, B., 2017. glmmTMB Balances Speed and Flexibility Among Packages for Zero-inflated Generalized Linear Mixed Modeling. R J. 9, 378–400. https://doi.org/doi:10.32614/RJ-2017-066

Brown, N.E.M., Bernhardt, J.R., Harley, C.D.G., 2020. Energetic context determines species and community responses to ocean acidification. Ecology 101, 1–15. https://doi.org/10.1002/ecy.3073

Buckley, Y.M., 2015. Generalized linear models. Ecol. Stat. Contemp. theory Appl. https://doi.org/10.1093/acprof:oso/9780199672547.003.0007

Burnham, K.P., Anderson, D.R., 2004. Multimodel inference: Understanding AIC and BIC in model selection. Sociol. Methods Res. 33, 261–304. https://doi.org/10.1177/0049124104268644

Cabillon, N.A.R., Lazado, C.C., 2019. Mucosal barrier functions of fish under changing environmental conditions. Fishes 4, 1–10. https://doi.org/10.3390/fishes4010002

Cao, W.Q., Song, J., Yang, G.P., 2017. An adsorption and thermodynamic study of ofloxacin on marine sediments. Environ. Chem. 14, 350–360. https://doi.org/10.1071/EN16188

Carl, C., Guenther, J., Sunde, L.M., 2011. Larval release and attachment modes of the hydroid Ectopleura larynx on aquaculture nets in Norway. Aquac. Res. 42, 1056–1060. https://doi.org/10.1111/j.1365-2109.2010.02659.x

Cattano, C., Claudet, J., Domenici, P., Milazzo, M., 2018. Living in a high CO2 world: a global meta-analysis shows multiple trait-mediated fish responses to ocean acidification. Ecol. Monogr. 88, 320–335. https://doi.org/10.1002/ecm.1297

Christensen, R.H.B., 2018. Cumulative link models for ordinal regression with the R Package ordinal. J. Stat. Softw. 1–40.

Clinton, M., Kintner, A.H., Delannoy, C.M.J.J., Brierley, A.S., Ferrier, D.E.K.K., 2020. Molecular identification of potential aquaculture pathogens adherent to cnidarian zooplankton. Aquaculture 518, 734801. https://doi.org/10.1016/j.aquaculture.2019.734801

Cook, E.J., Black, K.D., Sayer, M.D.J., Cromey, C.J., Angel, D.L., Spanier, E., Tsemel, A., Katz, T., Eden, N., Karakassis, I., Tsapakis, M., Apostolaki, E.T., Malej, A., 2006. The influence of caged mariculture on the early development of sublittoral fouling communities: a pan-European study. ICES J. Mar. Sci. 63, 637–649. https://doi.org/10.1016/j.icesjms.2005.12.007

Cornejo, P., Guerrero, N.M., Montes, R.M., Quiñones, R.A., Sepúlveda, H.H., 2020. Hydrodynamic effect of biofouling in fish cage aquaculture netting. Aquaculture 526, 735367. https://doi.org/10.1016/j.aquaculture.2020.735367

Crosbie, P.B.B., Bridle, A.R., Leef, M.J., Nowak, B.F., 2010. Effects of different batches of Neoparamoeba perurans and fish stocking densities on the severity of amoebic gill disease in experimental infection of Atlantic salmon, Salmo salar L. Aquac. Res. 41, 505–516. https://doi.org/10.1111/j.1365-2109.2010.02522.x

Dobretsov, S., Coutinho, R., Rittschof, D., Salta, M., Ragazzola, F., Hellio, C., 2019. The oceans are changing: impact of ocean warming and acidification on biofouling communities. Biofouling 35, 585–595. https://doi.org/10.1080/08927014.2019.1624727

Downes, J.K., Yatabe, T., Marcos-Lopez, M., Rodger, H.D., MacCarthy, E., O'Connor, I., Collins, E., Ruane, N.M., 2018. Investigation of co-infections with pathogens associated with gill disease in Atlantic salmon during an amoebic gill disease outbreak. J. Fish Dis. 41, 1217–1227. https://doi.org/10.1111/jfd.12814

Edwards, C.D., Pawluk, K.A., Cross, S.F., 2015. The effectiveness of several commercial antifouling treatments at reducing biofouling on finfish aquaculture cages in British Columbia. Aquac. Res. 46, 2225–2235. https://doi.org/10.1111/are.12380

Eliasen, K., Danielsen, E., Johannesen, Á., Joensen, L.L., Patursson, E.J., 2018. The cleaning efficacy of lumpfish (Cyclopterus lumpus L.) in Faroese salmon (Salmo salar L.) farming pens in relation to lumpfish size and seasonality. Aquaculture 488, 61–65. https://doi.org/10.1016/j.aquaculture.2018.01.026

Espmark, Å.M., Hjelde, K., Baeverfjord, G., 2010. Development of gas bubble disease in juvenile Atlantic salmon exposed to water supersaturated with oxygen. Aquaculture 306, 198–204. https://doi.org/10.1016/j.aquaculture.2010.05.001

FAO, 2020. The State of World Fisheries and Aquaculture 2020. In brief, FAO. FAO.

https://doi.org/10.4060/ca9231en

FAO, 2009. The State of World Fisheries and Aquaculture. Water Food Water Life A Compr. Assess. Water Manag. Agric.

Feely, R.A., Orr, J., Fabry, V.J., Kleypas, J.A., Sabine, C.L., Langdon, C., 2009. Present and future changes in seawater chemistry due to ocean acidification. Geophys. Monogr. Ser. 183, 175–188. https://doi.org/10.1029/2005GM000337

Ferguson, H.W., Delannoy, C.M.J.J., Hay, S., Nicolson, J., Sutherland, D., Crumlish, M., 2010. Jellyfish as vectors of bacterial disease for farmed salmon (Salmo salar). J. Vet. Diagnostic Investig. 22, 376–382. https://doi.org/10.1177/104063871002200305

Field, B., 1981. Marine Biofouling and Its Control: History and State-of-the-Art Review. Ocean. Conf. Rec. 1, 542–544. https://doi.org/10.1109/oceans.1981.1151477

Fisheries and Oceans Canada, 2003. Profile of the Blue Mussel Gulf Region, Profile of the Blue Mussel (Mytilus edulis).

Fitridge, I., Dempster, T., Guenther, J., de Nys, R., 2012. The impact and control of biofouling in marine aquaculture: a review. Biofouling 28, 649–669. https://doi.org/10.1080/08927014.2012.700478

Fitridge, I., Keough, M.J., 2013. Ruinous resident: The hydroid Ectopleura crocea negatively affects suspended culture of the mussel Mytilus galloprovincialis. Biofouling 29, 119–131. https://doi.org/10.1080/08927014.2012.752465

Fivelstad, S., Haavik, H., Løvik, G., Olsen, A.B., 1998. Sublethal effects and safe levels of carbon dioxide in seawater for Atlantic salmon postsmolts (Salmo salar L.): Ion regulation

and growth. Aquaculture 160, 305–316. https://doi.org/10.1016/S0044-8486(97)00166-X

Floerl, O., Sunde, L.M., Bloecher, N., 2016. Potential environmental risks associated with biofouling management in salmon aquaculture. Aquac. Environ. Interact. 8, 407–417. https://doi.org/10.3354/AEI00187

Fofonoff, P., Ruiz, G., Steves, B., Simkanin, C., Carlton, J., 2020. National Exotic Marine and Estuarine Species Information System [WWW Document]. URL http://invasions.si.edu/nemesis/ (accessed 12.4.20).

Foreman, M.G.G., Stucchi, D.J., Zhang, Y., Baptista, A.M., 2006. Estuarine and tidal currents in the Broughton Archipelago. Atmos. - Ocean 44, 47–63. https://doi.org/10.3137/ao.440104

Freeman, M.A., Sommerville, C., 2009. Desmozoon lepeophtherii n. gen., n. sp., (Microsporidia: Enterocytozoonidae) infecting the salmon louse Lepeophtheirus salmonis (Copepoda: Caligidae). Parasites and Vectors 2, 1–15. https://doi.org/10.1186/1756-3305-2-58

Frommel, A.Y., Maneja, R., Lowe, D., Malzahn, A.M., Geffen, A.J., Folkvord, A., Piatkowski, U., Reusch, T.B.H., Clemmesen, C., 2012. Severe tissue damage in Atlantic cod larvae under increasing ocean acidification. Nat. Clim. Chang. 2, 42–46. https://doi.org/10.1038/nclimate1324

Gansel, L.C., Plew, D.R., Endresen, P.C., Olsen, A.I., Misimi, E., Guenther, J., Jensen, Ø., 2015. Drag of Clean and Fouled Net Panels--Measurements and Parameterization of Fouling. PLoS One 10, e0131051. https://doi.org/10.1371/journal.pone.0131051

Gartner, H.N., Murray, C.C., Frey, M.A., Nelson, J.C., Larson, K.J., Ruiz, G.M., Therriault, T.W., 2016. Non-indigenous invertebrate species in the marine fouling communities of

British Columbia, Canada. BioInvasions Rec. 5, 205–212. https://doi.org/10.3391/bir.2016.5.4.03

Gil Martens, L., Witten, P.E., Fivelstad, S., Huysseune, A., Sævareid, B., Vikeså, V., Obach, A., 2006. Impact of high water carbon dioxide levels on Atlantic salmon smolts (Salmo salar L.): Effects on fish performance, vertebrae composition and structure. Aquaculture 261, 80–88. https://doi.org/10.1016/j.aquaculture.2006.06.031

Gjessing, M.C., Yutin, N., Tengs, T., Senkevich, T., Koonin, E., Rønning, H.P., Alarcon, M., Ylving, S., Lie, K.-I., Saure, B., Tran, L., Moss, B., Dale, O.B., 2015. Salmon Gill Poxvirus, the Deepest Representative of the Chordopoxvirinae. J. Virol. 89, 9348–9367. https://doi.org/10.1128/jvi.01174-15

Gormican, S.J., 1989. Water circulation dissolved oxygen and ammonia concentrations in fish net-cages. University of British Columbia.

Greene, J.K., Grizzle, R.E., 2007. Successional development of fouling communities on open ocean aquaculture fish cages in the western Gulf of Maine, USA. Aquaculture 262, 289–301. https://doi.org/10.1016/j.aquaculture.2006.11.003

Greene, R.M., Geider, R.J., Falkowski, P.G., 1991. Effect of iron limitation on photosynthesis in a marine diatom. Limnol. Oceanogr. 36, 1772–1782. https://doi.org/10.4319/lo.1991.36.8.1772

Guenther, J., Misimi, E., Sunde, L.M., 2010. The development of biofouling, particularly the hydroid Ectopleura larynx, on commercial salmon cage nets in Mid-Norway. Aquaculture 300, 120–127. https://doi.org/10.1016/j.aquaculture.2010.01.005

Guinotte, J.M., Fabry, V.J., 2008. Ocean acidification and its potential effects on marine ecosystems. Ann. N. Y. Acad. Sci. 1134, 320–342. https://doi.org/10.1196/annals.1439.013

Gustafson, L.L., Ellis, S.K., Beattie, M.J., Chang, B.D., Dickey, D.A., Robinson, T.L., Marenghi, F.P., Moffett, P.J., Page, F.H., 2007. Hydrographics and the timing of infectious salmon anemia outbreaks among Atlantic salmon (Salmo salar L.) farms in the Quoddy region of Maine, USA and New Brunswick, Canada. Prev. Vet. Med. 78, 35–56. https://doi.org/10.1016/j.prevetmed.2006.09.006

Hellebø, A., Stene, A., Aspehaug, V., 2017. PCR survey for Paramoeba perurans in fauna, environmental samples and fish associated with marine farming sites for Atlantic salmon (Salmo salar L.). J. Fish Dis. 40, 661–670. https://doi.org/10.1111/jfd.12546

Herrero, A., Thompson, K.D., Ashby, A., Rodger, H.D., Dagleish, M.P., 2018. Complex Gill Disease: an Emerging Syndrome in Farmed Atlantic Salmon (Salmo salar L.). J. Comp. Pathol. 163, 23–28. https://doi.org/10.1016/j.jcpa.2018.07.004

Hillebrand, H., Blasius, B., Borer, E.T., Chase, J.M., Downing, J.A., Eriksson, B.K., Filstrup, C.T., Harpole, W.S., Hodapp, D., Larsen, S., Lewandowska, A.M., Seabloom, E.W., Van de Waal, D.B., Ryabov, A.B., 2018. Biodiversity change is uncoupled from species richness trends: Consequences for conservation and monitoring. J. Appl. Ecol. 55, 169–184. https://doi.org/10.1111/1365-2664.12959

Hiroi, J., McCormick, S.D., 2012. New insights into gill ionocyte and ion transporter function in euryhaline and diadromous fish. Respir. Physiol. Neurobiol. 184, 257–268. https://doi.org/10.1016/j.resp.2012.07.019

Hodson, S.L., Lewis, T.E., Burke, C.M., 1997. Biofouling of fish-cage netting: Efficacy and

problems of in situ cleaning. Aquaculture 152, 77–90. https://doi.org/10.1016/S0044-8486(97)00007-0

Holloway, M.G., Keough, M.J., 2002. An Introduced Polychaete Affects Recruitment and Larval Abundance of Sessile Invertebrates. Ecol. Appl. 12, 1803. https://doi.org/10.2307/3099939

Howes, S., Herbinger, C.M., Darnell, P., Vercaemer, B., 2007. Spatial and temporal patterns of recruitment of the tunicate Ciona intestinalis on a mussel farm in Nova Scotia, Canada. J. Exp. Mar. Bio. Ecol. 342, 85–92. https://doi.org/10.1016/j.jembe.2006.10.018

Hubot, N.D., Giering, S.L.C., Füssel, J., Robidart, J., Birchill, A., Stinchcombe, M., Dumousseaud, C., Lucas, C.H., 2021. Evidence of nitrification associated with globally distributed pelagic jellyfish. Limnol. Oceanogr. 66, 2159–2173. https://doi.org/10.1002/lno.11736

IPCC (Intergovernmental Panel on Climate Change), 2023. Synthesis Report of the IPCC Sixth Assessment Report (AR6).

Jawed, M., 1973. Ammonia excretion by zooplankton and its significance to primary productivity during summer. Mar. Biol. 23, 115–120. https://doi.org/10.1007/BF00389168

Johnsen, T.M., Eikrem, W., Olseng, C.D., Tollefsen, K.E., Bjerknes, V., 2010. Prymnesium parvum: The norwegian experience. J. Am. Water Resour. Assoc. 46, 6–13. https://doi.org/10.1111/j.1752-1688.2009.00386.x

Jones, S.R.M., Price, D., 2022. Elevated Seawater Temperature and Infection with Neoparamoeba perurans Exacerbate Complex Gill Disease in Farmed Atlantic Salmon (Salmo salar) in British Columbia, Canada. Microorganisms 10.

https://doi.org/10.3390/microorganisms10051039

Kain, M.P., Bolker, B.M., McCoy, M.W., 2015. A practical guide and power analysis for GLMMs: Detecting among treatment variation in randomeffects. PeerJ 2015. https://doi.org/10.7717/peerj.1226

Karlsbakk, E., Olsen, A.B., Einen, A.C.B., Mo, T.A., Fiksdal, I.U., Aase, H., Kalgraff, C., Skår, S.Å., Hansen, H., 2013. Amoebic gill disease due to Paramoeba perurans in ballan wrasse (Labrus bergylta). Aquaculture 412–413, 41–44. https://doi.org/10.1016/j.aquaculture.2013.07.007

Keylock, C.J., 2005. Simpson diversity and the Shannon-Wiener index as special cases of a generalized entropy. Oikos 109, 203–207. https://doi.org/10.1111/j.0030-1299.2005.13735.x

Kim, T.W., Micheli, F., 2013. Decreased solar radiation and increased temperature combine to facilitate fouling by marine non-indigenous species. Biofouling 29, 501–512. https://doi.org/10.1080/08927014.2013.784964

Kintner, A., Brierley, A.S., 2019. Cryptic hydrozoan blooms pose risks to gill health in farmed North Atlantic salmon (Salmo salar). J. Mar. Biol. Assoc. United Kingdom 99, 539–550. https://doi.org/10.1017/S002531541800022X

Klein, R.D., Borges, V.D., Rosa, C.E., Colares, E.P., Robaldo, R.B., Martinez, P.E., Bianchini, A., 2017. Effects of increasing temperature on antioxidant defense system and oxidative stress parameters in the Antarctic fish Notothenia coriiceps and Notothenia rossii. J. Therm. Biol. 68, 110–118. https://doi.org/10.1016/j.jtherbio.2017.02.016

Krasnov, A., Burgerhout, E., Johnsen, H., Tveiten, H., Bakke, A.F., Lund, H., Afanasyev, S., Rebl, A., Johansen, L.H., 2021. Development of Atlantic Salmon (Salmo salar L.) Under Hypoxic Conditions Induced Sustained Changes in Expression of Immune Genes and Reduced Resistance to Moritella viscosa. Front. Ecol. Evol. 9, 1–11. https://doi.org/10.3389/fevo.2021.722218

Krkošek, M., Lewis, M.A., Volpe, J.P., 2005. Transmission dynamics of parasitic sea lice from farm to wild salmon. Proc. R. Soc. B Biol. Sci. 272, 689–696. https://doi.org/10.1098/rspb.2004.3027

LeBlanc, A.R.T., Landry, T., Miron, G., 2002. Fouling organisms in a mussel cultivation bay : their effect on nutrient uptake and release. Can. Tech. Rep. Fish. Aquat. Sci. 2431, 16 p.

Mackie, G.O., Pugh, P.R., Purcell, J.E., 1987. Siphonophore biology. Adv. Mar. Biol. Vol. 24 97–262.

Mangano, M.C., Ape, F., Mirto, S., 2019. The role of two non-indigenous serpulid tube worms in shaping artificial hard substrata communities: Case study of a fish farm in the central Mediterranean Sea. Aquac. Environ. Interact. 11, 41–51. https://doi.org/10.3354/aei00291

Marcos-López, M., Mitchell, S.O., Rodger, H.D., 2016. Pathology and mortality associated with the mauve stinger jellyfish Pelagia noctiluca in farmed Atlantic salmon Salmo salar L. J. Fish Dis. 39, 111–115. https://doi.org/10.1111/jfd.12267

Martell, L., Bracale, R., Carrion, S.A., Purcell, J.E., Lezzi, M., Gravili, C., Piraino, S., Boero, F., 2018. Successional dynamics of marine fouling hydroids (Cnidaria: Hydrozoa) at a finfish aquaculture facility in the Mediterranean Sea. PLoS One 13, e0195352.

Matey, V., Richards, J.G., Wang, Y., Wood, C.M., Rogers, J., Davies, R., Murray, B.W., Chen, X.Q., Du, J., Brauner, C.J., 2008. The effect of hypoxia on gill morphology and ionoregulatory status in the Lake Qinghai scaleless carp, Gymnocypris przewalskii. J. Exp. Biol. 211, 1063–1074. https://doi.org/10.1242/jeb.010181

Mhaddolkar, S., Dineshbabu, A., Sujitha, T., Jayasree, L., 2019. Impact of water quality parameters on diversity and intensity of biofouling at sea cage farm. Int. J. Life Sci. 7.

Midway, S., 2022. Random Effects, in: Data Analysis in R.

Miller, D.C., Poucher, S., Cardin, J.A., Hansen, D., 1990. The acute and chronic toxicity of ammonia to marine fish and a mysid. Arch. Environ. Contam. Toxicol. 19, 40–48. https://doi.org/10.1007/BF01059811

Mineur, F., Cook, E.J., Minchin, D., Bohn, K., Macleod, A., Maggs, C.A., 2012. Changing coasts: Marine aliens and artificial structures. Oceanogr. Mar. Biol. An Annu. Rev. 50, 189–234.

Mitchell, S.O., Baxter, E.J., Rodger, H.D., 2011. Gill pathology in farmed salmon associated with the jellyfish Aurelia aurita. Vet. Rec. 169, 1–3. https://doi.org/10.1136/vr.100045

Mitchell, S.O., Rodger, H.D., 2011. A review of infectious gill disease in marine salmonid fish. J. Fish Dis. 34, 411–432. https://doi.org/10.1111/j.1365-2761.2011.01251.x

Montalto, V., Rinaldi, A., Ape, F., Mangano, M.C., Gristina, M., Sarà, G., Mirto, S., 2020. Functional role of biofouling linked to aquaculture facilities in Mediterranean enclosed locations. Aquac. Environ. Interact. 12, 11–22. https://doi.org/10.3354/aei00339

Morton, A.B., Williams, R., 2003. First report of a sea louse, Lepeophtheirus salmonis,

infestation on juvenile Pink Salmon, Oncorhynchus gorbuscha, in nearshore habitat. Can. Field-Naturalist 117, 634–641. https://doi.org/10.22621/cfn.v117i4.834

Mota, V.C., Nilsen, T.O., Gerwins, J., Gallo, M., Kolarevic, J., Krasnov, A., Terjesen, B.F., 2020. Molecular and physiological responses to long-term carbon dioxide exposure in Atlantic salmon (Salmo salar). Aquaculture 519, 734715. https://doi.org/10.1016/j.aquaculture.2019.734715

Mowi, 2023. Salmon Farming Industry Handbook. Report. https://mowi.com/investors/resources/

Murray, C.S., Malvezzi, A., Gobler, C.J., Baumann, H., 2014. Offspring sensitivity to ocean acidification changes seasonally in a coastal marine fish. Mar. Ecol. Prog. Ser. 504, 1–11. https://doi.org/10.3354/meps10791

Nellis, P., Bourget, E., 1996. Influence of physical and chemical factors on settlement and recruitment of the hydroid Tubularia larynx. Mar. Ecol. Prog. Ser. 140, 123–139. https://doi.org/10.3354/meps140123

Ngatia, L., M. Grace III, J., Moriasi, D., Taylor, R., 2019. Nitrogen and Phosphorus Eutrophication in Marine Ecosystems. Monit. Mar. Pollut. 1–17. https://doi.org/10.5772/intechopen.81869

Oldham, T., Dempster, T., Crosbie, P., Adams, M., Nowak, B., 2020. Cyclic hypoxia exposure accelerates the progression of amoebic gill disease. Pathogens 9, 1–14. https://doi.org/10.3390/pathogens9080597

Østevik, L., Stormoen, M., Nødtvedt, A., Alarcón, M., Lie, K.I., Skagøy, A., Rodger, H., 2021.

Assessment of acute effects of in situ net cleaning on gill health of farmed Atlantic salmon (Salmo salar L). Aquaculture 545. https://doi.org/10.1016/j.aquaculture.2021.737203

Øvrelid, M.S., 2017. Characterization of planktonic sea lice distribution and association to fish farm installations. Norwegian University of Science and Technology.

Palma, S., Apablaza, P., Silva, N., 2007. Hydromedusae (Cnidaria) of the Chilean southern channels (from the Corcovado Gulf to the Pulluche-Chacabuco channels). Sci. Mar. 71, 65–74. https://doi.org/10.3989/scimar.2007.71n165

Parihar, M.S., Javeri, T., Hemnani, T., Dubey, A.K., Prakash, P., 1997. Responses of superoxide dismutase, glutathione peroxidase and reduced glutathione antioxidant defenses in gills of the freshwater catfish (Heteropneustes fossilis) to short-term elevated temperature. J. Therm. Biol. 22, 151–156. https://doi.org/10.1016/S0306-4565(97)00006-5

Pelis, R.M., Zydlewski, J., McCormick, S.D., 2001. Gill Na+-K+-2Cl- cotransporter abundance and location in Atlantic salmon: Effects of seawater and smolting. Am. J. Physiol. - Regul. Integr. Comp. Physiol. 280, 1844–1852. https://doi.org/10.1152/ajpregu.2001.280.6.r1844

Person-Le Ruyet, J., Pichavant, K., Vacher, C., Le Bayon, N., Sévère, A., Boeuf, G., 2002. Effects of O2 supersaturation on metabolism and growth in juvenile turbot (Scophthalmus maximus l.). Aquaculture 205, 373–383. https://doi.org/10.1016/S0044-8486(01)00689-5

Pica, D., Bloecher, N., Dell'Anno, A., Bellucci, A., Pinto, T., Pola, L., Puce, S., 2019. Dynamics of a biofouling community in finfish aquaculture: a case study from the South Adriatic Sea. Biofouling 35, 696–709. https://doi.org/10.1080/08927014.2019.1652817

Piraino, S., Boero, F., Aeschbach, B., Schmid, V., 1996. Reversing the life cycle: Medusae

transforming into polyps and cell transdifferentiation in Turritopsis nutricula (Cnidaria, Hydrozoa). Biol. Bull. 190, 302–312. https://doi.org/10.2307/1543022

Powell, M.D., Åtland, Dale, T., 2018. Acute lion's mane jellyfish, Cyanea capillata (Cnideria: Scyphozoa), exposure to Atlantic salmon (Salmo salar L.). J. Fish Dis. 41, 751–759. https://doi.org/10.1111/jfd.12771

Powell, M.D., Reynolds, P., Kristensen, T., 2015. Freshwater treatment of amoebic gill disease and sea-lice in seawater salmon production: Considerations of water chemistry and fish welfare in Norway. Aquaculture 448, 18–28. https://doi.org/10.1016/j.aquaculture.2015.05.027

Purcell, J., Grover, J., 1990. Predation and food limitation as causes of mortality in larval herring at a spawning ground in British Columbia. Mar. Ecol. Prog. Ser. 59, 55–61. https://doi.org/10.3354/meps059055

Purcell, J.E., 2005. Climate effects on formation of jellyfish and ctenophore blooms: A review. J. Mar. Biol. Assoc. United Kingdom 85, 461–476. https://doi.org/10.1017/S0025315405011409

Purcell, J.E., Baxter, E.J., Fuentes, V.L., 2013. Jellyfish as products and problems of aquaculture. Adv. Aquac. Hatch. Technol. 404–430. https://doi.org/10.1533/9780857097460.2.404

Purcell, J.E., Uye, S.I., Lo, W.T., 2007. Anthropogenic causes of jellyfish blooms and their direct consequences for humans: A review. Mar. Ecol. Prog. Ser. 350, 153–174. https://doi.org/10.3354/meps07093

R Core Team, 2021. R: A language and environment for statistical computing.

Remen, M., Oppedal, F., Torgersen, T., Imsland, A.K., Olsen, R.E., 2012. Effects of cyclic environmental hypoxia on physiology and feed intake of post-smolt Atlantic salmon: Initial responses and acclimation. Aquaculture 326–329, 148–155. https://doi.org/10.1016/j.aquaculture.2011.11.036

Rensel, J.E., Whyte, J.N.. I., 2003. Manual on Harmful Marine Microalgae, in: Manual on Harmful Marine Microalgae.

Rodger, H.D., 2007. Gill disorders: an emerging problem for farmed Atlantic salmon (Salmo salar) in the marine environment? Fish Vet. J. 9, 38–48.

Rodger, H.D., Henry, L., Mitchell, S.O., 2011. Non-infectious gill disorders of marine salmonid fish. Rev. Fish Biol. Fish. 21, 423–440. https://doi.org/10.1007/s11160-010-9182-6

Roveta, C., Marrocco, T., Pica, D., Pulido Mantas, T., Rindi, F., Musco, L., Puce, S., 2022. The effect of substrate and depth on hydroid assemblages: a comparison between two islands of the Tuscan Archipelago (Tyrrhenian Sea). Mar. Biodivers. 52. https://doi.org/10.1007/s12526-021-01254-0

Rozas-Serri, M., 2019. Gill diseases in marine salmon aquaculture with an emphasis on amoebic gill disease. CAB Rev. Perspect. Agric. Vet. Sci. Nutr. Nat. Resour. 14. https://doi.org/10.1079/PAVSNNR201914032

Russ, G.R., 1980. Effects of predation by fishes, competition, and structural complexity of the substratum on the establishment of a marine epifaunal community. J. Exp. Mar. Bio. Ecol. 42, 55–69. https://doi.org/10.1016/0022-0981(80)90166-5

Sampaio, L.A., Wasielesky, W., Campos Miranda-Filho, K., 2002. Effect of salinity on acute toxicity of ammonia and nitrite to juvenile Mugil platanus. Bull. Environ. Contam. Toxicol. 68, 668–674. https://doi.org/10.1007/s001280306

Samsing, F., Solstorm, D., Oppedal, F., Solstorm, F., Dempster, T., 2015. Gone with the flow: Current velocities mediate parasitic infestation of an aquatic host. Int. J. Parasitol. 45, 559–565. https://doi.org/10.1016/j.ijpara.2015.03.006

Schielzeth, H., 2010. Simple means to improve the interpretability of regression coefficients. Methods Ecol. Evol. 1, 103–113. https://doi.org/10.1111/j.2041-210x.2010.00012.x

Sievers, M., Dempster, T., Keough, M.J., Fitridge, I., 2019. Methods to prevent and treat biofouling in shellfish aquaculture. Aquaculture 505, 263–270. https://doi.org/10.1016/j.aquaculture.2019.02.071

Simkanin, C., Davidson, I.C., Dower, J.F., Jamieson, G., Therriault, T.W., 2012. Anthropogenic structures and the infiltration of natural benthos by invasive ascidians. Mar. Ecol. 33, 499–511. https://doi.org/10.1111/j.1439-0485.2012.00516.x

Sollid, J., De Angelis, P., Gundersen, K., Nilsson, G.E., 2003. Hypoxia induces adaptive and reversible gross morphological changes in crucian carp gills. J. Exp. Biol. 206, 3667–3673. https://doi.org/10.1242/jeb.00594

Sundh, H., Finne-Fridell, F., Ellis, T., Taranger, G.L., Niklasson, L., Pettersen, E.F., Wergeland, H.I., Sundell, K., 2019. Reduced water quality associated with higher stocking density disturbs the intestinal barrier functions of Atlantic salmon (Salmo salar L.). Aquaculture 512, 734356. https://doi.org/10.1016/j.aquaculture.2019.734356

Swift, M.R., Fredriksson, D.W., Unrein, A., Fullerton, B., Patursson, O., Baldwin, K., 2006. Drag force acting on biofouled net panels. Aquac. Eng. 35, 292–299. https://doi.org/10.1016/j.aquaeng.2006.03.002

Tezcan, Ö.D., Sarp, S., 2013. An unusual marine envenomation following a rope contact: A report on nine cases of dermatitis caused by Pennaria disticha. Toxicon 61, 125–128. https://doi.org/10.1016/j.toxicon.2012.10.019

Toenshoff, E.R., Kvellestad, A., Mitchell, S.O., Steinum, T., Falk, K., Colquhoun, D.J., Horn, M., 2012. A novel betaproteobacterial agent of gill epitheliocystis in seawater farmed Atlantic salmon (Salmo salar). PLoS One 7, 1–7. https://doi.org/10.1371/journal.pone.0032696

Tommasi, D.A.G., Routledge, R.D., Hunt, B.P.V., Pakhomov, E.A., 2013. The seasonal development of the zooplankton community in a British Columbia (Canada) fjord during two years with different spring bloom timing. Mar. Biol. Res. 9, 129–144. https://doi.org/10.1080/17451000.2012.708044

Tully, O., Poole, W.R., Whelan, K.F., 1993. Infestation parameters for Lepeophtheirus salmonis (Kroyer) (Copepoda: Caligidae) parasitic on sea trout, Salmo trutta L., off the west coast of Ireland during 1990 and 1991. Aquac. Res. 24, 545–555. https://doi.org/10.1111/j.1365-2109.1993.tb00629.x

Tzaneva, V., Bailey, S., Perry, S.F., 2011. The interactive effects of hypoxemia, hyperoxia, and temperature on the gill morphology of goldfish (Carassius auratus). Am. J. Physiol. - Regul. Integr. Comp. Physiol. 300, 1344–1351. https://doi.org/10.1152/ajpregu.00530.2010

Vargas-Chacoff, L., Regish, A.M., Weinstock, A., McCormick, S.D., 2018. Effects of elevated

temperature on osmoregulation and stress responses in Atlantic salmon Salmo salar smolts in fresh water and seawater. J. Fish Biol. 93, 550–559. https://doi.org/10.1111/jfb.13683

Venables, W., Ripley, B., 2002. Modern Applied Statistics with S, Fourth Edi. ed. New York.

Visch, W., Nylund, G.M., Pavia, H., 2020. Growth and biofouling in kelp aquaculture (Saccharina latissima): the effect of location and wave exposure. J. Appl. Phycol. 32, 3199–3209. https://doi.org/10.1007/s10811-020-02201-5

Wetzel, R.G., 2001. Oxygen, in: Limnology, Lake and River Ecosystems. pp. 151–168.

Whyte, J.N.. I., Haigh, N., Ginther, N., Keddy, L., Norma, G., Laurie, J., Whyte, J.N.. I., Haigh, N., Ginther, N., Keddy, L., Norma, G., Laurie, J., 2001. First record of blooms of Cochlodinium sp . Gymnodiniales , ... Phycologia 40, 298–304.

Willcox, S., Moltschaniwskyj, N.A., Crawford, C.M., 2008. Population dynamics of natural colonies of Aurelia sp. scyphistomae in Tasmania, Australia. Mar. Biol. 154, 661–670. https://doi.org/10.1007/s00227-008-0959-2

Williams, C.R., Dittman, A.H., McElhany, P., Busch, D.S., Maher, M.T., Bammler, T.K., MacDonald, J.W., Gallagher, E.P., 2019. Elevated CO 2 impairs olfactory-mediated neural and behavioral responses and gene expression in ocean-phase coho salmon (Oncorhynchus kisutch). Glob. Chang. Biol. 25, 963–977. https://doi.org/10.1111/gcb.14532

Winfree, R., Fox, J.W., Williams, N.M., Reilly, J.R., Cariveau, D.P., 2015. Abundance of common species, not species richness, drives delivery of a real-world ecosystem service. Ecol. Lett. 18, 626–635. https://doi.org/10.1111/ele.12424

Appendices

Appendix A

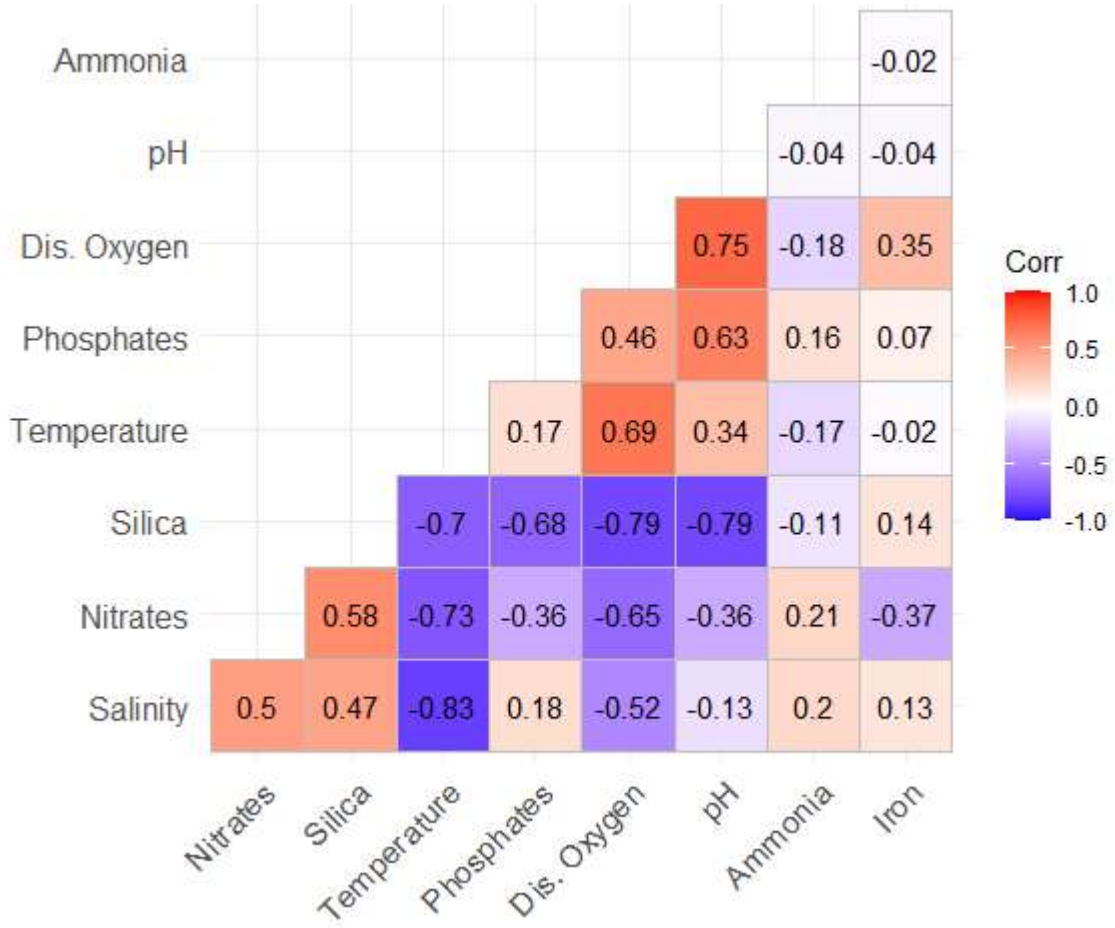

Figure A2.1: Correlation plot of the continuous variables used to supplement the model selection process for the models examining the effects of water parameters on biofouling counts and grams of hydroids collected from the net-patches for Doctor Islets. Correlation values greater than ±0.60 were taken into consideration.

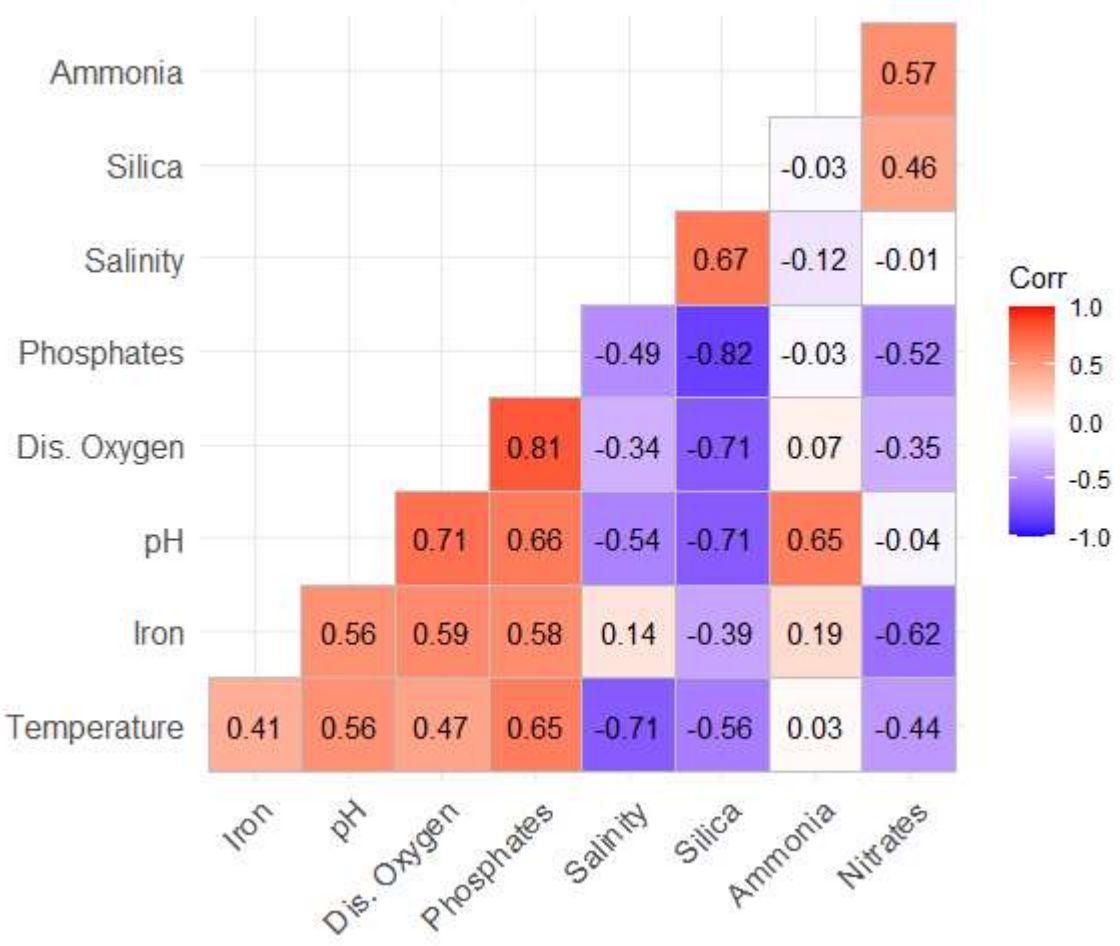

Figure A2.2: Correlation plot of the continuous variables used to supplement the model selection process for the models examining the effects of water parameters on biofouling counts and grams of hydroids collected from the net-patches for Wicklow Point. Correlation values greater than ±0.60 were taken into consideration.

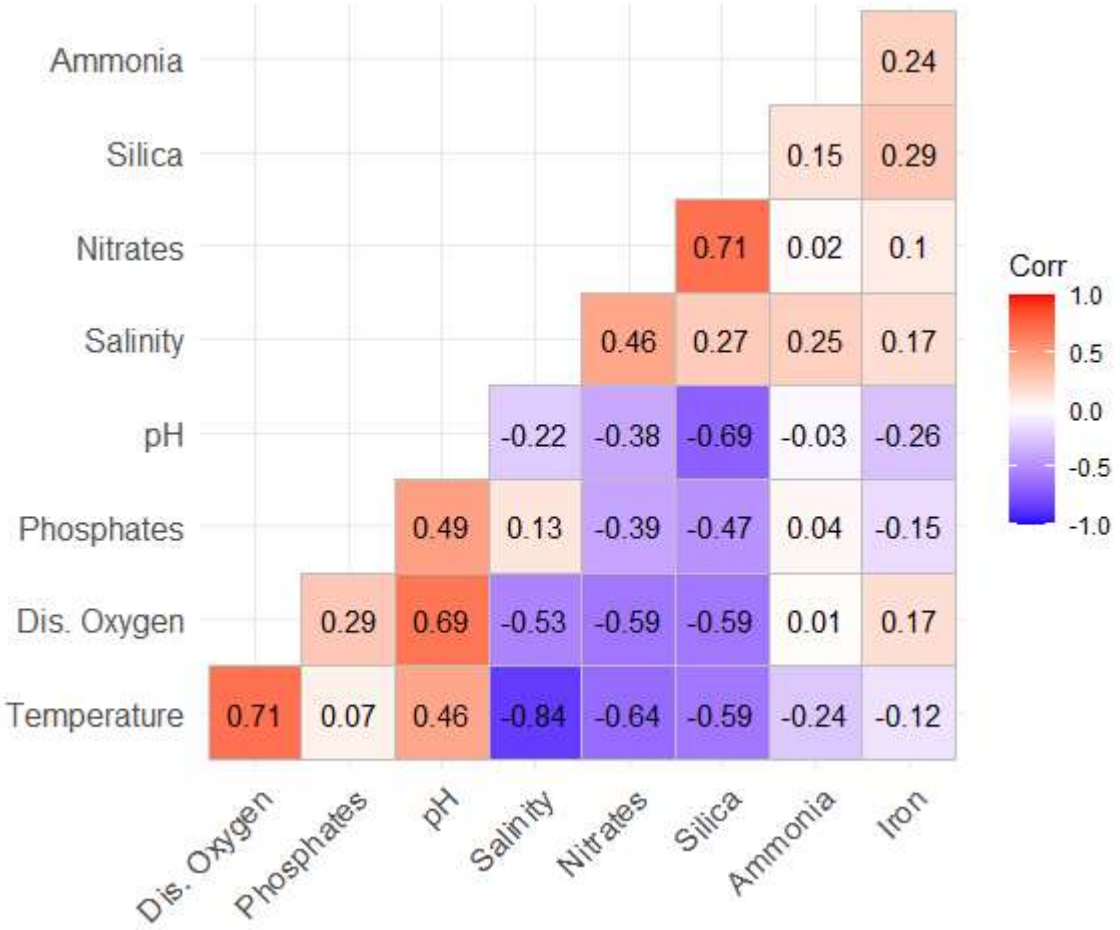

Figure A2.3: Correlation plot of the continuous variables used to supplement the model selection process for the models examining the effects of water parameters on the stinging-capable species in tow samples for Doctor Islets. Correlation values greater than ±0.60 were taken into consideration.

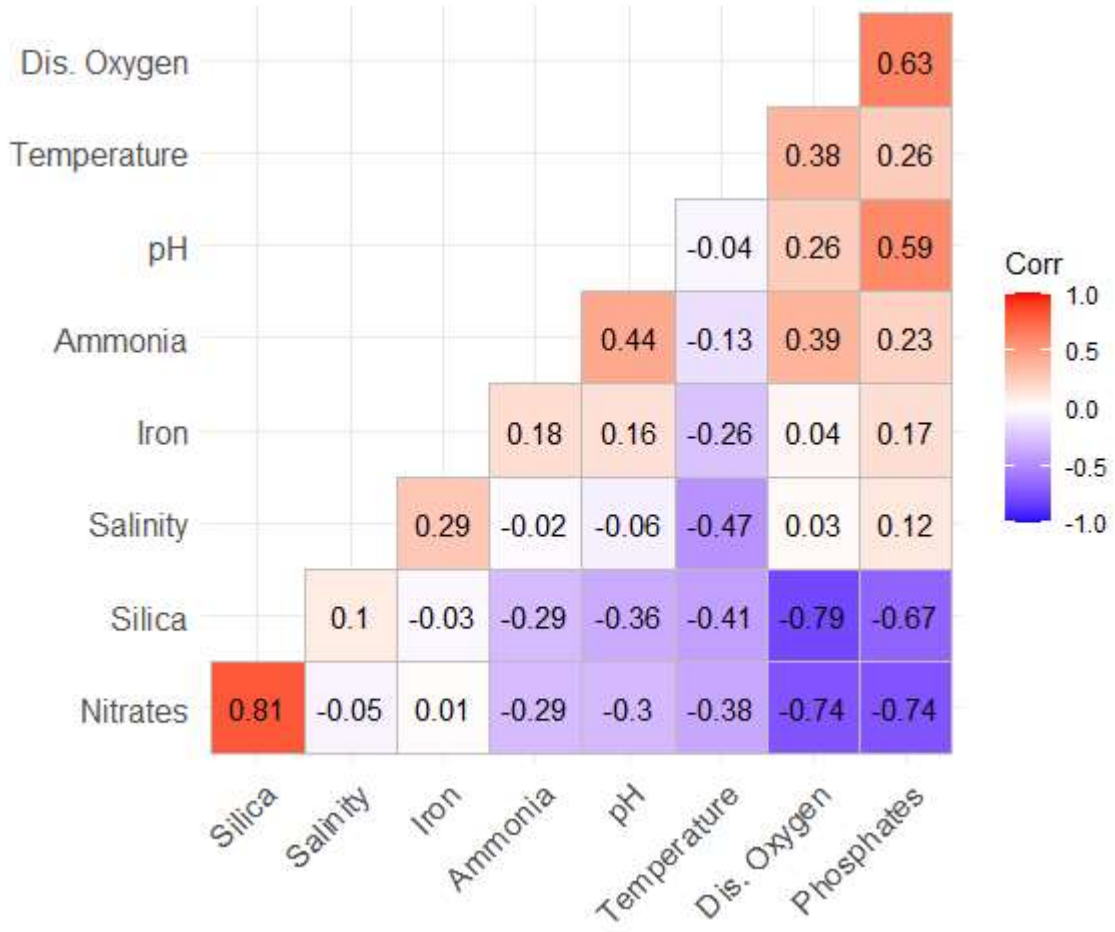

Figure A2.4: Correlation plot of the continuous variables used to supplement the model selection process for the models examining the effects of water parameters on the stinging-capable species in tow samples for Wicklow Point. Correlation values greater than ±0.60 were taken into consideration.

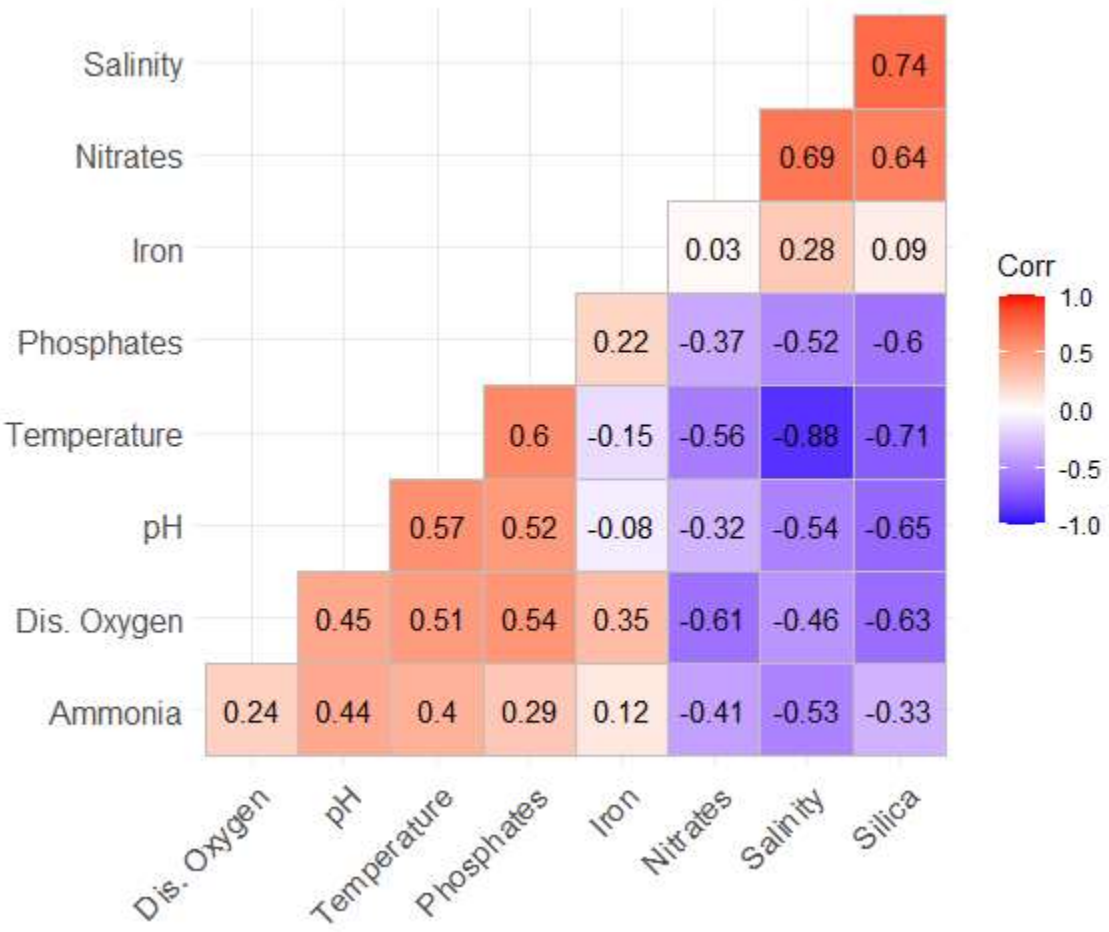

Figure A3.1: Correlation plot of the continuous variables used to supplement the model selection process for the models examining the effects of water parameters on the gill health scores for Doctor Islets. Correlation values greater than ±0.60 were taken into consideration.

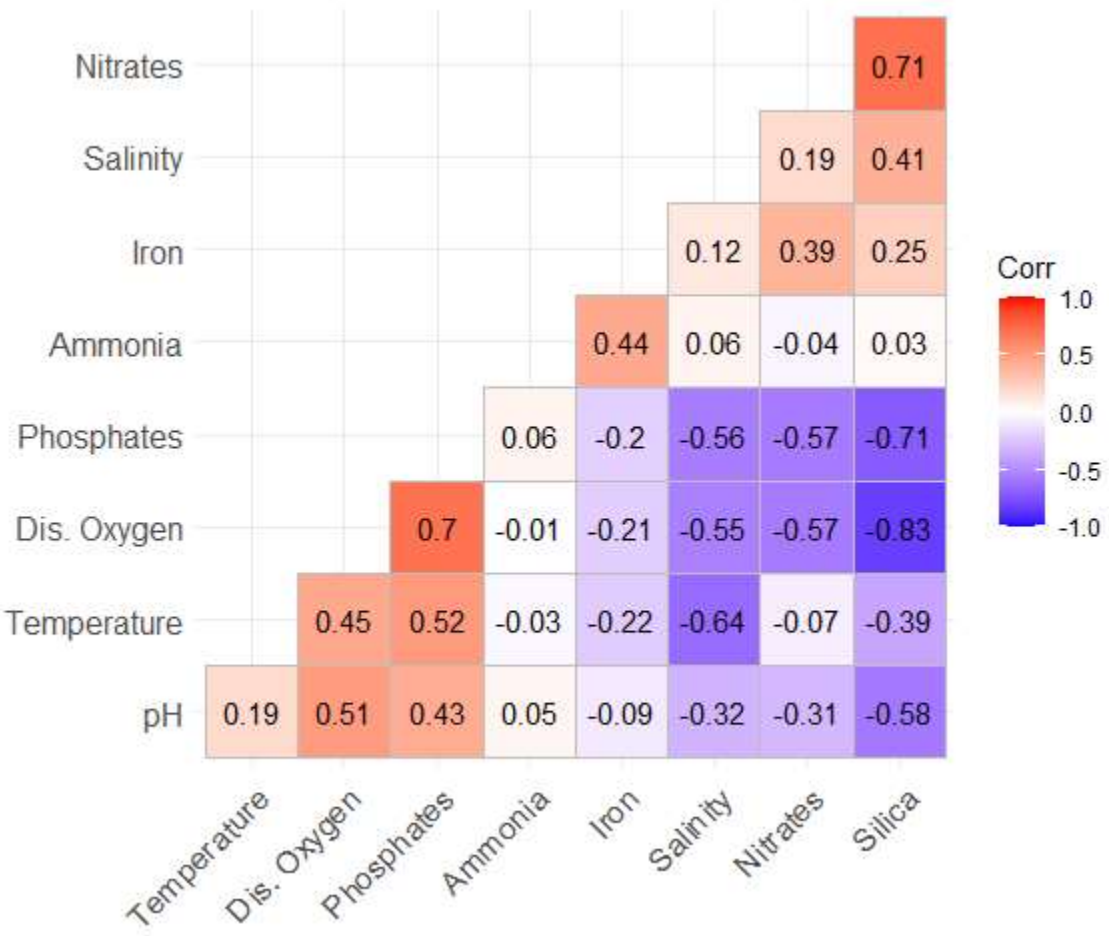

Figure A3.2: Correlation plot of the continuous variables used to supplement the model selection process for the models examining the effects of water parameters on the gill health scores for Wicklow Point. Correlation values greater than ±0.60 were taken into consideration.

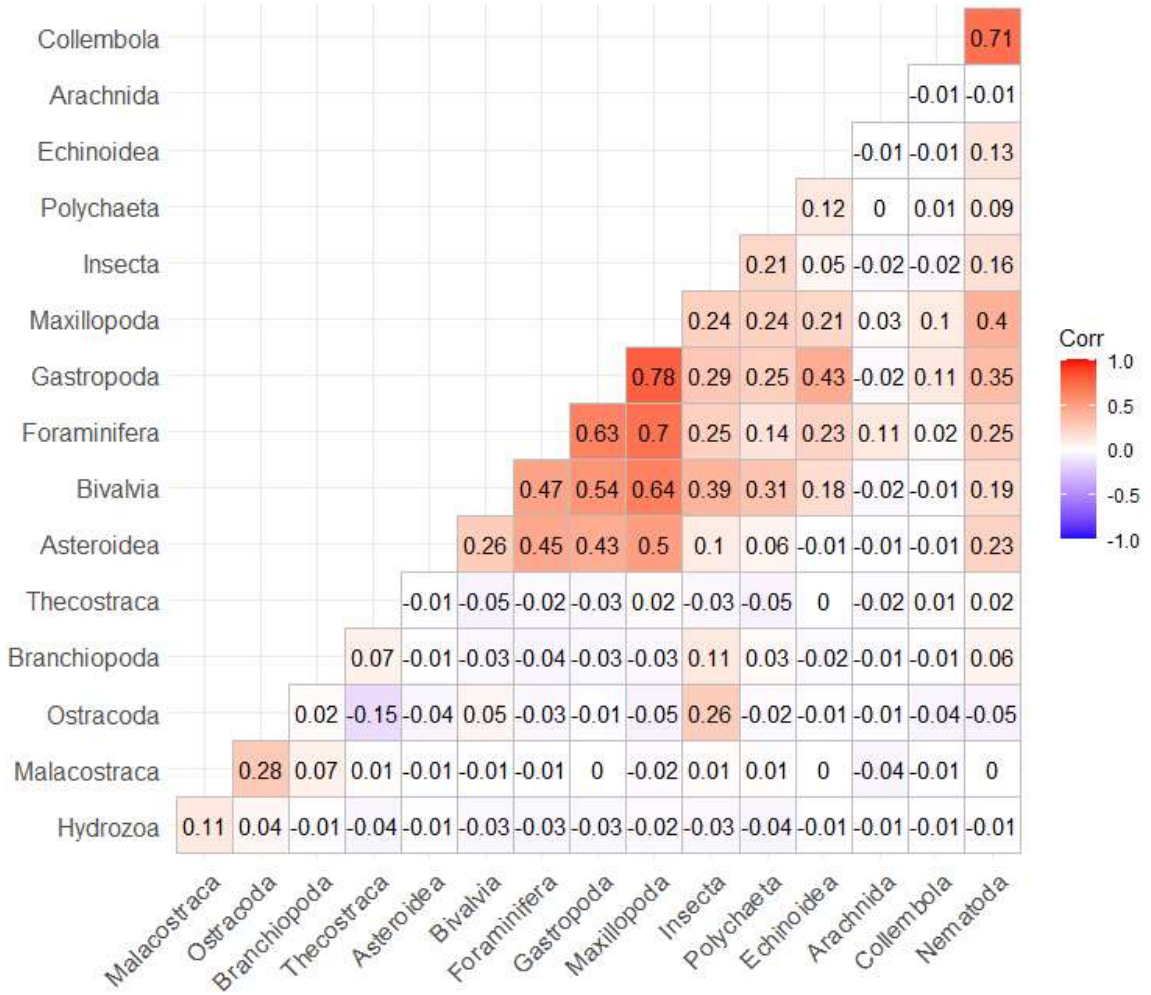

Figure A3.3: Correlation plot of the biofoulant species counts used to supplement the model selection process for the models examining the effects of biofoulant species counts on the gill health scores for Doctor Islets. Correlation values greater than ±0.60 were taken into consideration.

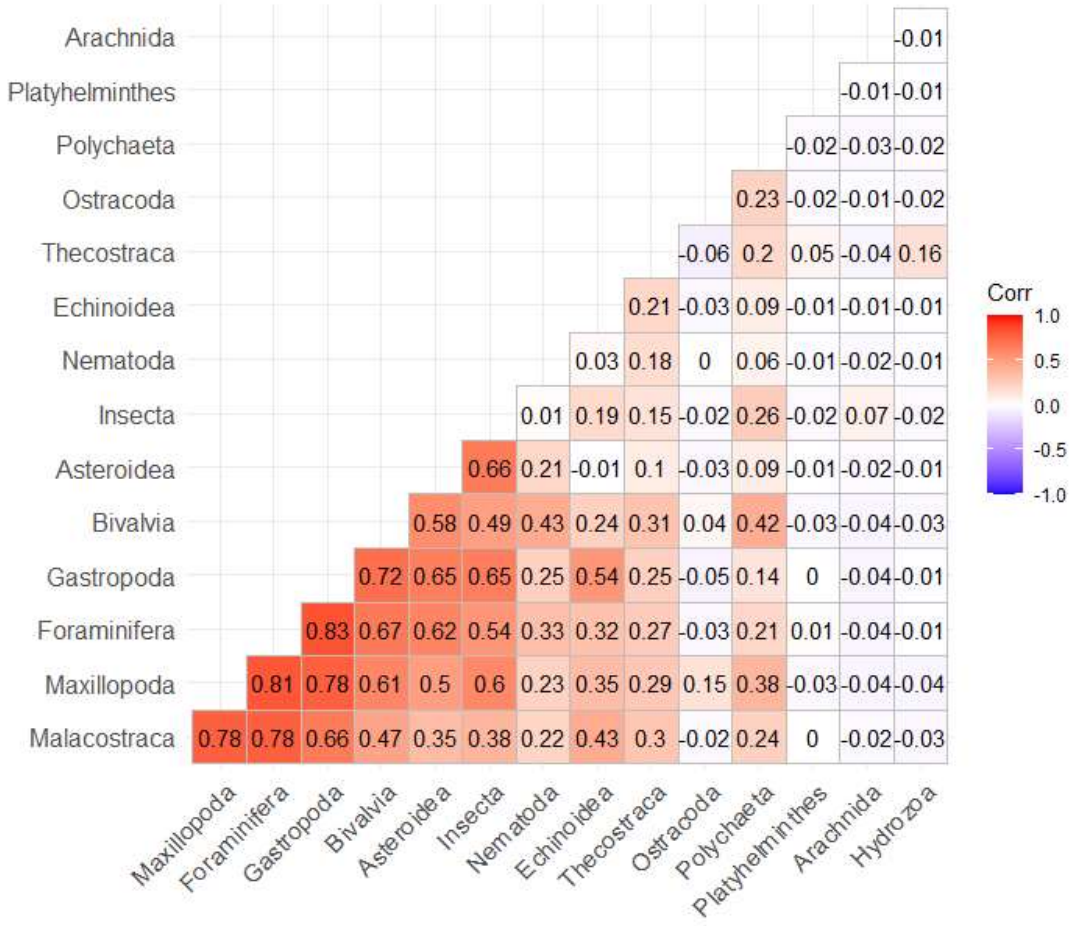

Figure A3.4: Correlation plot of the biofoulant species counts used to supplement the model selection process for the models examining the effects of biofoulant species counts on the gill health scores for Wicklow Point. Correlation values greater than ±0.60 were taken into consideration.

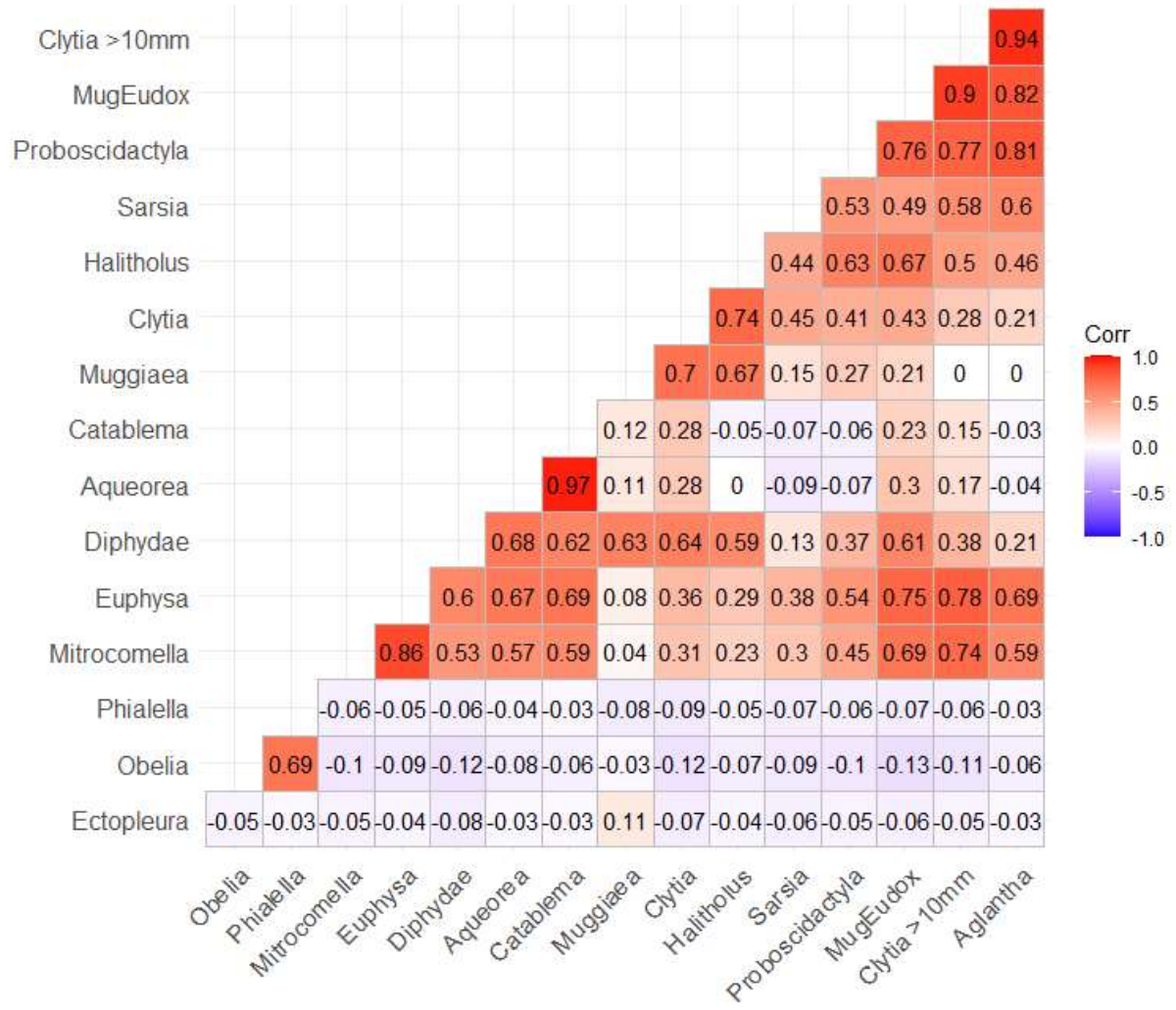

Figure A3.5: Correlation plot of the counts of stinging-capable species in the tow samples used to supplement the model selection process for the models examining the effects of stinging species counts in tow samples on the gill health scores for Doctor Islets. Correlation values greater than ±0.60 were taken into consideration.

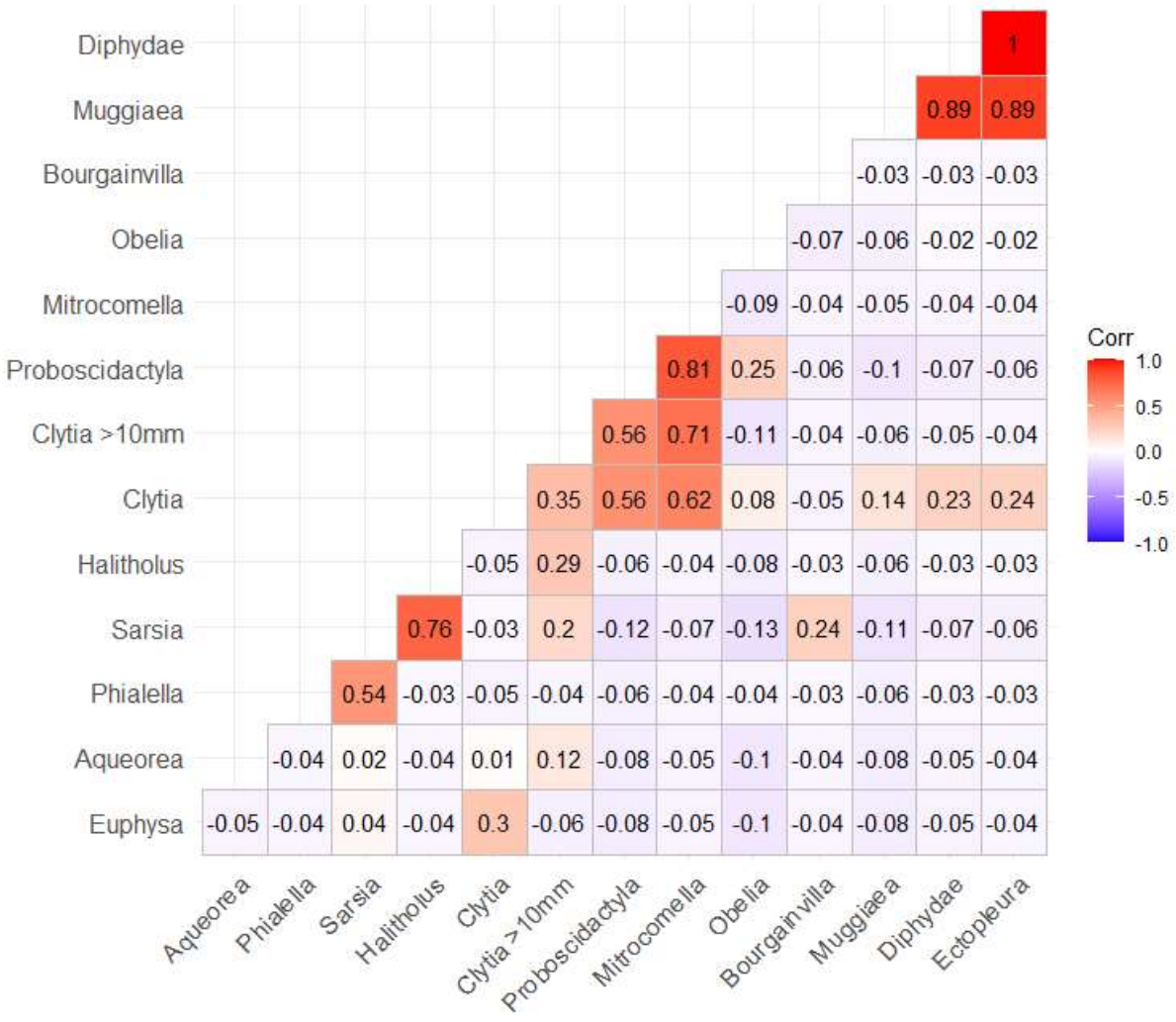

Figure A3.6: Correlation plot of the counts of stinging-capable species in the tow samples used to supplement the model selection process for the models examining the effects of stinging species counts in tow samples on the gill health scores for Wicklow Point. Correlation values greater than ±0.60 were taken into consideration.